Non-abelian braiding in abelian lattice models from lattice dislocations

Icke-abelsk flätning i abelska gittermodeller genom dislokationer

Mattias Flygare

Faculty of Health, Science and Technology, Department of Engineering and Physics

Subject: Master's thesis in physics

Credits: 30 ECTS

Supervisor: Jürgen Fuchs

Examiner: Claes Uggla

Date: 2014-03-10

Abstract

Topological order is a new field of research involving exotic physics. Among other things it has been suggested as a means for realising fault-tolerant quantum computation. Topological degeneracy, i.e. the ground state degeneracy of a topologically ordered state, is one of the quantities that have been used to characterize such states. Topological order has also been suggested as a possible quantum information storage.

We study two-dimensional lattice models defined on a closed manifold, specifically on a torus, and find that these systems exhibit topological degeneracy proportional to the genus of the manifold on which they are defined. We also find that the addition of lattice dislocations increases the ground state degeneracy, a behaviour that can be interpreted as artificially increasing the genus of the manifold. We derive the fusion and braiding rules of the model, which are then used to calculate the braiding properties of the dislocations themselves. These turn out to resemble non-abelian anyons, a property that is important for the possibility to achieve universal quantum computation. One can also emulate lattice dislocations synthetically, by adding an external field. This makes them more realistic for potential experimental realisations.

Sammanfattning – Abstract in Swedish

Topologisk ordning är ett nytt område inom fysik som bland annat verkar lovande som verktyg för förverkligandet av kvantdatorer. En av storheterna som karakteriserar topologiska tillstånd är det totala antalet degenererade grundtillstånd, den topologiska degenerationen. Topologisk ordning har också föreslagits som ett möjligt sätt att lagra kvantdata.

Vi undersöker tvådimensionella gittermodeller definierade på en sluten mångfald, specifikt en torus, och finner att dessa system påvisar topologisk degeneration som är proportionerlig mot mångfaldens topologiska genus. När dislokationer introduceras i gittret finner vi att grundtillståndets degeneration ökar, något som kan ses som en artificiell ökning av mångfaldens genus. Vi härleder sammanslagningsregler och flätningsregler för modellen och använder sedan dessa för att räkna ut flätegenskaperna hos själva dislokationerna. Dessa visar sig likna icke-abelska anyoner, en egenskap som är viktiga för möjligheten att kunna utföra universella kvantberäkningar. Det går också att emulera dislokationer i gittret genom att lägga på ett yttre fält. Detta gör dem mer realistiska för eventuella experimentella realisationer.

Acknowledgements

Thank you to my supervisor Jürgen Fuchs for all your time and efforts into making this work as good as it could be. To my wife Anna-Lena for your support and love. To my sons Sixten and Alexander for making me happy. To Martin Carlsson and Per Sallnäs for being good friends, your support counts. To my father Kent, Gun-Britt and to the memory of my mother Bodil. Thanks to Per Folkesson for all your wise words and to Igor Buchberger for inspiring and fun conversations. Finally, to all the boys and girls at Karlstad university who have made my life better during my time there, you know who you are!

Contents

1 Introduction

In the last decade of the twentieth century and the start of the twenty-first, a small revolution has been taking place in the theory of mechanisms determining different phases of matter. Not long ago it was considered a confirmed fact that all phases of matter, be it solid, liquid, magnetic, conducting or insulating, were characterized by a *spontaneous symmetry breaking order* which in essence is the presence or non-presence of symmetries in the system. For example, take the discreet translation symmetry in a lattice of atoms in a solid crystal compared to the continuous translation symmetry of the "randomly" ordered atoms of a liquid.

In the late 1980's, the study of superconductors and fractional quantum Hall (FQH) states led to the conclusion that spontaneous symmetry breaking is not enough to explain all phases of matter. A new concept emerged, termed *topological order*, due to its apparent dependence on the topological properties of the system. Topological order introduced new quantum numbers to characterize the new exotic phases of matter, such as ground state degeneracy and the non-abelian Berry phase of those degenerate ground states. An excellent introduction to the concept of topological order can be found in [23].

In systems that can be described in $2+1$ dimensions (two spatial and time), and which exhibit topological order, a special type of *quasi-particle* excitation has been found to exist, one that neither has the particle exchange statistics of bosons or fermions, but instead follows

$$|a\rangle \otimes |b\rangle = \mathrm{e}^{\mathrm{i}\theta}\ |b\rangle \otimes |a\rangle$$

for the exchange of particles a and b, where θ is an arbitrary phase. For $\theta = 0$ and $\theta = \pi$ we thus get bosonic and fermionic statistics, respectively, but for other phases we say that the particles are *anyons*. Furthermore, if the exchanges of two different pairs of particles do not commute, as can also be the case, we say that the particles are *non-abelian anyons*.

As pointed out in [15], it is rare for a new scientific theory to develop in parallel with a potential application, however in this case, topological order and *quantum computing* are evolving alongside each other, each field bleeding into the other. Abelian anyons are not suitable for quantum computing given their inability to produce a complete set of logical gates, however, there are attempts to exploit the existence of non-abelian anyons to create fault-tolerant quantum computers. The basic idea is to use the different degenerate ground states to store information, since these are insensitive to local disturbances due to their topological origin. The unitary gate operations needed to perform calculations are made possible by the *braiding* of non-abelian anyons, and the information is then read by measuring the resulting Berry phase. More information on how $2+1$ dimensional anyon systems can be considered quantum computers can be found in [12]. The role of non-abelian anyons for quantum computing is explored in [15]. In [8] suggestions are made on how to achieve universal topological quantum computation in a FQH state. Also see [11] as a reference for quantum error correction codes (stabilizer codes) and [16] for a general textbook on quantum computation.

In 1997, A. Yu. Kitaev suggested a theoretical model featuring a square lattice with a spin degree of freedom assigned to each site [12]. The Hamiltonian proposed by Kitaev was based on particle interaction grouped in vertices and squares, where each vertex and square (or plaquette) in the lattice had its own 4-particle interaction term in the Hamiltonian. The model was also equipped with periodic boundary conditions which, by giving the lattice the topological shape of a torus, was the origin of the name; the Kitaev toric code model. In this model the ground state degeneracy proved to be non-trivial (larger than 1) and it also featured abelian anyons. The fusion and braiding rules of the anyons allow for at least two symmetries, or *dualities*, within the model.

Besides the square lattice model, other types of lattices have also been considered, for instance the honeycomb model in [17].

Later, it was also pointed out by Kitaev in [13] that it should be possible and interesting to consider dislocated toric code lattices. This possibility is explored, for instance in [6] and

[26], and indeed the dislocations themselves, sometimes called *twist defects* or *genons*, effectively realize the dualities expected from the fusion and braiding properties of the anyons. In addition, the dislocations themselves turn out to resemble anyons with non-abelian braiding statistics, as is explored in detail in [2]. They can however not be considered as non-abelian anyons, since they are by nature extrinsic, i.e. do not have an interaction term in the Hamiltonian. Another problem with such lattice dislocations is the inability to create, annihilate and move them in a controlled way. These problems make lattice dislocations unsuitable for quantum computation. As a remedy, Hamiltonians that realize such dislocations "synthetically", by applying an external field, have been suggested for instance in [25]. The hope is for such non-abelian anyons to allow for a complete set of logical gates, and thus for universal quantum computation.

The defects of square lattice models also have certain aspects in common with defects in abelian bilayer systems, such as the ones considered in [10], [21] and [4].

A number of possible experimental settings to realize synthetic dislocations have been suggested, for example for a bilayer FQH system in [4]. An experiment to detect topological degeneracy is proposed in [3], also for a bilayer FQH system. In 2012 it was reported in [24] that topological error correction had been experimentally confirmed to be viable. There are many more experiments related to topological order to date, and new ones seem to emerge every month.

In this thesis we explore the toric code lattice model in detail, including the introduction of dislocations both by "physically" altering the lattice as in [26], here treated in Section 2, and synthetically as in [25], treated in Section 4. In Section 3 we also generalize the model from having spin states at each site to having an N-fold angular momentum rotor assigned to each site. The generalization to N opens up the possibility of another type of dislocation which is explored in Section 3.7. The ground state degeneracy of undislocated and dislocated models are calculated and a basis for the space of ground states is found. The braiding statistics of the abelian anyons of the generalized model are determined in Section 3.3, and then used to calculate the braiding properties of the non-abelian anyons of the dislocations in Section 3.6 and 3.9.

A few results previously not found in the literature will be presented, such as the special cases of ground state degeneracy when introducing the first pair of dislocations found in Section 3.4 and 3.8, and similar unusual situations that have not been explicitly calculated before. The fusion rules of Section 3.2 and braiding rules of Section 3.3 of the modular tensor categories that characterize anyon models like this are linked to, and confirmed by, the microscopic details of the model, in more detail than previously found. Furthermore, the equations leading to the non-abelian Berry phase of dislocations in Section 3.6 and 3.9 are expanded by several steps and are supported by a solid list of identities derived from the braiding properties, all of which are necessary for a complete understanding of the equations. The proofs of Appendix A.2-A.7 can also not be found in the literature.

2 The $\mathbb{Z}_2$ toric plaquette model

In this section we explore a two-dimensional lattice model with periodic boundary conditions. The latter means that we are actually dealing with a lattice that has the topological shape of a torus. At each vertex of the lattice we assign a two-dimensional complex state space which, together with the specific form of the Hamiltonian of this model, gives rise to a $\mathbb{Z}_2$-symmetry, hence the name. Actually, one should expect that many features we find are not dependent on a specific Hamiltonian, but rather on the universality classes of the systems. For explicit calculations, however, we use a concrete Hamiltonian. Moreover, lattices used in examples are typically very small, but one should keep in mind that in realistic applications the number of sites is very large. The toric plaquette model is also called the Kitaev toric code model, developed by Kitaev in [12].

First we will set up the basic rules of the model and see how the boundary conditions together with the parity of the lattice determine the ground state degeneracy. Then we will see how this degeneracy can be altered by the introduction of defects, and finally we explore the braiding properties of such defects and how these processes can be used to go from one ground state to another.

2.1 The state space

We start with a square lattice with $L_x \times L_y$ nodes. For concreteness we mainly restrict our considerations to the case that L_x and L_y are both even, considering cases when one or both sides are odd only when it is relevant in order to better understand the even case. A node (or vertex) of the lattice is from now on referred to interchangeably as a *site*. The set of all sites is denoted M. The total number of sites is

$$|\mathrm{M}| = L_x \times L_y. \tag{2.1.1}$$

Each square defined by 4 adjacent sites is referred to as a *plaquette*, the set of all plaquettes is denoted P and the total number of plaquettes is denoted |P|.

To begin with, this lattice is defined on the plane, but we can add some boundary conditions to compactify the space into the sphere. It turns out that it is also interesting to consider higher genus surfaces, which is the motivation for us to consider this lattice to be mapped onto a torus. When applying the periodic boundary conditions that define a torus we create new plaquettes on the right and bottom sides and identify the new sites with the corresponding ones on the opposing side to glue together the lattice.

Example 2.1. The identifications of the periodic boundary conditions are illustrated in the following picture, for the 4×2 site lattice:

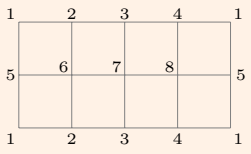

(2.1.2)

This process of identifying nodes also means that the number of columns of plaquettes is equal to L_x and the number of rows of plaquettes is equal to L_y, so we get $|\mathrm{M}| = |\mathrm{P}|$. From now on we refer to the numbers L_x and L_y as the *periods* of the lattice.

To each site $i \in \mathrm{M}$ assign a state space $\mathcal{H}_i = \mathbb{C}^2$, and choose as basis the two eigenstates of the Pauli operator σ_i^z:

$$|m_i\rangle, \quad m_i \in \{0, 1\}, \tag{2.1.3}$$

so that

$$\sigma_i^z \left|m_i\right\rangle = \mathrm{e}^{\mathrm{i}\pi m_i} \left|m_i\right\rangle = (-1)^{m_i} \left|m_i\right\rangle . \tag{2.1.4}$$

Then the Pauli operator σ_i^x exchanges $|0\rangle$ and $|1\rangle$ according to

$$\sigma_i^x \left|m_i\right\rangle = \left|(m_i - 1)_{\mathrm{mod}\ 2}\right\rangle . \tag{2.1.5}$$

The full system state space is the tensor product of state spaces at all sites:

$$\mathcal{H} = \bigotimes_{i \in \mathrm{M}} \mathcal{H}_i \cong \mathbb{C}^{2|\mathrm{M}|} \tag{2.1.6}$$

with basis

$$\mathcal{B}_s = \left\{ \left|m_1\right\rangle \otimes \left|m_2\right\rangle \otimes \cdots \otimes \left|m_i\right\rangle \otimes \cdots \otimes \left|m_{|\mathrm{M}|-1}\right\rangle \otimes \left|m_{|\mathrm{M}|}\right\rangle \ \middle|\ m_i \in \{0,1\} \right\}, \tag{2.1.7}$$

of dimension $2^{|\mathrm{M}|}$. With abbreviated notation the basis states (2.1.7) are written as

$$\left|m_1 m_2 \cdots m_i \cdots m_{|\mathrm{M}|-1} m_{|\mathrm{M}|}\right\rangle . \tag{2.1.8}$$

An operator $\mathcal{Q}_i$ on the state space $\mathcal{H}_i$ induces an operator on $\mathcal{H}$ given by

$$\mathbf{1}_1 \otimes \mathbf{1}_2 \otimes \cdots \otimes \mathcal{Q}_i \otimes \cdots \otimes \mathbf{1}_{|\mathrm{M}|-1} \otimes \mathbf{1}_{|\mathrm{M}|}. \tag{2.1.9}$$

By abuse of notation we still call this operator $\mathcal{Q}_i$.

We will adopt the graphical notation for the Pauli matrices introduced in [26] where

$\sigma_i^z =$, (2.1.10)

$\sigma_i^x =$ (2.1.11)

and

$\sigma_i^y = \mathrm{i}$ $= \mathrm{i}\,\sigma_i^x \sigma_i^z$. (2.1.12)

2.2 The Hamiltonian and plaquette operators

The Hamiltonian we use is not the one suggested by Kitaev in [12], but was first suggested by Wen in [22]. Kitaev's and Wen's Hamiltonians alike have been shown to be exactly solvable on square lattices and the two models also correspond to one another on the honeycomb lattice, upon taking certain limits of the involved parameters [22, p. 2].

We denote the Hamiltonian by H_0, and defined it as

$$H_0 = -\sum_{p \in \mathrm{P}} O_p. \tag{2.2.1}$$

Each operator O_p, with the plaquette p defined by the sites $\{1,2,3,4\}$ arranged as

 , (2.2.2)

is a product over Pauli operators at the four sites:

$$O_p = \sigma_1^z \, \sigma_2^x \, \sigma_3^z \, \sigma_4^x. \tag{2.2.3}$$

We call O_p a *plaquette operator*. The order of operators in O_p does not matter because the Pauli operators involved all commute (see (A.1.1)). It is convenient to draw each plaquette operator as

$O_p =$  (2.2.4)

so that O_p describes a "circle" around the plaquette p.

It is easily checked (see equations (A.1.1) and (A.1.2)) that

$$(O_p)^2 = (\sigma_1^z\,\sigma_2^x\,\sigma_3^z\,\sigma_4^x)^2 = (\sigma_1^z)^2\;(\sigma_2^x)^2\;(\sigma_3^z)^2\;(\sigma_4^x)^2 = 1. \tag{2.2.5}$$

This tells us in particular that the eigenvalues of O_p are ± 1, and thus there exists a basis

$$\mathcal{B}_p = \left\{ |q_1 q_2 \cdots q_i \cdots q_{|\mathrm{P}|-1} q_{|\mathrm{P}|}\rangle \;\middle|\; q_i \in \{0,1\} \right\}. \tag{2.2.6}$$

of $\mathcal{H}$ where

$$O_p\,|q_1 \cdots q_{|\mathrm{P}|}\rangle = (-1)^{q_p}\,|q_1 \cdots q_{|\mathrm{P}|}\rangle\,, \qquad \forall p \in \mathrm{P}. \tag{2.2.7}$$

2.3 Strings and string operators

A *string* S is a collection of site crossings. Each crossing is represented by

$$\sigma_i^z = \tag{2.3.1}$$

$$\sigma_i^x = \tag{2.3.2}$$

$$\sigma_i^z\,\sigma_i^x = \tag{2.3.3}$$

or

$$\sigma_i^x\,\sigma_i^z = \tag{2.3.4}$$

The string is thus represented by a product of σ_z and/or σ_x operators, involving one or more sites. A plaquette operator is a string operator.

The strings are not oriented, that is, there is no direction that the string is going so there is no real distinction between a string entering or leaving a plaquette but for concreteness we will always say that a string is entering a plaquette to describe the situation. A plaquette that is entered by a string an odd number of times is called an *endpoint* of the string. An *open string* is a string that has one or more endpoints. On a compact surface an open string always has exactly two endpoints.

Example 2.2. As an illustration, the following open string has endpoints at the top and lower leftmost plaquettes:

$$\sigma_6^z\,\sigma_5^z\,\sigma_4^x\,\sigma_3^z\,\sigma_2^x\,\sigma_1^x = \tag{2.3.5}$$

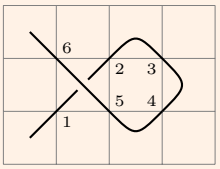

A *closed string* is a string without endpoints.

Example 2.3. The following picture shows an example of a closed string S:

$$\begin{aligned} S &= \sigma_8^z\,\sigma_7^x\,\sigma_6^z\,\sigma_5^z\,\sigma_4^x\,\sigma_3^z\,\sigma_2^x\,\sigma_1^x \\ &= (\sigma_8^z\,\sigma_1^x\,\sigma_6^z\,\sigma_7^x)\;(\sigma_5^z\,\sigma_4^x\,\sigma_3^z\,\sigma_2^x) \\ &= O_{p'}\,O_p = \end{aligned} \tag{2.3.6}$$

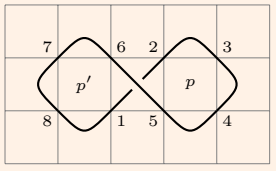

The example also demonstrates how the operators in S, since they commute, can be rearranged such that the string is simply a product of plaquette operators.

At any plaquette a string either continues into an adjacent plaquette or stops at an end point. In this sense strings are continuous. Since strings can only go from one plaquette to another diagonally, a string starting from an "odd" plaquette can never enter an "even" plaquette. Thus is makes sense to locally label the strings with two colors, say red and blue, leading to the notion of a *colored string*. *Locally* in this context means "somewhere inside the lattice, not crossing over any topological boundary conditions". We choose to color strings that only live on even plaquettes in red, and strings on odd plaquettes in blue. To help us keep track we also color the corresponding plaquettes.

For an $even \times even$ lattice on a torus, the strings are globally distinguishable: a red string can never enter a blue plaquette and vice versa, so in this case it makes sense to also globally color the plaquettes/strings. This distinction between strings is special for the $even \times even$ lattice on a torus.

Example 2.4. The coloring of plaquettes can be seen in the following open string examples:

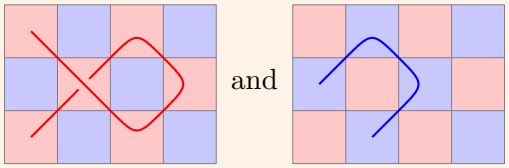
and

. (2.3.7)

2.4 Commutation relations of plaquette operators

If we consider the plaquette p as a set containing the 4 sites that define p then it is obvious that

$$[O_p, O_{p'}] = 0, \quad \text{if } p \cap p' = \emptyset, \tag{2.4.1}$$

that is; O_p and $O_{p'}$ commute if p and p' have zero sites of overlap. As for the possible cases with overlaps, let the plaquette p defined by the set $\{1, 2, 3, 4\}$ be neighbour to the plaquettes A,B,C,D,E,F,G and H according to

A	B	C
D	$\overset{4}{\underset{1}{p}}\ \overset{3}{\underset{2}{}}$	E
F	G	H

. (2.4.2)

The first case is when we have one site overlapping p, as with plaquettes A, C, F and H. Recall equation (2.2.3) so the two points 1 and 3 both correspond to a σ^z operator. Seeing that F and C overlaps with p only on this diagonal, the overlapping operators are of the type σ^z. Since σ^z commutes with itself, so we have

$$[O_p, O_C] = [O_p, O_F] = 0. \tag{2.4.3}$$

By the same reasoning, on the points 2 and 4 with the σ^x operator we get

$$[O_p, O_A] = [O_p, O_H] = 0. \tag{2.4.4}$$

As for the remaining plaquettes B, D, E and G, we have two sites of overlap, and these two are both mixed, that is, if a site has a σ^x from O_p then it has a σ^z from the overlapping plaquette, and vice versa. For example, take the product of O_p with O_D, denoting the two non-overlapping sites in D by the labels $i, j \notin p$:

$$\begin{aligned} O_p\, O_D &= \sigma_1^z\, \sigma_2^x\, \sigma_3^z\, \sigma_4^x\, \sigma_i^z\, \sigma_1^x\, \sigma_4^z\, \sigma_j^x \\ &= \sigma_i^z\, \sigma_j^x\, \sigma_1^z\, \sigma_1^x\, \sigma_4^x\, \sigma_4^z\, \sigma_2^x\, \sigma_3^z \\ &= \sigma_i^z\, \sigma_j^x\, (-\sigma_1^x\, \sigma_1^z)\, \sigma_4^x\, \sigma_4^z\, \sigma_2^x\, \sigma_3^z \\ &= \sigma_i^z\, \sigma_j^x\, (-\sigma_1^x\, \sigma_1^z)\, (-\sigma_4^z\, \sigma_4^x)\, \sigma_2^x\, \sigma_3^z \\ &= \sigma_i^z\, \sigma_1^x\, \sigma_4^z\, \sigma_j^x\, \sigma_1^z\, \sigma_2^x\, \sigma_3^z\, \sigma_4^x = O_D\, O_p. \end{aligned} \tag{2.4.5}$$

Reasoning in the same way, commutativity can also be shown for B, E and G. So indeed we have

$$\left[O_p, O_{p'}\right] = 0 \quad \forall p, p' \in \mathrm{P}. \tag{2.4.6}$$

Graphically, the commutation of plaquette operators can be expressed as the fact that two plaquette operators that overlap are either tangent to each other in one point or cross each other in exactly two points.

Example 2.5. Equation (2.4.7) illustrates a situation where O_A is tangent to O_p at site 4 and O_E crosses O_p at sites 2 and 3:

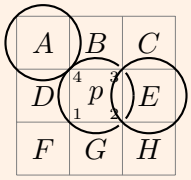

(2.4.7)

The commutation relations of plaquette operators can be generalized as follows:

Proposition 2.1. *In the graphical representation, if two string operators S_1 and S_2 cross paths orthogonally at an even number of sites, then*

$$[S_1, S_2] = 0. \tag{2.4.8}$$

2.5 Charges/excitations on plaquettes

By inspecting the Hamiltonian H_0 in (2.2.1) it is apparent that the lowest possible energy state, and thus the *ground state* is the state for which the plaquette operator O_p has the eigenvalue $+1$ for each p. Thus the state $|\Omega\rangle$ is a ground state if and only if

$$O_p\, |\Omega\rangle = |\Omega\rangle \quad \forall p \in \mathrm{P}. \tag{2.5.1}$$

Furthermore, since the operator O_p is associated with the plaquette p, it makes sense to say that if

$$O_p\, |\Omega\rangle = -\, |\Omega\rangle\,, \tag{2.5.2}$$

then there exists an excitation or a *charge* located on plaquette p. We have already agreed to color the plaquettes red and blue; now we may also make distinctions between the two different types of charges. If a charge is resident on a red (even) plaquette then we say that it is an *electric charge* and if a charge is resident on a blue (odd) plaquette then we say that it is a

magnetic charge. Electric and magnetic charges will be denoted by e and m respectively. From this point on we use interchangeably that

$$\text{even} = \text{red} = \text{electric}, \tag{2.5.3}$$

and

$$\text{odd} = \text{blue} = \text{magnetic}. \tag{2.5.4}$$

Charges can be created in pairs by the action of an open string operator. An open string operator with endpoints at plaquette p and p' creates charges on those plaquettes, which can be detected by the action of O_p and $O_{p'}$. This follows considering a string operator entering the plaquette q an even number of times has an even number of operators σ_i^z or σ_i^x which overlap the operators σ_i^x or σ_i^z in the corresponding plaquette operator O_q. Each pair of overlapping operators anti-commute and since there is an even number of them, the total resulting sign factor is $+1$. In other words, if S is an open string operator that runs through the plaquette q but does not have an endpoint in q, then

$$O_q S |\Omega\rangle = S O_q |\Omega\rangle = S |\Omega\rangle , \tag{2.5.5}$$

so that no charge is created on q by the action of S. On the other hand, a string operator entering a plaquette p an odd number of times will anti-commute in total with O_p, so if S is an open string operator that has an endpoint in the plaquette p then

$$O_p S |\Omega\rangle = -S O_p |\Omega\rangle = -S |\Omega\rangle , \tag{2.5.6}$$

so a charge is created on p by the action of S. Due to the fact that the eigenvalues of the plaquette operators O_p are ± 1, the charge is measured modulo 2. Thus the charge of the entire string S will always be neutral, since measuring the charge of one endpoint is "cancelled out" by the charge at the other endpoint. For the *even* $\times$ *even* lattice this also means that the total charge of all the electric plaquettes is neutral and the total charge of all magnetic plaquettes is neutral, individually, since any string is confined to either electric or magnetic plaquettes.

2.6 Fusion of charges

We can now, within the setting of this model, define a notion of *fusion product* of charges. Imagine that you want to measure the total charge of some region of the system. The fusion rules determine the possible outcomes of such a measurement from the local charges.

We indicate the fusion product of two charges a and b by $a * b$. We also introduce the symbol $\mathbf{1}$ indicating no charge, or an *invisible* charge.

To begin with, the fusion of an invisible charge and an electric charge is

$$\mathbf{1} * e = e * \mathbf{1} = e. \tag{2.6.1}$$

In a similar way, we get

$$m * \mathbf{1} = \mathbf{1} * m = m. \tag{2.6.2}$$

The fusion of electric and magnetic charges becomes something new, denote it by ϵ, so that we have

$$e * m = m * e = \epsilon, \tag{2.6.3}$$

and then we also get

$$\epsilon * \mathbf{1} = \mathbf{1} * \epsilon = \epsilon. \tag{2.6.4}$$

Thus ϵ corresponds to having "both electric and magnetic charge". Such a combination is sometimes called a "dyon" [7, p. 3489].

Measuring of charge can only have the outcome ± 1 due to the eigenvalues of the O_p-operators. Thus measuring two charges of the same type is the same as measuring no charge, so we also have

$$e * e = m * m = \epsilon * \epsilon = \mathbf{1}. \tag{2.6.5}$$

This also implies

$$e * \epsilon = \epsilon * e = m \tag{2.6.6}$$

and

$$m * \epsilon = \epsilon * m = e. \tag{2.6.7}$$

These fusion rules have a natural interpretation in the language of monoidal semisimple $\mathbb{C}$-linear categories

$$\mathcal{C} \equiv (\mathcal{C}, \otimes, \mathbf{1}), \tag{2.6.8}$$

where $\otimes$ is the tensor product functor and $\mathbf{1}$ is the tensor unit. The category in question has

$$\{\mathbf{1}, e, m, \epsilon\} \tag{2.6.9}$$

as representatives for the isomorphism classes of simple objects in $\mathcal{C}$. The tensor product functor is associative in the sense that for all simple objects x, y and z in $\mathcal{C}$ we have isomorphisms such that

$$(x \otimes y) \otimes z \cong x \otimes (y \otimes z)\,. \tag{2.6.10}$$

For all objects x in $\mathcal{C}$ there exists an isomorphisms such that

$$\mathbf{1} \otimes x \cong x \quad \text{and} \quad x \otimes \mathbf{1} \cong x. \tag{2.6.11}$$

Note that for what we are doing we do not need the actual isomorphisms, we only need their existence.

The fusion rules in (2.6.3) and (2.6.5) mean that there exist isomorphisms in $\mathcal{C}$ such that

$$e \otimes e \cong \mathbf{1}, \tag{2.6.12}$$

$$m \otimes m \cong \mathbf{1} \tag{2.6.13}$$

and

$$e \otimes m \cong m \otimes e \cong \epsilon. \tag{2.6.14}$$

Then it follows using (2.6.10) and (2.6.11) that

$$\epsilon \otimes \epsilon \cong \mathbf{1}, \tag{2.6.15}$$

$$\epsilon \otimes e \cong e \otimes \epsilon \cong m, \tag{2.6.16}$$

and

$$\epsilon \otimes m \cong m \otimes \epsilon \cong e. \tag{2.6.17}$$

2.7 Braiding of charges

In the context of monoidal categories, the possibility to change the order of operators σ_i^a amounts to a *braiding*. For each simple object x in $\mathcal{C}$ we denote by

$$\mathrm{id}_x : x \to x, \tag{2.7.1}$$

the identity morphism of x. We depict the identity morphisms as follows:

$\mathrm{id}_e =$, $\mathrm{id}_m =$, (2.7.2)

e m

and we denote the various braiding isomorphisms as

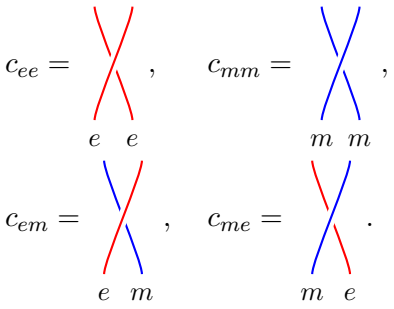

(2.7.3)

Here c_{12} indicates that the "world line" of object 1 crosses "over" the world line of object 2. We also have the inverse isomorphism denoted by c_{12}^{-1}, which indicate that the world line of object 1 crosses "under" the world line of object 2.

In c_{ee} from (2.7.3) we have $e \otimes e \to e \otimes e$, so, according to the fusion rule in equation (2.6.12), this is isomorphic to $1 \to 1$, which in turn is an isomorphism from a simple object to itself and therefore proportional to an identity isomorphism. Thus the morphism c_{ee} must be some number $R_{ee} \in \mathbb{C}$ times the identity isomorphism:

$$c_{ee} = R_{ee}\, \mathrm{id}_e \otimes \mathrm{id}_e. \tag{2.7.4}$$

Likewise we have

$$c_{mm} = R_{mm}\, \mathrm{id}_m \otimes \mathrm{id}_m. \tag{2.7.5}$$

In c_{em} and c_{me} from (2.7.3) we have the morphisms $e \otimes m \to m \otimes e$ and $m \otimes e \to e \otimes m$ which are again characterized by the numbers R_{me} and R_{em} respectively, since both $e \otimes m$ and $m \otimes e$ are isomorphic to the simple object ϵ. However, these numbers depend on a choice of basis in their respective isomorphism space. Even so, a basis independent number can be found characterizing the morphism

$c_{me}\, c_{em} =$

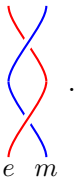

(2.7.6)

Here we have $e \otimes m \to e \otimes m$ which according to (2.6.14) is isomorphic to $\epsilon \to \epsilon$. Again we have an isomorphism from a simple object to itself, and thus

$$c_{me}\, c_{em} = (R_{me}\, R_{em})\ \mathrm{id}_e \otimes \mathrm{id}_m, \quad (R_{me}\, R_{em}) \in \mathbb{C}. \tag{2.7.7}$$

The numbers R_{ee}, R_{mm} and $R_{me}R_{em}$ are not arbitrary. Consider two open electric (or magnetic) strings crossing at plaquette p. These two strings have no common nodes and so they have no common Pauli operators. If we have strings entering a plaquette p through all 4 nodes it is therefore completely arbitrary in which order they cross, or indeed whether they cross at all, or simply "meet" inside the plaquette and go out again without crossing, as illustrated by

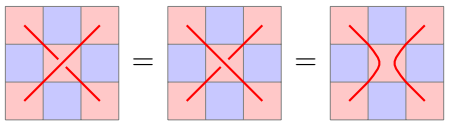

(2.7.8)

Thus we have

(2.7.9)

and

$$c_{mm} = \quad = \quad = \quad = R_{mm}\,\mathrm{id}_m \otimes \mathrm{id}_m \tag{2.7.10}$$

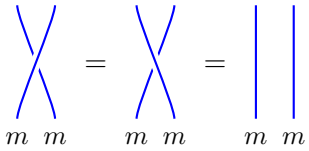

and so we get the two relations

$$R_{ee} = 1, \tag{2.7.11}$$

and

$$R_{mm} = 1. \tag{2.7.12}$$

This means that the self-braidings of both e and m are trivial.

Slightly less trivial is braiding an electric charge with a magnetic charge. If the strings cross at node i then we have either $\sigma_i^x\sigma_i^z$ or $\sigma_i^z\sigma_i^x$ depending on the order of the crossing. Since $\sigma_i^x\sigma_i^z = -\sigma_i^z\sigma_i^x$ we get

$$(R_{me}\,R_{em})\,\mathrm{id}_e \otimes \mathrm{id}_m = c_{me}\,c_{em} = \quad = - \quad = - \quad , \tag{2.7.13}$$

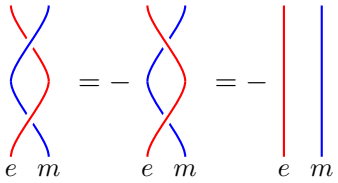

so that

$$R_{me}\,R_{em} = -1. \tag{2.7.14}$$

We can also determine the braiding of ϵ with ϵ, by considering

$$R_{\epsilon\epsilon}\,\mathrm{id}_\epsilon \otimes \mathrm{id}_\epsilon = c_{\epsilon\epsilon} = \quad = \quad = - \quad = - \quad , \tag{2.7.15}$$

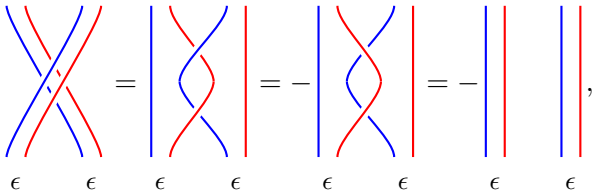

so we get

$$R_{\epsilon\epsilon} = -1. \tag{2.7.16}$$

Notably, the braiding rules are invariant to the outer automorphism

$$e \longleftrightarrow m \tag{2.7.17}$$

which exchanges e-charge with m-charge, a $\mathbb{Z}_2 \times \mathbb{Z}_2$ symmetry of the model. Such braiding symmetries are significant, and are sometimes referred to as *dualities*. This particular symmetry will be called the *e-m duality*.

2.8 Ground state degeneracy

Now we determine the degeneracy of the ground state $|\Omega\rangle$, that is, the dimension of the space of ground states $\{|\Omega\rangle\}$ that obey the constraints

$$O_p\,|\Omega\rangle = |\Omega\rangle\,, \quad \forall p \in \mathrm{P}. \tag{2.8.1}$$

The charges are always created in pairs, one at each end point of an open string, and thus we always have a globally neutral charge. For a lattice of even periods we can color the plaquettes

red and blue globally to indicate that red and blue strings are *distinguishable*. Global neutrality for red and blue independently can be expressed with the two equations

$$\prod_{p\in \mathrm{P}_e} O_p = 1 \tag{2.8.2}$$

and

$$\prod_{p\in \mathrm{P}_m} O_p = 1, \tag{2.8.3}$$

where P_e is the subset of P including only the electric plaquettes, and P_m is the subset of P including only the magnetic plaquettes, so that

$$\mathrm{P} = \mathrm{P}_e \cup \mathrm{P}_m \tag{2.8.4}$$

and

$$\mathrm{P}_e \cap \mathrm{P}_m = \emptyset. \tag{2.8.5}$$

From (2.1.3) we know that each site i contributes with dimension 2, and there are $|\mathrm{M}|$ sites in the lattice, which gives a total dimension of $2^{|\mathrm{M}|}$. Also, since each O_p has 2 different eigenvalues, -1 or 1, each independent constraint in (2.8.1) reduces the total number of ground states by a factor of 2. Having in mind equation (2.8.2), we can independently impose the constraint $O_p = 1$ for all electric plaquettes except for one. (Say we impose the constraints $O_p = 1$ for all $p \in \mathrm{P}_e$ except for p'. Then we have $\prod_{p\in \mathrm{P}_e, p\neq p'} O_p = 1$. But then if we multiply with $O_{p'}$ we get $O_{p'} \prod_{p\in \mathrm{P}_e, p\neq p'} O_p = \prod_{p\in \mathrm{P}_e} O_p$, but this is already known to be equal to 1 from equation (2.8.2). Thus we already know that $O_{p'} = 1$.) The same reasoning can be made with magnetic plaquette operators.

In summary, since the number of constraint equations in (2.8.1) is $|\mathrm{P}|$, we get $|\mathrm{P}| - 2$ independent constraints. Thus the ground state degeneracy for an *even* $\times$ *even* lattice with $|\mathrm{M}|$ sites and $|\mathrm{P}|$ plaquettes is

$$\bar{D}_\Omega = \frac{2^{|\mathrm{M}|}}{2^{|\mathrm{P}|-2}} = 2^{|\mathrm{M}|-|\mathrm{P}|+2}. \tag{2.8.6}$$

For a $L_x \times L_y$ lattice where at least one of L_x or L_y is odd we can no longer globally distinguish red plaquettes from blue ones. This means that in this case we do not have the two equalities (2.8.2) and (2.8.3) but instead we have only a single equality, namely

$$\prod_{p\in \mathrm{P}} O_p = 1. \tag{2.8.7}$$

The number of independent constraint equations are therefore $|\mathrm{P}| - 1$ and so the ground state degeneracy for a lattice with at least one period odd, with $|\mathrm{M}|$ sites and $|\mathrm{P}|$ plaquettes is

$$\tilde{D}_\Omega = \frac{2^{|\mathrm{M}|}}{2^{|\mathrm{P}|-1}} = 2^{|\mathrm{M}|-|\mathrm{P}|+1}. \tag{2.8.8}$$

2.9 Dislocations and *e-m* duality

Take an *even* $\times$ *even* lattice with a ground state degeneracy $\bar{D}_\Omega$ given by (2.8.6), and then remove a complete row of sites in one of the lattice directions. The resulting lattice is then an *odd* $\times$ *even* with a ground state degeneracy $\tilde{D}_\Omega$ given by (2.8.8). Recall that when the lattice is mapped to a torus, the numbers $|\mathrm{M}|$ and $|\mathrm{P}|$ are equal so, having this in mind, when comparing $\bar{D}_\Omega$ with $\tilde{D}_\Omega$ we conclude that the process of removing a row of sites changes the degeneracy.

This motivates us to consider *lattice dislocations* of the type illustrated by

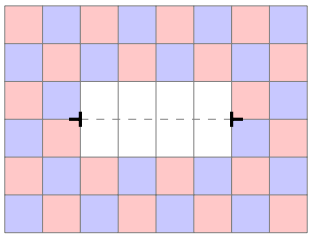

(2.9.1)

where the symbol ⊣ denotes dislocations with a dashed *defect line* or *branch cut* between them, denoted by $\mathcal{C}$. In the context of conformal field theory such dislocations are called "disorder fields" [9]. The new plaquettes, to be called *double plaquettes*, are colored in white. The reason for only considering a straight horizontal defect line and not a vertical or mixed one is that ultimately we should be able to identify these defect lines with real physical defects and since any continuous line can be made straight and horizontal in some specific local coordinates, they are locally equivalent.

In terms of operators it is now natural to introduce double plaquette operators. Let $\mathrm{P}_{\mathcal{C}} \subset \mathrm{P}$ be the set of all double plaquettes in the defect line and let $\partial\mathrm{P}_{\mathcal{C}} \subset \mathrm{P}_{\mathcal{C}}$ be the set of the two double plaquettes at the ends of the defect line. Then, similarly to what is suggested in [25, p. 3], there are two types of double plaquettes: those in the "interior" of the defect line have 4 vertices, those at the edges have 5 vertices. Accordingly the natural definition of plaquette operators is

$$P_q = \quad = \sigma_1^z\,\sigma_2^x\,\sigma_3^z\,\sigma_4^x \quad \text{for } q \in \mathrm{P}_{\mathcal{C}} \setminus \partial\mathrm{P}_{\mathcal{C}} \tag{2.9.2}$$

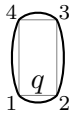

and the operators at the edges are defined for $q \in \partial\mathrm{P}_{\mathcal{C}}$ by

$$P_q = \mathrm{i}\quad = \mathrm{i}\,\sigma_1^z\,\sigma_2^x\,\sigma_3^z\,\sigma_4^x\,\sigma_5^z\sigma_5^x = \sigma_1^z\,\sigma_2^x\,\sigma_3^z\,\sigma_4^x\,\sigma_5^y \quad \text{(right dislocation)}, \tag{2.9.3}$$

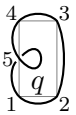

and

$$P_q = \mathrm{i}\quad = \mathrm{i}\,\sigma_1^z\,\sigma_2^x\,\sigma_3^z\,\sigma_4^x\,\sigma_5^z\sigma_5^x = \sigma_1^z\,\sigma_2^x\,\sigma_3^z\,\sigma_4^x\,\sigma_5^y \quad \text{(right dislocation)} \tag{2.9.4}$$

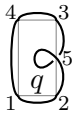

where the phase factor i is present to ensure that $P_q^2 = 1$ so that all plaquette operators still have eigenvalues ± 1. The latter are referred to as *pentagonal plaquette operators* since they involve 5 sites.

By the same kind of reasoning as the one leading to (2.4.7), we see that

$$[P_q, P_{q'}] = 0 \quad \text{for } q, q' \in \mathrm{P}_{\mathcal{C}}. \tag{2.9.5}$$

We can also see that

$$[O_p, P_q] = 0 \quad \text{for } p \in \mathrm{P} \setminus \mathrm{P}_{\mathcal{C}},\ q \in \mathrm{P}_{\mathcal{C}} \setminus \partial\mathrm{P}_{\mathcal{C}}. \tag{2.9.6}$$

Finally, we can check the remaining situation, which is shown in the following picture:

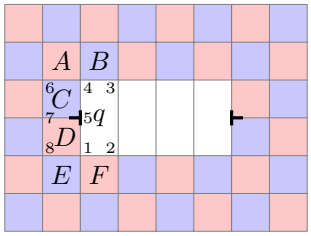

(2.9.7)

O_A and O_E commute with P_q because they are only tangent to P_q. Also, O_B and O_F commute with P_q because they cross at 2 sites. O_C and O_D also cross P_q at 2 sites, but on this side, P_q is different from the ordinary plaquette operators so we check this explicitly. We find

$$\begin{aligned} O_C\, P_q &= (\sigma_7^z\, \sigma_5^x\, \sigma_4^z\, \sigma_6^x)\, (\mathrm{i}\, \sigma_1^z\, \sigma_2^x\, \sigma_3^z\, \sigma_4^x\, \sigma_5^z\, \sigma_5^x) \\ &= \mathrm{i}\, \sigma_1^z\, \sigma_2^x\, \sigma_3^z\, \sigma_4^z\, \sigma_4^x\, \sigma_5^x\, \sigma_5^z\, \sigma_5^x \sigma_7^z\, \sigma_6^x \\ &= \mathrm{i}\, \sigma_1^z\, \sigma_2^x\, \sigma_3^z\, (-\sigma_4^x\, \sigma_4^z)\, (-\sigma_5^z\, \sigma_5^x)\, \sigma_5^x \sigma_7^z\, \sigma_6^x \\ &= (\mathrm{i}\, \sigma_1^z\, \sigma_2^x\, \sigma_3^z\, \sigma_4^x\, \sigma_5^z\, \sigma_5^x)\, (\sigma_7^z\, \sigma_5^x\, \sigma_4^z\, \sigma_6^x) = P_q\, O_C, \end{aligned} \tag{2.9.8}$$

and

$$\begin{aligned} O_D\, P_q &= (\sigma_8^z\, \sigma_1^x\, \sigma_5^z\, \sigma_7^x)\, (\mathrm{i}\, \sigma_1^z\, \sigma_2^x\, \sigma_3^z\, \sigma_4^x\, \sigma_5^z\, \sigma_5^x) \\ &= \mathrm{i}\, \sigma_2^x\, \sigma_3^z\, \sigma_4^x\, \sigma_1^x\, \sigma_1^z\, \sigma_5^z\, \sigma_5^z\, \sigma_5^x\, \sigma_8^z\, \sigma_7^x \\ &= \mathrm{i}\, \sigma_2^x\, \sigma_3^z\, \sigma_4^x\, (-\sigma_1^z\, \sigma_1^x)\, \sigma_5^z\, (-\sigma_5^x\, \sigma_5^z)\, \sigma_8^z\, \sigma_7^x \\ &= (\mathrm{i}\, \sigma_1^z\, \sigma_2^x\, \sigma_3^z\, \sigma_4^x\, \sigma_5^z\, \sigma_5^x)\, (\sigma_8^z\, \sigma_1^x\, \sigma_5^z\, \sigma_7^x) = P_q\, O_D. \end{aligned} \tag{2.9.9}$$

In summary, we have

$$[O_p, P_q] = 0 \quad \forall\, p \in \mathrm{P} \setminus \mathrm{P}_{\mathcal{C}},\, \forall q \in \mathrm{P}_{\mathcal{C}}. \tag{2.9.10}$$

The Hamiltonian that is naturally associated with the new set of commuting plaquette operators is

$$H_0^{\mathcal{C}} = -\sum_{p \in \mathrm{P} \setminus \mathrm{P}_{\mathcal{C}}} O_p - \sum_{q \in \mathrm{P}_{\mathcal{C}}} P_q. \tag{2.9.11}$$

So the new constraints on the ground state are

$$O_p = 1 \quad \forall p \in \mathrm{P} \setminus \mathrm{P}_{\mathcal{C}} \tag{2.9.12}$$

and

$$P_q = 1 \quad \forall q \in \mathrm{P}_{\mathcal{C}}, \tag{2.9.13}$$

a total of $|\mathrm{P}|$ equations.

The double plaquettes can be used to measure charge modulo 2 as with the original plaquette operators. Following the rule that a string must continue by entering a diagonally adjacent plaquette, it follows that an open string S commutes with all P_q in $\mathrm{P}_{\mathcal{C}}$.

Example 2.6. The following picture shows an open string S crossing a defect line:

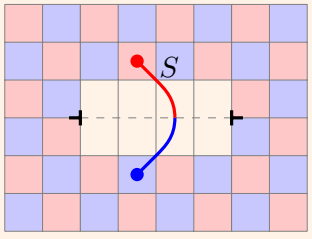

(2.9.14)

Example 2.6 shows that the defect line realizes the *e-m* duality. Passing through it changes an electric charge into a magnetic charge and thus the plaquettes/charges are again indistinguishable, just as after a full row dislocation. In particular we can no longer require the electric and magnetic plaquettes to be neutral independently.

Adding a pair of dislocations to the lattice is a process involving removing sites and plaquettes. Thereby the numbers $|\mathrm{M}|$ and $|\mathrm{P}|$ will change. Since the number $|\mathrm{M}| - |\mathrm{P}|$ then also might

change, and since it has been shown in (2.8.6) to be an important number for the ground state degeneracy, we separately introduce the quantity

$$\Lambda := (|\mathrm{M}| - |\mathrm{P}|)_{\text{no dislocations}}\,. \tag{2.9.15}$$

Automatically, this quantity is a constant through the processes we have considered. We also introduce the new notation $\bar{D}^n_\Omega$ denoting the ground state degeneracy of an *even* $\times$ *even* lattice with n pair(s) of dislocations. Then from equation (2.8.6) we see that

$$\bar{D}^0_\Omega = \bar{D}_\Omega = 2^{\Lambda+2}. \tag{2.9.16}$$

If we remove k sites, then we also remove $2(k+1)$ plaquettes. In replacement we obtain $(k+1)$ double plaquettes, so a net loss of k sites results in a net loss of $k+1$ plaquettes, and thus after the process we end up with $|\mathrm{M}| - |\mathrm{P}| = \Lambda + 1$.

Since charges are now indistinguishable, this in turn means that there are $|\mathrm{P}|-1$ independent constraint equations on the ground state space. Before the defect we had $|\mathrm{P}| - 2$ independent constraints, so this number increases by 1.

Proposition 2.2. *The degeneracy of the ground state does not change when adding one pair of defects to an even* $\times$ *even lattice.*

Adding a pair of dislocations to an *odd* $\times$ *even* lattice, however, will increase the degeneracy by a factor of 2, since now $|\mathrm{M}| - |\mathrm{P}| = \Lambda + 1$ but we have $|\mathrm{P}| - 1$ independent constraints both before and after. This means that, starting with an *even* $\times$ *even* lattice, first removing a complete row, as in the introductory example of this section, and then adding a pair of dislocations amounts to the same degeneracy as only adding one pair of dislocations to the lattice directly.

Topologically we may look at the *even* $\times$ *even* situation in the following way, as suggested in [26, p. 3]: On a torus with an *even* $\times$ *even* lattice, the electric and magnetic strings are distinguishable, as if they were defined on two separate layers of the torus. Each of these has $\frac{|\mathrm{M}|}{2}$ sites, $\frac{|\mathrm{P}|}{2}$ plaquettes and $\frac{|\mathrm{P}|}{2}+1$ independent constraint equations. We can thus view the topological space as two disjoint tori, each with a ground state degeneracy of

$$D_1 = D_2 = 2^{\frac{|\mathrm{M}|-|\mathrm{P}|}{2}+1}, \tag{2.9.17}$$

so that the total degeneracy becomes

$$\bar{D}^0_\Omega = D_1 D_2 = \left(2^{\frac{|\mathrm{M}|-|\mathrm{P}|}{2}+1}\right)\left(2^{\frac{|\mathrm{M}|-|\mathrm{P}|}{2}+1}\right) = 2^{|\mathrm{M}|-|\mathrm{P}|+2}. \tag{2.9.18}$$

Adding a pair of dislocations thus connects the two layers and the topological space can be glued together in the form of a "double torus" as prescribed in [26, p. 3], with unchanged ground state degeneracy.

For each additional pair of dislocations, however, $|\mathrm{M}| - |\mathrm{P}|$ increases by 1, but there is no longer any *even* $\times$ *even* effect to be broken. Adding n pairs of dislocations results in $|\mathrm{M}| - |\mathrm{P}| = \Lambda + n$. Also, when we start with a lattice defined on a torus in the way prescribed in connection to Example (2.1.2), we start with $|\mathrm{M}| = |\mathrm{P}|$ so $\Lambda = 0$. In summary we have the following theorems:

Theorem 2.3. *(i) For an even* $\times$ *even lattice with periodic boundary conditions and with* n *pairs of e-m duality dislocations, the ground state degeneracy is given by*

$$\bar{D}^n_\Omega = \begin{cases} 2^2 & \text{for } n = 0, \\ 2^{n+1} & \text{for } n = 1, 2, \ldots \end{cases} \tag{2.9.19}$$

(ii) For a lattice with at least one odd period and with periodic boundary conditions, adding n pairs of e-m duality dislocations results in the ground state degeneracy

$$\tilde{D}_{\Omega}^{n} = 2^{n+1} \quad \text{for } n = 0, 1, ... \tag{2.9.20}$$

For $n \geq 2$, adding another pair of dislocations increases the ground state degeneracy by a factor of 2. Therefore we can say, formally, that to each *e-m* duality dislocation we can attribute a quantum dimension $\sqrt{2}$.

2.10 A basis for the space of ground states without dislocations

Now that we have calculated the ground state degeneracy, we also want to be able to give a convenient orthogonal basis for the space of ground states. We know that all closed strings, or *loops*, commute with the Hamiltonian and thus leave the system in the ground state. The question is, is the system left in the same ground state or does it change, and if so, what operators leave the state invariant and which operators can be used to transform one ground state into another? From (2.9.19) we see that the degeneracy for an *even* $\times$ *even* lattice on a torus without defects is 4, so we need to find 4 mutually orthogonal basis states that are all ground states.

In the mathematical language of topology, a *contractible loop* is a loop that can be continuously deformed to a point. As we shall see, in this model the notion of a contractible loop means any closed string that is equal to a product of plaquette operators, and thus can be "contracted" and annihilated with plaquette operators only.

Proposition 2.4. *A closed string that can be expressed in terms of a product of plaquette operators is a contractible loop. In particular, if ∂L is the operator representing an electric (magnetic) loop enclosing the area L on the lattice then*

$$\partial L = \prod_{p \in L_{m(e)}} O_p, \tag{2.10.1}$$

where $L_{m(e)}$ denotes the set of all magnetic (electric) plaquettes in the area L.

Example 2.7. Locally a loop is always confined to either blue or red plaquettes. A blue loop that encompasses n red plaquettes is always tangent to $1, 2, 3$ or 4 sites of some specific red plaquette. By operating on the loop with the corresponding plaquette operator, which is a closed blue string encircling the red plaquette, we can "shrink" the loop, meaning that we can make it encompass $n - 1$ red plaquettes. An example is indicated in the following picture:

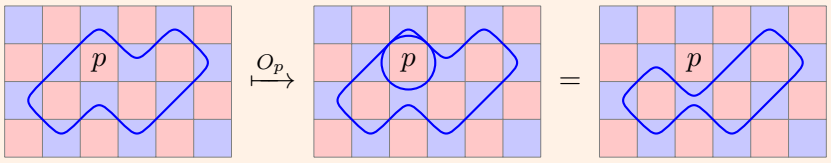

(2.10.2)

This process of deformation can be continued until the loop encompasses only a single red plaquette, in which case it is given by a single plaquette operator. This operator in turn annihilates the loop completely, so that it is fully contracted.

To understand why this new notion is important we need to look at the ground state. Any ground state of a system without defects can be written as

$$|\Omega\rangle = \prod_{p \in \mathrm{P}} (\mathbf{1} + O_p) \, |\omega\rangle \,, \tag{2.10.3}$$

where

$$\mathbf{1} := \mathbf{1}_1 \otimes \mathbf{1}_2 \otimes \cdots \otimes \mathbf{1}_i \otimes \cdots \otimes \mathbf{1}_{|\mathrm{M}|-1} \otimes \mathbf{1}_{|\mathrm{M}|} \tag{2.10.4}$$

and $|\omega\rangle$ is an arbitrary linear combination of states from the basis $\mathcal{B}_s$ in equation (2.1.7). The ground state is thus a superposition of $|\omega\rangle$, $O_1 |\omega\rangle$, $O_1 O_2 |\omega\rangle$ and so on, including all $2^{|\mathrm{P}|}$ possible ordered products between plaquette operators and the identity operator. To prove that (2.10.3) is indeed a ground state, consider

$$O_{p'} |\Omega\rangle = O_{p'} \prod_{p\in\mathrm{P}} (\mathbf{1} + O_p) |\omega\rangle \,. \tag{2.10.5}$$

Since $O_{p'}$ commutes with all O_p we get

$$\begin{aligned} O_{p'} |\Omega\rangle &= O_{p'} \prod_{p\in\mathrm{P}} (\mathbf{1} + O_p) |\omega\rangle = O_{p'} (\mathbf{1} + O_{p'}) \prod_{\substack{p\in\mathrm{P} \\ p\neq p'}} (\mathbf{1} + O_p) \\ &= (O_{p'}\mathbf{1} + O_{p'} O_{p'}) \prod_{\substack{p\in\mathrm{P} \\ p\neq p'}} (\mathbf{1} + O_p) \\ &= (O_{p'} + \mathbf{1}) \prod_{\substack{p\in\mathrm{P} \\ p\neq p'}} (\mathbf{1} + O_p) = \prod_{p\in\mathrm{P}} (\mathbf{1} + O_p) |\omega\rangle = |\Omega\rangle \,. \end{aligned} \tag{2.10.6}$$

This holds for all p', so

$$O_p |\Omega\rangle = |\Omega\rangle \quad \forall p \in \mathrm{P}, \tag{2.10.7}$$

and thus, by comparison with (2.5.1), $|\Omega\rangle$ as given by (2.10.3) is a ground state. From (2.10.6) we see that actually

$$O_{p'} \prod_{p\in\mathrm{P}} (\mathbf{1} + O_p) = \prod_{p\in\mathrm{P}} (\mathbf{1} + O_p) \quad \forall =_{p'} \in \mathrm{P}, \tag{2.10.8}$$

so

$$H \prod_{p\in\mathrm{P}} (\mathbf{1} + O_p) = -\sum_{p'\in\mathrm{P}} O_{p'} \prod_{p\in\mathrm{P}} (\mathbf{1} + O_p) = -|\mathrm{P}| \prod_{p\in\mathrm{P}} (\mathbf{1} + O_p) \,. \tag{2.10.9}$$

The operation on $|\Omega\rangle$ with any contractible loops never "touches" the state $|\omega\rangle$ but leaves the system in the state $|\Omega\rangle$. The different degenerate ground states must therefore depend on the choice of $|\omega\rangle$, and the different orthogonal choices must be obtainable from one another by some set of operators that commute with the Hamiltonian but cannot be written as a product of plaquette operators. The only operators that commute with all plaquette operators and thus with the Hamiltonian are loop operators, and since contractible loops are products of plaquette operators, these operators must be non-contractible loops.

Searching for the proper set of operators and orthogonal basis states follows the following steps:

1. Choose one non-contractible loop L_1 acting on $|\omega\rangle$ such that $L_1 |\omega\rangle$ is orthogonal to $|\omega\rangle$.

2. Choose a second non-contractible loop L_2 such that $L_2 |\omega\rangle$ is orthogonal to $|\omega\rangle$.

3. Confirm that $L_1 |\omega\rangle$ is orthogonal to $L_2 |\omega\rangle$. This can in particular be done by checking that L_1 can not be contracted to L_2, which means that no operator $\mathcal{Q}$ exists such that $L_1 = \mathcal{Q} L_2$, where $\mathcal{Q}$ is any product of plaquette operators.

4. The above steps imply that the operator $L_1 L_2$ is also a non-contractible loop satisfying the above conditions.

We may now search for the relevant set of operators with the aid of the graphical representation. Without loss of generality we choose

$$|\omega\rangle = |\, \underbrace{0 \cdots 0}_{|M| \text{ times}} \,\rangle \,, \tag{2.10.10}$$

from the basis $\mathcal{B}_s$ in equation (2.1.7). This choice of $|\omega\rangle$ is made to simplify the following considerations. Another choice could make the arguments very different but the end result would be the same.

First note that for any set of sites $\mathrm{I} \subset \mathrm{M}$ we have

$$\prod_{i\in \mathrm{I}} \sigma_i^x |\omega\rangle = \prod_{i\in \mathrm{I}} \sigma_i^x |0\,0\,\cdots 0\,0\rangle = |0\,0\,\cdots 0\,0\rangle = |\omega\rangle\,. \tag{2.10.11}$$

Apparently, any action by σ^x operators leaves $|\omega\rangle$ unchanged. Therefore a non-contractible loop operator that can be written as a product of σ^x can not produce a state orthogonal to $|\omega\rangle$. We will call a loop that is isomorphic to such a diagonal by the operation of plaquette operators a *backslash loop*. The corresponding operator is called a backslash loop operator.

Graphically, (2.1.5) is represented by the symbol $\not|$. A pair of σ^x operators can be created on the top left and lower right corners of the plaquette p by operation with O_p. If a pair already resides on the corners of p they are annihilated and if only one corner is occupied the action of σ^x is "moved" to the opposing corner. Thus O_p can either add two, remove two or move one, so that any combination of plaquette operators can only change the total number of σ^x operators by an even number. The "movement" of any such operator is confined to the top/left to bottom/right diagonal that it is on.

First we consider the *even* $\times$ *even* case. Since there are a number of complicating factors to consider, we first try to decompose the problem into smaller constituents.

We want to see how many independent top/left to bottom/right diagonals are created by imposing the periodic boundary conditions which give rise to the torus. As we shall see later, this is related to the number of independent diagonals there are on square lattices. On a square lattice with $n \times n$ sites/plaquettes there are n such independent diagonals.

Example 2.8. As an illustration of independent diagonals, consider the following example which shows the four diagonals (two blue and two red) of a 4×4 lattice:

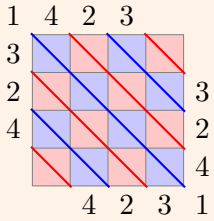

(2.10.12)

With plaquette operators, we can move, create and annihilate $\not|$ operators along every such diagonal, but we can only create or annihilate them in pairs, which as we shall later see is an important fact.

Now consider the 4 types of loops that can be defined on a square lattice, labelled by E_x, M_x, E_y and M_y, meaning electric and magnetic loops going from boundary to boundary in the x- and y-direction, respectively, as shown in the following picture:

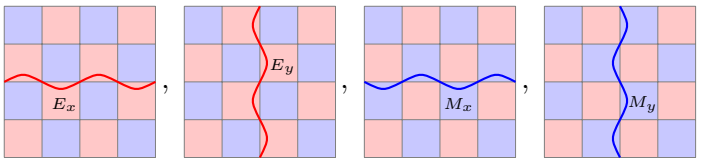

(2.10.13)

All such loops can be deformed by plaquette operators but since they must connect at the boundaries at the corresponding sites, they must have an even number of $\not|$ and $\not\backslash$-operators

independently; thus each operator really represents a class of operators. As we said before, the ⧸ are the important ones, and these can be moved along a diagonal by operating with the proper choice of O_p. The ⧸ operator created by the magnetic loops can be moved by using plaquette operators encircling red plaquettes and the ones created by the electric loops can be moved by using operators encircling blue plaquettes. If a pair of ⧸ operators are on the same diagonal then they can be moved together, which annihilates them. It is however clear by inspection of (2.10.13) that the ⧸ operators are all on different diagonals in all 4 cases, which means that a state produced by operation on $|\omega\rangle$ with any of E_x, M_x, E_y or M_y can not be produced in the same way by contractible loop operators. Thus E_x, M_x, E_y or M_y are all non-contractible loops, which makes them candidates for creating a complete set of basis states for the ground state.

Even though for instance M_x and M_y are topologically distinct loops, they can still be deformed to produce the same state. Consider the following operation:

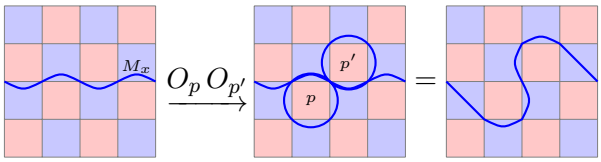

(2.10.14)

Having in mind that only the operator σ^z changes the state of $|\omega\rangle$, now compare the positions of the ⧸ operators with the loop M_y from equation (2.10.13) to see that $M_y\,|\omega\rangle$ and $O_pO_{p'}M_x\,|\omega\rangle$ are in fact the same state. We also see that M_xM_y is a backslash loop operator. The same is true for E_x and E_y, so for a square lattice we must choose one electric and one magnetic non-contractible loop when trying to produce an orthogonal basis for the ground state.

The boundary conditions of an arbitrary lattice of dimension $L_x \times L_y$ can be reconstructed by taking one square lattice, hereby referred to as the *primary lattice*, and placing copies of this lattice in rows and columns according to a *secondary lattice*. The primary lattice is the square lattice of size

$$\gcd(L_x, L_y) \times \gcd(L_x, L_y), \tag{2.10.15}$$

where $\gcd(\,,\,)$ denotes the greatest common divisor, and the secondary lattice is then of size

$$\frac{L_x}{\gcd(L_x, L_y)} \times \frac{L_y}{\gcd(L_x, L_y)}. \tag{2.10.16}$$

Since the boundary conditions of the primary lattice are repeated along the secondary lattice, the original lattice has the same number of independent diagonals as the primary lattice, namely $\gcd(L_x, L_y)$.

Example 2.9. A lattice with size 9×6 has $\gcd(9, 6) = 3$ and thus the primary lattice is 3×3, and the secondary lattice is 3×2. The 9×6 lattice thus has 3 independent diagonals.

We are considering the case that the original lattice is *even* $\times$ *even*, which means that $\gcd(L_x, L_y)$ must be even, so that we have a primary lattice that is even and square, as in the above example. For one such lattice we know that E_x, M_x, E_y and M_y are all non-contractible. But what happens when placing two such lattices next to each other?

Example 2.10. Take E_x on an 8×4 lattice for example:

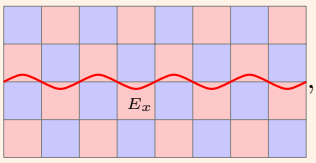

(2.10.17)

Now we actually have two $\not$ operators on each blue diagonal instead of one. They can be brought together for annihilation by two diagonal chains of plaquette operators:

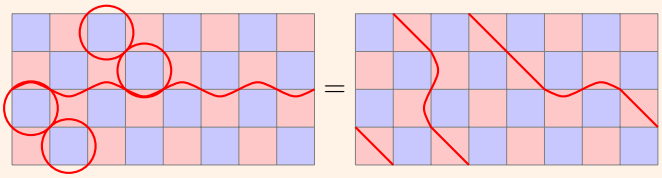

(2.10.18)

and

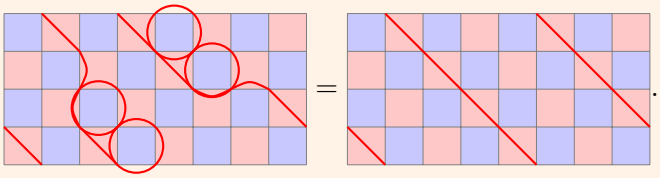

(2.10.19)

So in this case E_x is a backslash loop operator.

Proposition 2.5. *For loops defined on an even $\times$ even lattice we have the following:*

(i) A loop that crosses the boundaries in a direction in which the secondary lattice is even is backslash loop.

(ii) A loop that crosses the boundaries in a direction in which the secondary lattice is odd is not a backslash loop.

Since $\gcd(L_x, L_y)$ is even, we must have "divided out" all prime factors 2 from at least one of L_x and L_y when obtaining the periods of the secondary lattice, and thus we also have the following:

Proposition 2.6. *For any even lattice, the secondary lattice has at least one odd period.*

The above statements guarantee that we can find a non-contractible loop in at least one of the directions, when the lattice is even, and that we should take the direction in which the secondary lattice is odd.

If only one period of the secondary lattice is odd, then the E- and M-loops in the even direction cannot produce a state orthogonal to $|\omega\rangle$. It is however also true that both of the E- and M-loops in the odd direction can achieve this, and since electric strings are distinct from magnetic ones, we also know that these two loops produce states that are orthogonal to each other, and the state given by the combination of the two is then orthogonal to the other three states as well.

In the case that both periods of the secondary lattice are odd, $E_x|\omega\rangle$ and $E_y|\omega\rangle$ are both orthogonal to $|\omega\rangle$ but, as we saw before, in this case the loops E_xE_y and M_xM_y are backslash loop operators so we cannot use those combinations. In this case we must choose a combination of one electric and one magnetic loop, and the directions do not matter.

In all cases of an *even* $\times$ *even* lattice we can see that exactly two of the loops produce mutually orthogonal states and thus there are exactly four orthogonal basis states. This result is consistent with equation (2.9.19) which predicts that the ground state degeneracy is 4 for an *even* $\times$ *even* lattice on a torus without defects.

Theorem 2.7. *For an even × even lattice with a secondary lattice with an odd period in the x-direction we can choose an orthogonal basis for the ground state as*

$$\{|\omega\rangle, E_x|\omega\rangle, M_x|\omega\rangle, E_x M_x|\omega\rangle\}, \tag{2.10.20}$$

where

$$|\omega\rangle = |\underbrace{0\cdots 0}_{|M| \text{ times}}\rangle, \tag{2.10.21}$$

chosen from the basis $\mathcal{B}_s$ in equation (2.1.7).

Since it is arbitrary which direction we call the x-direction, Theorem 2.7 is completely general for all even lattices.

It is possible to show with similar arguments that for an *odd* × *odd* or *odd* × *even* lattice it is only possible to choose one independent non-contractible loop C_x and that this loop can always be chosen to be in a direction which the lattice is odd. The ground state basis for an *odd* × *odd* or *odd* × *even* lattice can thus be chosen as

$$\{|\omega\rangle, C_x|\omega\rangle\}, \tag{2.10.22}$$

where

$$|\omega\rangle = |\underbrace{0\cdots 0}_{|M| \text{ times}}\rangle, \tag{2.10.23}$$

chosen from the basis $\mathcal{B}_s$.

2.11 A concrete example – a 2 × 2 site $\mathbb{Z}_2$ lattice model

Now that we have developed the $\mathbb{Z}_2$ toric plaquette model thoroughly it could be nice to see an example before moving on to investigating the defects further.

Example 2.11. Consider the system of 4 sites in a 2 × 2 lattice with periodic boundary conditions:

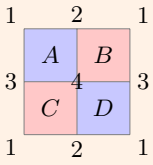

(2.11.1)

This system has 4 plaquette operators defined by

$$\begin{aligned} O_A &= \sigma_3^z \sigma_4^x \sigma_2^z \sigma_1^x, \quad O_B = \sigma_4^z \sigma_3^x \sigma_1^z \sigma_2^x, \\ O_C &= \sigma_1^z \sigma_2^x \sigma_4^z \sigma_3^x, \quad O_D = \sigma_2^z \sigma_1^x \sigma_3^z \sigma_4^x. \end{aligned} \tag{2.11.2}$$

Since Pauli operators on different sites commute, we really only have 2 independent plaquette operators, which we name O_m and O_e, defined by

$$O_m := O_A = O_D, \tag{2.11.3}$$

and

$$O_e := O_B = O_C. \tag{2.11.4}$$

The Hamiltonian is

$$H = -\sum_{p \in \mathrm{P}} O_p = -2(O_m + O_e) \tag{2.11.5}$$

and a system state basis is

$$\mathcal{B}_p = \{|q_1\, q_2\, q_3\, q_4\rangle \;\mid\; q_i \in \{0,1\}\}\,. \tag{2.11.6}$$

The ground state is given by

$$\begin{aligned} |\Omega\rangle &= \prod_{p\in \mathrm{P}} (\mathbf{1}+O_p)\,|\omega\rangle = (\mathbf{1}+O_m)^2\,(\mathbf{1}+O_e)^2\,|\omega\rangle \\ &= 4\,(\mathbf{1}+O_m)\,(\mathbf{1}+O_e)\,|\omega\rangle = 4\,(\mathbf{1}+O_m+O_e+O_mO_e)\,|\omega\rangle\,. \end{aligned} \tag{2.11.7}$$

We choose

$$|\omega\rangle = |0000\rangle \tag{2.11.8}$$

so that

$$O_m\,|\omega\rangle = O_m\,|0000\rangle = \sigma_1^x\sigma_2^z\sigma_3^z\sigma_4^x\,|0000\rangle = |1001\rangle\,, \tag{2.11.9}$$

$$O_e\,|\omega\rangle = O_e\,|0000\rangle = \sigma_1^z\sigma_2^x\sigma_3^x\sigma_4^z\,|0000\rangle = |0110\rangle \tag{2.11.10}$$

and

$$O_mO_e\,|\omega\rangle = O_mO_e\,|0000\rangle = |1111\rangle\,. \tag{2.11.11}$$

Now we can write the (unnormalized) ground state explicitly as

$$|\Omega\rangle = 4\,(|0000\rangle + |1001\rangle + |0110\rangle + |1111\rangle)\,. \tag{2.11.12}$$

We see that this state spans 1/4 of the full system state space, as was expected.

The lattice (2.11.1) is square and even, so according to (2.10.16) the secondary lattice is 1×1. According to Proposition 2.5 we can thus find non-contractible loops that are not backslash loops in any direction of the lattice. Furthermore, according to Theorem 2.7 we need one electric and one magnetic loop, and we choose

$$E_x = \sigma_3^z\sigma_4^x = $$ 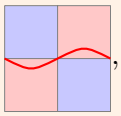 , (2.11.13)

$$M_x = \sigma_3^x\sigma_4^z = $$ 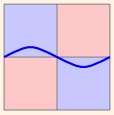 (2.11.14)

and the combination

$$E_xM_x = \sigma_3^z\sigma_3^x\sigma_4^x\sigma_4^z = $$ 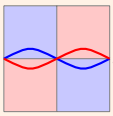 . (2.11.15)

We see that

$$E_xO_e = \sigma_3^z\sigma_4^x\sigma_3^z\sigma_4^x\sigma_2^z\sigma_1^x = \sigma_3^z\sigma_4^x\sigma_2^z\sigma_1^x\sigma_3^z\sigma_4^x = O_eE_x, \tag{2.11.16}$$

$$E_xO_m = \sigma_3^z\sigma_4^x\sigma_4^z\sigma_3^x\sigma_1^z\sigma_2^x = -\sigma_3^z\sigma_4^z\sigma_3^x\sigma_1^z\sigma_2^x\sigma_4^x = \sigma_4^z\sigma_3^x\sigma_1^z\sigma_2^x\sigma_3^z\sigma_4^x = O_mE_x, \tag{2.11.17}$$

$$M_xO_e = \sigma_3^x\sigma_4^z\sigma_3^z\sigma_4^x\sigma_2^z\sigma_1^x = -\sigma_3^x\sigma_3^z\sigma_4^x\sigma_2^z\sigma_1^x\sigma_4^z = \sigma_3^z\sigma_4^x\sigma_2^z\sigma_1^x\sigma_3^x\sigma_4^z = O_eM_x \tag{2.11.18}$$

and

$$M_xO_m = \sigma_3^x\sigma_4^z\sigma_4^z\sigma_3^x\sigma_1^z\sigma_2^x = \sigma_4^z\sigma_3^x\sigma_1^z\sigma_2^x\sigma_3^x\sigma_4^z = O_mM_x, \tag{2.11.19}$$

which confirms that they all commute with the plaquette operators, which in turn means that they are loops. Moreover, they can not be constructed by plaquette operators, which means they are non-contractible loops. We get

$$E_x\,|0000\rangle = \sigma_3^z\sigma_4^x\,|0000\rangle = |0001\rangle\,, \tag{2.11.20}$$

$$M_x \left|0000\right\rangle = \sigma_3^x \sigma_4^z \left|0000\right\rangle = \left|0010\right\rangle \tag{2.11.21}$$

and

$$E_x M_x \left|0000\right\rangle = \sigma_3^z \sigma_4^x \sigma_3^x \sigma_4^z \left|0000\right\rangle = \left|0011\right\rangle, \tag{2.11.22}$$

which are all orthogonal to the state (2.11.12), and to each other. Thus we have found our set of mutually orthogonal states. The 4 different ground states are explicitly given by

$$\begin{gathered} 4\left(\left|0000\right\rangle + \left|1001\right\rangle + \left|0110\right\rangle + \left|1111\right\rangle\right), \\ 4\left(\left|0001\right\rangle + \left|1000\right\rangle + \left|0111\right\rangle + \left|1110\right\rangle\right), \\ 4\left(\left|0010\right\rangle + \left|1011\right\rangle + \left|0100\right\rangle + \left|1101\right\rangle\right), \\ \text{and} \\ 4\left(\left|0011\right\rangle + \left|1010\right\rangle + \left|0101\right\rangle + \left|1100\right\rangle\right). \end{gathered} \tag{2.11.23}$$

2.12 A basis for the ground state space with *e-m* duality dislocations

In previous sections we have seen that the lattice dimensions L_x and L_y, and specifically if they are odd or even has an effect on the ground state degeneracy. We also saw that we can find a set of non-contractible loop-operators that form an algebra so that the irreducible representation space of the algebra spans the space of ground states.

In (2.9.20) and (2.9.19) we see that the number of pairs of dislocations also has effect on the ground state degeneracy. In particular, for $n \geq 2$ pairs of dislocations, the degeneracy is increased by a factor of 2^{n-1}. Adding one pair of dislocations does not alter the ground state degeneracy for an *even* $\times$ *even* lattice. For two pairs of dislocations, however, the degeneracy is changed from 4 to 8, and thus we need to extend the algebra by adding new generators. We do this by adding two new non-contractible loops to the old ones, so that we can again form an algebra whose irreducible representation space spans the space of ground states.

The dislocations that we have considered can be compared to the "twist defects" in [2] for which it is stated that for $n \geq 1$ pair(s) of dislocations it is possible to choose $2(n-1)$ distinct non-contractible loops such that every loop only crosses one other loop once and none of the others. We choose these loops in accordance with the homology basis from [25, p. 4, fig. 3] developed for the $\mathbb{Z}_N$ model in [5], the main difference here being that since we are dealing with the $\mathbb{Z}_2$ model, the loops are not oriented. It should also be pointed out that this is an arbitrary choice and that there are many equivalent choices of loops.

The process for choosing loops for each added pair of dislocations is:

1. Add one loop that goes through the defect line between the new pair and the defect line of the first pair.

2. Add one loop encircling the new pair.

The graphical representation of the system state has up until now included lattice sites, plaquettes, dislocations and colored strings. We now want to represent different ground states graphically. Any ground state is a superposition of all possible "deformations" of some initial state $\left|\omega\right\rangle$, that can be made by plaquette operators. This means that the precise lattice structure is no longer important when it comes to distinguish different ground states, but only the class of the non-contractible loop(s) of the initial state $\left|\omega\right\rangle$. The quantities that matter now are thus:

1. The number of dislocation pairs.

2. The number and type of non-contractible loops around the dislocations.

3. The different coloring of the loops that may arise from crossing a defect line.

Example 2.12. The following figure illustrates two pairs of dislocations with non-contractible loops to label the additional degenerate ground states induced by the presence of the dislocations:

(2.12.1)

As shown in Example 2.12, a cross now indicates a dislocation and the dashed line indicates the defect line. We henceforth refer to this new picture as the continuous picture or the *macroscopic picture*, and the previous one as the *microscopic picture*. These new loops used in combination with the previous loops labelling the different ground states then form a complete basis for the ground state with two pairs of defects.

Example 2.13. To illustrate the process further, when adding a third pair of dislocations ($n = 3$) we choose the $2(3-1) = 4$ loops as shown by

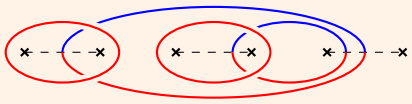

(2.12.2)

in combination with the loops already found labelling the four original ground states.

In terms of operators, for n pairs of defects lined up in a horizontal row and numbered increasingly from left to right. Defect lines expand between every odd defect and the right adjacent even defect. Let $\mathcal{O}_{ij}$ denote the non-contractible loop that encircles the defects i and j as well as all defects k, where $i < j$ and $i < k < j$. Then we choose non-contractible loop operators $\mathcal{O}_{ij}$ for the $2(n-1)$ pairs (i, j) given by

$$i = 2k-1,\ j = 2k \quad \text{for} \quad 1 \leq k \leq n-1, \tag{2.12.3}$$

or

$$i = 2k,\ j = 2n-1 \quad \text{for} \quad 1 \leq k \leq n-1. \tag{2.12.4}$$

Each loop overlaps exactly one other loop, and any operators corresponding to non-overlapping loops obviously commute. The loops that overlap correspond to the two operators $\mathcal{O}_{ij}$ satisfying (2.12.3) and $\mathcal{O}_{kl}$ satisfying (2.12.4) with $j = k$. As an example, take the two loops from (2.12.1). From the braiding relations (2.7.11) and (2.7.14) it follows that the operators anti-commute. In general we have the commutation rules given by

$$\mathcal{O}_{ij}\,\mathcal{O}_{kl} = \begin{cases} \mathcal{O}_{kl}\,\mathcal{O}_{ij}, & j \neq k \\ -\mathcal{O}_{kl}\,\mathcal{O}_{ij}, & j = k. \end{cases} \tag{2.12.5}$$

For each pair of dislocations, one pair of loops is added which commute with all previous loops but anti-commute with each other, so each new pair of loops extends the algebra. The resulting representation space then spans the space of ground states.

Example 2.14. Take the two pairs of loops with the defects numbered as

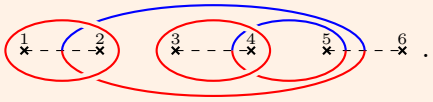

(2.12.6)

Then we have a basis specified for $k, l \in \{0, 1\}$ by

$$\mathcal{O}_{12} |k\rangle \otimes |l\rangle = (-1)^k |k\rangle \otimes |l\rangle , \tag{2.12.7}$$

$$\mathcal{O}_{25} |k\rangle \otimes |l\rangle = |(k-1)_{\text{mod } 2}\rangle \otimes |l\rangle , \tag{2.12.8}$$

$$\mathcal{O}_{34} |k\rangle \otimes |l\rangle = (-1)^l |k\rangle \otimes |l\rangle , \tag{2.12.9}$$

and

$$\mathcal{O}_{45} |k\rangle \otimes |l\rangle = |k\rangle \otimes |(l-1)_{\text{mod } 2}\rangle . \tag{2.12.10}$$

2.13 Braiding properties of *e*-*m* duality dislocations

In a similar way as we considered braiding of charges, we may now consider braiding properties of dislocations. In order to do this, we need to use the braiding relations from Section 2.7. Also, the operator P_q with $q \in \partial \mathrm{P}_{\mathcal{C}}$ defined for the edge of the defect line in equation (2.9.3) looks in the macroscopic picture as

$P_q =$, (2.13.1)

and the operator P_q with $q \in \mathrm{P}_{\mathcal{C}} \setminus \partial \mathrm{P}_{\mathcal{C}}$ defined on the defect line in equation (2.9.2) can be represented in the macroscopic picture by

$P_q =$. (2.13.2)

The plaquette operators all act as the identity when restricted to the ground state subspace, so in accordance with Theorem A.1 with $N = 2$, we have

 (2.13.3)

and

 (2.13.4)

Also, according to Theorem A.2, for the special case of $N = 2$, we have

 (2.13.5)

Now we consider two pairs of dislocations labeled by 1, 2, 3 and 4, and the corresponding loop operators displayed in the following picture:

 (2.13.6)

$\mathcal{O}_{12}$ $\mathcal{O}_{23}$

Let B_{12} denote the operation of changing places of dislocations 1 and 2 by rotating them 180° counter-clockwise, as is shown in the following picture:

 (2.13.7)

Thus B_{12} denotes the braiding of dislocations 1 and 2. A more detailed description on how loops get deformed by the rotation of dislocations can be found in [5, p. 6].

Following the lines of [25, p. 5], we see that

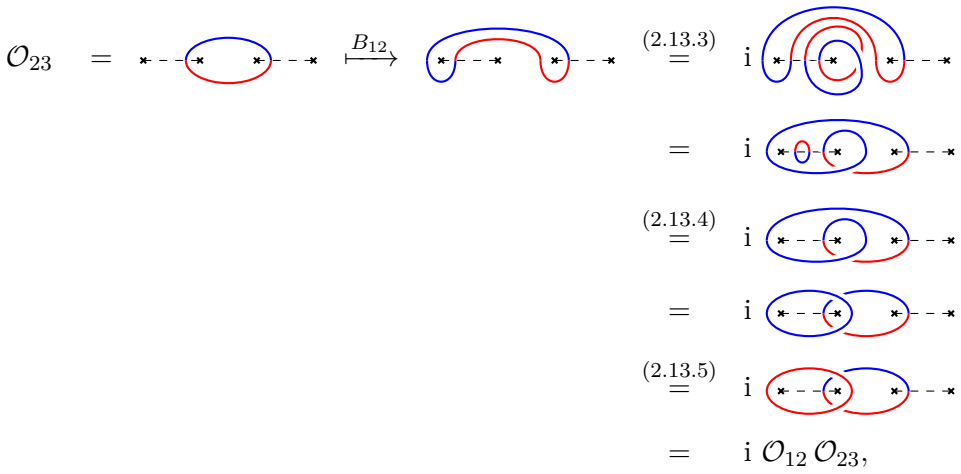

(2.13.8)

where we have fused and unfused both the electric and magnetic lines and used the braiding rules (2.7.11),(2.7.12) and (2.7.14).

It is equally interesting to consider the braiding properties of dislocations 2 and 3. Let B_{23} denote the braiding of dislocations 2 and 3 by rotating them 180° counter-clockwise, as is shown in the following picture:

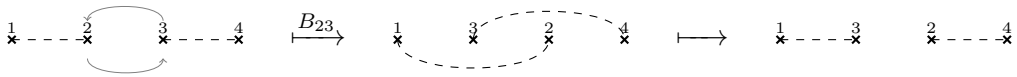

(2.13.9)

where in the last step the defect lines are rearranged. Then we find that

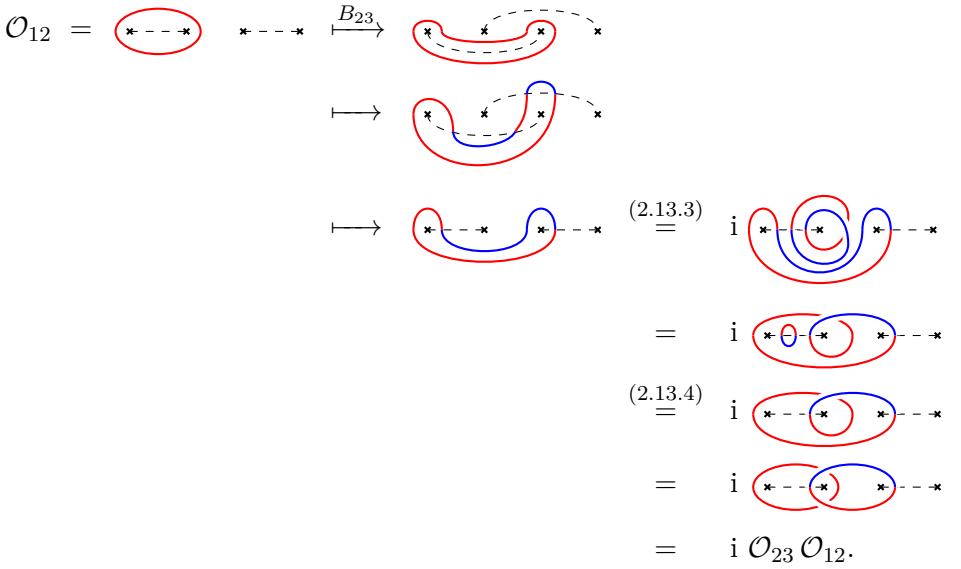

(2.13.10)

Also we have

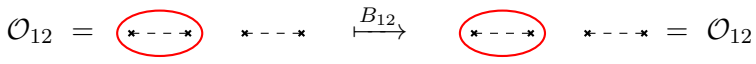

(2.13.11)

and

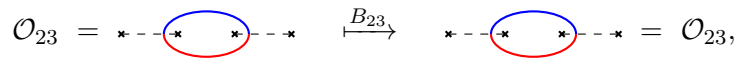

(2.13.12)

so that in summary we have the following transformations that define the braiding properties for dislocations 1, 2 and 3:

$$B_{12}: \begin{cases} \mathcal{O}_{12} \mapsto \mathcal{O}_{12} \\ \mathcal{O}_{23} \mapsto \mathrm{i}\,\mathcal{O}_{12}\,\mathcal{O}_{23} \end{cases} \tag{2.13.13}$$

and

$$B_{23} : \begin{cases} \mathcal{O}_{12} \mapsto \mathrm{i}\, \mathcal{O}_{23}\, \mathcal{O}_{12} \\ \mathcal{O}_{23} \mapsto \mathcal{O}_{23}. \end{cases} \tag{2.13.14}$$

We now want to represent these operations by unitary operators T_{12} and T_{23} in the ground state subspace. The operators should satisfy the four equations

$$T_{12}^\dagger\, \mathcal{O}_{12}\, T_{12} = \mathcal{O}_{12}, \tag{2.13.15}$$

$$T_{12}^\dagger\, \mathcal{O}_{23}\, T_{12} = \mathrm{i}\, \mathcal{O}_{12}\, \mathcal{O}_{23}, \tag{2.13.16}$$

$$T_{23}^\dagger\, \mathcal{O}_{12}\, T_{23} = \mathrm{i}\, \mathcal{O}_{23}\, \mathcal{O}_{12}, \tag{2.13.17}$$

and

$$T_{23}^\dagger\, \mathcal{O}_{23}\, T_{23} = \mathcal{O}_{23}. \tag{2.13.18}$$

Two unitary operators that solve the generalized version of these equations for the $\mathbb{Z}_N$ case were suggested in [25, p. 5]; they are given here in equations (A.3.5) and (A.3.6). Theorem A.4 assures that the operators are indeed solutions; a proof is given in Appendix A.3. The phases ψ_{12} and ψ_{23} are chosen to satisfy (A.4.1).

In these equations, let $N = 2$ which in particular implies that $\zeta := \mathrm{e}^{\mathrm{i}\pi}$, let $\psi_{12} = 0$ and $\psi_{23} = -\frac{\pi}{4}$ so as to satisfy (A.4.1). Then we get the two operators

$$\begin{aligned} T_{12} &= \sum_{n=0}^{1} \zeta^{\frac{n(2-n)}{2}}\ |n\rangle\langle n| \\ &= \zeta^0\ |0\rangle\langle 0| + \zeta^{\frac{1}{2}}\ |1\rangle\langle 1| \\ &= |0\rangle\langle 0| + \mathrm{e}^{\mathrm{i}\frac{\pi}{2}}\ |1\rangle\langle 1| \\ &= |0\rangle\langle 0| + \mathrm{i}\ |1\rangle\langle 1| \end{aligned} \tag{2.13.19}$$

and

$$\begin{aligned} T_{23} &= \tfrac{\mathrm{e}^{-\mathrm{i}\pi/4}}{\sqrt{2}} \sum_{n,n'=0}^{1} \zeta^{\frac{1}{2}(n-n'-1)^2}\ |n\rangle\langle n'| \\ &= \tfrac{1-\mathrm{i}}{2}\ \left(\zeta^{\frac{1}{2}}\ |0\rangle\langle 0| + \zeta^0\ |1\rangle\langle 0| + \zeta^2\ |0\rangle\langle 1| + \zeta^{\frac{1}{2}}\ |1\rangle\langle 1|\right) \\ &= \tfrac{1-\mathrm{i}}{2}\ \left(\mathrm{i}\ |0\rangle\langle 0| + |1\rangle\langle 0| + |0\rangle\langle 1| + \mathrm{i}\ |1\rangle\langle 1|\right). \end{aligned} \tag{2.13.20}$$

We will check explicitly that these two operators are indeed unitary and that they also satisfy the braid group relation

$$T_{12}\, T_{23}\, T_{12} = T_{23}\, T_{12}\, T_{23} \tag{2.13.21}$$

(a full proof that the operators are unitary also for the more general $\mathbb{Z}_N$ case can be found in Appendix A.3, and a proof of (2.13.21) for general N can be found in Appendix A.4).

We represent the operators by matrices:

$$T_{12} = \begin{pmatrix} 1 & 0 \\ 0 & \mathrm{i} \end{pmatrix} \tag{2.13.22}$$

and

$$T_{23} = \frac{1-\mathrm{i}}{2} \begin{pmatrix} \mathrm{i} & 1 \\ 1 & \mathrm{i} \end{pmatrix}. \tag{2.13.23}$$

The two loop operators are represented by

$$\mathcal{O}_{12} = |0\rangle\langle 0| - |1\rangle\langle 1| = \begin{pmatrix} 1 & 0 \\ 0 & -1 \end{pmatrix} \tag{2.13.24}$$

and

$$\mathcal{O}_{23} = |0\rangle\langle 1| + |1\rangle\langle 0| = \begin{pmatrix} 0 & 1 \\ 1 & 0 \end{pmatrix} . \tag{2.13.25}$$

Proof that the operators T_{12} and T_{23} are unitary. Take

$$T_{12}^{\dagger}\, T_{12} = \begin{pmatrix} 1 & 0 \\ 0 & -\mathrm{i} \end{pmatrix} \begin{pmatrix} 1 & 0 \\ 0 & \mathrm{i} \end{pmatrix} = \begin{pmatrix} 1 & 0 \\ 0 & 1 \end{pmatrix} \tag{2.13.26}$$

and

$$T_{23}^{\dagger}\, T_{23} = \frac{(1+\mathrm{i})(1-\mathrm{i})}{4} \begin{pmatrix} -\mathrm{i} & 1 \\ 1 & -\mathrm{i} \end{pmatrix} \begin{pmatrix} \mathrm{i} & 1 \\ 1 & \mathrm{i} \end{pmatrix} = \frac{1}{2} \begin{pmatrix} 2 & 0 \\ 0 & 2 \end{pmatrix} = \begin{pmatrix} 1 & 0 \\ 0 & 1 \end{pmatrix} . \tag{2.13.27}$$

□

Proof of the braid group equation (2.13.21) *for* $N = 2$. The left hand side of (2.13.21) is

$$\begin{aligned} T_{12}\, T_{23}\, T_{12} &= \frac{1-\mathrm{i}}{2} \begin{pmatrix} 1 & 0 \\ 0 & \mathrm{i} \end{pmatrix} \begin{pmatrix} \mathrm{i} & 1 \\ 1 & \mathrm{i} \end{pmatrix} \begin{pmatrix} 1 & 0 \\ 0 & \mathrm{i} \end{pmatrix} \\ &= \frac{1-\mathrm{i}}{2} \begin{pmatrix} 1 & 0 \\ 0 & \mathrm{i} \end{pmatrix} \begin{pmatrix} \mathrm{i} & \mathrm{i} \\ 1 & -1 \end{pmatrix} = \frac{1-\mathrm{i}}{2} \begin{pmatrix} \mathrm{i} & \mathrm{i} \\ \mathrm{i} & -\mathrm{i} \end{pmatrix} = \frac{1+\mathrm{i}}{2} \begin{pmatrix} 1 & 1 \\ 1 & -1 \end{pmatrix} . \end{aligned} \tag{2.13.28}$$

The right hand side of equation (2.13.21) is

$$\begin{aligned} T_{23}\, T_{12}\, T_{23} &= \frac{(1-\mathrm{i})^2}{4} \begin{pmatrix} \mathrm{i} & 1 \\ 1 & \mathrm{i} \end{pmatrix} \begin{pmatrix} 1 & 0 \\ 0 & \mathrm{i} \end{pmatrix} \begin{pmatrix} \mathrm{i} & 1 \\ 1 & \mathrm{i} \end{pmatrix} \\ &= -\frac{\mathrm{i}}{2} \begin{pmatrix} \mathrm{i} & \mathrm{i} \\ 1 & -1 \end{pmatrix} \begin{pmatrix} \mathrm{i} & 1 \\ 1 & \mathrm{i} \end{pmatrix} \\ &= -\frac{\mathrm{i}}{2} \begin{pmatrix} -1+\mathrm{i} & -1+\mathrm{i} \\ -1+\mathrm{i} & 1-\mathrm{i} \end{pmatrix} \\ &= -\mathrm{i}\, \frac{-1+\mathrm{i}}{2} \begin{pmatrix} 1 & 1 \\ 1 & -1 \end{pmatrix} \\ &= \frac{1+\mathrm{i}}{2} \begin{pmatrix} 1 & 1 \\ 1 & -1 \end{pmatrix} , \end{aligned} \tag{2.13.29}$$

which is equal to (2.13.28) and completes the proof. □

It is worth noting that the overall U(1) phase of both T_{12} and T_{23} is unimportant when it comes to solving equations (2.13.15) - (2.13.15), but essential for solving the braid group equation (2.13.21). By choosing the phase factors ψ_{12} and ψ_{23} to satisfy (A.4.1) we see that the space of ground states carries a genuine representation of the braid group. For general phase factors, the braid group equation is only satisfied up to a phase Ψ, so that

$$T_{12}\, T_{23}\, T_{12} = \mathrm{e}^{\mathrm{i}\Psi}\, T_{23}\, T_{12}\, T_{23}, \tag{2.13.30}$$

where

$$\Psi = \psi_{12} - \psi_{23} - \frac{\pi}{4}. \tag{2.13.31}$$

For all phases $\Psi \neq 0$ we have a *projective* representation, or equivalently, a central extension, of the braid group.

The different degenerate ground states are represented by the loop operators $\mathcal{O}_{ij}$ and $\mathcal{O}_{jk}$ and after the braiding of defects i and j the loops are deformed. The final ground state is related to the initial via the unitary operator T_{ij} which represents the non-abelian Berry phase that is acquired over the course of braiding defects i and j [25, p. 5].

3 Generalization to the $\mathbb{Z}_N$ plaquette model

In this section we generalize the results of Section 2 to a model that assigns an N-dimensional complex state space to each vertex of the lattice, which now gives rise to a $\mathbb{Z}_N$-symmetry. We may think of it as an N-fold angular momentum rotor instead of the spin up/down of the $\mathbb{Z}_2$ model. The boundary conditions are again periodic, but some details are quite different. The section largely follows the reasoning in [26], with some supplements from [25].

Once the model is set up and the *e-m* duality dislocations are generalized, we will also introduce a new type of duality and the type of dislocations with which it can be realized.

3.1 Setting up the model

We start with a similar lattice as in the previous section with M being the set of all sites and P the set of all plaquettes. We assign to each vertex $i \in \mathrm{M}$ a state space $\mathcal{H}_i = \mathbb{C}^N$. We choose an orthogonal basis

$$|m_i\rangle\,, \quad m_i \in \{0, 1, ..., N-1\}, \tag{3.1.1}$$

and define the operators Z_i and X_i by

$$Z_i\,|m_i\rangle = \zeta^{m_i}\,|m_i\rangle\,, \tag{3.1.2}$$

and

$$X_i\,|m_i\rangle = |(m_i - 1)_{\text{mod } N}\rangle\,, \tag{3.1.3}$$

where

$$\zeta := \mathrm{e}^{\mathrm{i}\frac{2\pi}{N}}. \tag{3.1.4}$$

The operator X_i thus lowers the angular momentum according by 1, modulo N. From (3.1.2) and (3.1.3) it is clear that

$$(X_i\,)^N = (Z_i\,)^N = \mathbf{1}. \tag{3.1.5}$$

For $N > 2$, the operators X and Z are not self-adjoint, as was the case with the Pauli operators of Section 2, but have hermitian conjugates $Z_i^\dagger$ and $X_i^\dagger$ which act as

$$Z_i^\dagger\,|m_i\rangle = \zeta^{-m_i}\,|m_i\rangle\,, \tag{3.1.6}$$

$$X_i^\dagger\,|m_i\rangle = |(m_i + 1)_{\text{mod } N}\rangle\,. \tag{3.1.7}$$

By considering

$$X_i\,Z_i\,|m_i\rangle = X_i\,\zeta^{m_i}\,|m_i\rangle = \zeta^{m_i}\,|(m_i - 1)_{\text{mod } N}\rangle \tag{3.1.8}$$

and then

$$Z_i\,X_i\,|m_i\rangle = Z_i\,|(m_i - 1)_{\text{mod } N}\rangle = \zeta^{m_i - 1}\,|(m_i - 1)_{\text{mod } N}\rangle\,. \tag{3.1.9}$$

we find that the operators X and Z obey the commutation rule

$$X_i\,Z_i = \zeta\,Z_i\,X_i. \tag{3.1.10}$$

By similar reasoning one also shows that

$$X_i^\dagger\,Z_i^\dagger = \zeta\,Z_i^\dagger\,X_i^\dagger, \tag{3.1.11}$$

$$Z_i^\dagger\,X_i = \zeta\,X_i\,Z_i^\dagger, \tag{3.1.12}$$

and

$$Z_i\,X_i^\dagger = \zeta\,X_i^\dagger\,Z_i. \tag{3.1.13}$$

We now introduce the operator

$$Y_i = -\zeta^{-\frac{1}{2}} Z_i \, X_i^\dagger, \tag{3.1.14}$$

with hermitian conjugate

$$Y_i^\dagger = -\zeta^{\frac{1}{2}} X_i \, Z_i^\dagger. \tag{3.1.15}$$

The factor $-\zeta^{-\frac{1}{2}}$ is introduced to make sure that

$$(Y_i\,)^N = \mathbf{1}. \tag{3.1.16}$$

That (3.1.16) holds can be seen as follows:

$$\begin{aligned}
(Y_i\,)^N &= (-1)^N \zeta^{-\frac{N}{2}} \underbrace{X_i \, Z_i^\dagger \, \cdots \, X_i \, Z_i^\dagger}_{N \text{ times}} = (-1)^N \zeta^{-\frac{N}{2}} \, \zeta^{-1} \, Z_i^\dagger \, X_i \underbrace{X_i \, Z_i^\dagger \, \cdots \, X_i \, Z_i^\dagger}_{N-1 \text{ times}} \\
&= (-1)^N \zeta^{-\frac{N}{2}} \, \zeta^{-1} \, \zeta^{-2} \, Z_i^\dagger \, Z_i^\dagger \, X_i \, X_i \underbrace{X_i \, Z_i^\dagger \, \cdots X_i \, Z_i^\dagger}_{N-2 \text{ times}} = \cdots \\
&= (-1)^N \zeta^{-\frac{N}{2}} \, \zeta^{\left(-\sum_{k=1}^{N-1} k\right)} \left(Z_i^\dagger\right)^N \left(X_i\right)^N = (-1)^N \zeta^{-\frac{N}{2}} \zeta^{-\frac{N(N-1)}{2}} \\
&= (-1)^N \zeta^{-\frac{N^2}{2}} = \left(\mathrm{e}^{\mathrm{i}\pi}\right)^N \left(\mathrm{e}^{\mathrm{i}\frac{2\pi}{N}}\right)^{-\frac{N^2}{2}} = \left(\mathrm{e}^{\mathrm{i}\frac{\pi}{N}}\right)^{N^2} \left(\mathrm{e}^{\mathrm{i}\frac{\pi}{N}}\right)^{-N^2} = \mathbf{1},
\end{aligned} \tag{3.1.17}$$

where we have used the commutation rule (3.1.12) multiple times.

Note that for $N = 2$ we get

$$Z_i = \sigma_i^z, \;\; X_i = \sigma_i^x \quad \text{and} \quad Y_i = -\sigma_i^y. \tag{3.1.18}$$

The difference in sign of the operator Y from the $\mathbb{Z}_2$ model of Section 2 is unimportant; it is chosen here for convenience.

The operators are unitary, as is evidenced by

$$Z_i^\dagger \, Z_i \, |m_i\rangle = Z_i^\dagger \, \zeta^{m_i} \, |m_i\rangle = \zeta^{-m_i} \, \zeta^{m_i} \, |m_i\rangle = |m_i\rangle \,, \tag{3.1.19}$$

$$X_i^\dagger X_i \, |m_i\rangle = X_i^\dagger \, |(m_i - 1)_{\text{mod } N}\rangle = |(m_i - 1 + 1)_{\text{mod } N}\rangle = |m_i\rangle \,, \tag{3.1.20}$$

and

$$Y_i^\dagger Y_i = \left(-\zeta^{\frac{1}{2}} X_i \, Z_i^\dagger\right) \left(-\zeta^{-\frac{1}{2}} Z_i \, X_i^\dagger\right) = X_i \, Z_i^\dagger \, Z_i \, X_i^\dagger = X_i \, X_i^\dagger = \mathbf{1}. \tag{3.1.21}$$

The full system state space is the tensor product of state spaces at all sites:

$$\mathcal{H} = \bigotimes_{i \in \mathrm{M}} \mathcal{H}_i \cong \mathbb{C}^{N|\mathrm{M}|}. \tag{3.1.22}$$

As before, by abuse of notation, we denote also with $\mathcal{Q}_i$ an operator on the full system space defined by

$$\mathbf{1}_1 \otimes \mathbf{1}_2 \otimes \cdots \otimes \mathcal{Q}_i \otimes \cdots \otimes \mathbf{1}_{|\mathrm{M}|-1} \otimes \mathbf{1}_{|\mathrm{M}|}, \tag{3.1.23}$$

where $\mathcal{Q}_i$ originally denotes an operator on the state space of site i. The commutation rules are the same as before, with the addition that an operator on the site i commutes with all operators on the site i' if $i \neq i'$.

Again, for $N > 2$ these operators are not self-adjoint, which is one of the main differences from the $\mathbb{Z}_2$ model. In the graphical representation this amounts to having a direction on strings, according to

$$Z_i = \text{} \,, \tag{3.1.24}$$

$$Z_i^\dagger = \text{} \,, \tag{3.1.25}$$

$$X_i = \text{  }\,, \tag{3.1.26}$$

$$X_i^\dagger = \text{  }\,, \tag{3.1.27}$$

$$Y_i = -\zeta^{-\frac{1}{2}} \text{  } \tag{3.1.28}$$

and

$$Y_i^\dagger = -\zeta^{-\frac{1}{2}} \text{  }\,. \tag{3.1.29}$$

We say that the string is *oriented*. With the graphical representation the commutation rule from (3.1.10) becomes

$$\text{  } \tag{3.1.30}$$

The plaquette operator of plaquette $p \in \mathrm{P}$ defined by the four sites labeled $1, 2, 3, 4 \in M$, is defined by

$$O_p = Z_1\, X_2\, Z_3^\dagger\, X_4^\dagger = \text{  }\,. \tag{3.1.31}$$

The Hamiltonian for the $\mathbb{Z}_N$ toric plaquette model is then defined as

$$H_0 = -\frac{1}{2}\sum_{p\in\mathrm{P}} O_p + h.c. = -\frac{1}{2}\sum_{p\in\mathrm{P}} \left(O_p + O_p^\dagger\right), \tag{3.1.32}$$

where *h.c.* denotes the hermitian conjugate, which is needed to ensure that the Hamiltonian is hermitian.

The plaquette operators have the property

$$O_p^N = \mathbf{1}, \tag{3.1.33}$$

since

$$\left(X_i\right)^N = \left(X_i^\dagger\right)^N = \left(Z_i\right)^N = \left(Z_i^\dagger\right)^N = \mathbf{1}. \tag{3.1.34}$$

This means that there are N distinct eigenvalues for each plaquette operator. Thus there exists a basis

$$\mathcal{B}_p = \left\{ |q_1 q_2 \cdots q_i \cdots q_{|\mathrm{P}|-1} q_{|\mathrm{P}|}\rangle \;\middle|\; q_i \in \{0, 1, ..., N-1\} \right\}. \tag{3.1.35}$$

of $\mathcal{H}$ obeying

$$O_p\, |q_1 \cdots q_{|\mathrm{P}|}\rangle = \zeta^{q_p}\, |q_1 \cdots q_{|\mathrm{P}|}\rangle\,, \qquad \forall p \in \mathrm{P}. \tag{3.1.36}$$

For each pair O_p and $O_p^\dagger$ in the Hamiltonian we have

$$\frac{1}{2}\left(O_p + O_p^\dagger\right)|q_p\rangle = \frac{1}{2}\left(\zeta^{q_p} + \zeta^{-q_p}\right)|q_p\rangle = \cos\left(\frac{2\pi q_p}{N}\right)|q_p\rangle \tag{3.1.37}$$

which shows that the lowest energy state is the eigenstate with eigenvalue 1. Put another way, the ground state subspace is the state space $\mathcal{H}$ subjected to the constraints

$$O_p = \mathbf{1} \quad \forall p \in \mathrm{P}. \tag{3.1.38}$$

The eigenvalue 1 of the plaquette state $|q_p\rangle$ corresponds to $q_p = 0$. We call q_p the $\mathbb{Z}_N$ charge of the plaquette p, so that the ground state is the state having zero $\mathbb{Z}_N$ charge on all plaquettes.

As before, if the plaquette is odd, we call it an electric charge (e-charge), and we call it a magnetic charge (m-charge) if the plaquette is even. In some but not all cases we can make this distinction globally, but it is always possible to make it locally.

The distinction between entering and exiting a plaquette is determined by the direction of the involved operator. A string can only enter and exit a plaquette through one of four corners. A given corner has an operator associated with it through (3.1.31), and this in turn determines which operator can be used to enter or exit through that specific corner.

Example 3.1. Consider the graphical representation of plaquette operators from equation (3.1.31). A string can only enter this plaquette through node 1 by the operator X_1 and can only exit it through the operator $X_1^\dagger$. It enters through node 2 by the operator $Z_2^\dagger$ and exits through Z_2.

All entering and exiting operators for a general plaquette are listed in the following table:

Corresponding factor in O_p	Entering operator	Exiting operator
X	$Z^\dagger$	Z
$X^\dagger$	Z	$Z^\dagger$
Z	X	$X^\dagger$
$Z^\dagger$	$X^\dagger$	X

(3.1.39)

A string that enters a plaquette but doesn't exit is called an *open string*; the corresponding plaquette is called an *end point* of the string. A string that exits a plaquette that it has not entered is also an open string; the corresponding plaquette is called a *start point* of the string. The distinction between start and end point is often irrelevant and usually they are both referred to as end points. A string without end points is called a *closed string*.

To create a $q_p = +1$ charge on plaquette p we need a string operator S with the property

$$O_p\, S = \zeta\, S\, O_p. \tag{3.1.40}$$

Comparing (3.1.39) with equations (3.1.10), (3.1.11), (3.1.12) and (3.1.13) we see that the string represented by the operator S should exit the plaquette p but not enter it, that is, plaquette p must be a starting point of the string. We can also conclude by the same reasoning that to create a $q_{p'} = -1$ charge on plaquette p' we need a string operator S with the property

$$O_{p'}\, S = \zeta^{-1}\, S\, O_{p'}. \tag{3.1.41}$$

which means that the string represented by the operator S should enter the plaquette p' but not exit it, thus plaquette p' must be an end point of the string. We summarize this in the following proposition:

Proposition 3.1. *At the starting point p of an open string S the $\mathbb{Z}_N$ charge of the plaquette p is raised by 1 modulo N. At the end point p' of S the $\mathbb{Z}_N$ charge of the plaquette p' is lowered by 1 modulo N.*

A point of a string S that is neither a starting nor an end point is called an *interior point* of the string. From the definition of a string above it is apparent that the string S both enters and exits all interior points. We conclude:

Proposition 3.2. *If the plaquette p is an interior point of a string S, the $\mathbb{Z}_N$ charge of the plaquette p is invariant under the action of S.*

The above proposition trivially leads to the following corollary:

Corollary 3.3. *A closed string does not alter the $\mathbb{Z}_N$ charge of any plaquette.*

This finally leads to the theorem of commutativity of closed strings:

Theorem 3.4. *All closed strings commute with all plaquette operators.*

Proof. Assume the system is in an energy eigenstate $|\alpha\rangle$. Then for some plaquette p there is an operator O_p satisfying

$$O_p \, |\alpha\rangle = \zeta^q \, |\alpha\rangle \,, \tag{3.1.42}$$

with $q \in \{0, 1, ..., N-1\}$. Let S be a closed string. Then

$$O_p \, S \, |\alpha\rangle = O_p \, (S \, |\alpha\rangle) = \zeta^q \, (S \, |\alpha\rangle) = \zeta^q \, S \, |\alpha\rangle \,, \tag{3.1.43}$$

since by Corollary 3.3, S does not alter the charge of any plaquette. On the other hand

$$S \, O_p \, |\alpha\rangle = S \, \zeta^q \, |\alpha\rangle = \zeta^q \, S \, |\alpha\rangle \,. \tag{3.1.44}$$

Since both $|\alpha\rangle$ and O_p are arbitrary, S commutes with all plaquette operators, and since S is an arbitrary closed string the proof is complete. □

Example 3.2. The following figure shows two open strings, one electric and one magnetic. The positive and negative charges at the start and end points are denoted by ⊕ and ⊖ respectively:

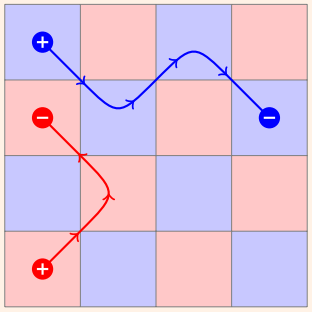

(3.1.45)

3.2 Fusion of charges

As in the $N = 2$ case, charges can be fused and unfused, i.e. we have the notion of a fusion product. As before, we express these rules in the language of monoidal semisimple $\mathbb{C}$-linear categories $\mathcal{C} \equiv (\mathcal{C}, \otimes, \mathbf{1})$. The category in question has

$$\{W_{i,j} \mid i, j = 0, 1, ..., N-1\} \tag{3.2.1}$$

as the set of representatives for the isomorphism classes of simple objects in $\mathcal{C}$, where

$$W_{i,j} = e^{\otimes i} \otimes m^{\otimes j} = \overbrace{e \otimes \cdots \otimes e}^{i \text{ factors}} \otimes \overbrace{m \otimes \cdots \otimes m}^{j \text{ factors}} \tag{3.2.2}$$

and where

$$e^{\otimes 0} = \mathbf{1} = m^{\otimes 0}. \tag{3.2.3}$$

It follows that

$$W_{0,0} = \mathbf{1}. \tag{3.2.4}$$

From (3.2.2) we see that there are N^2 different isomorphism classes of simple objects. Also, for any object x there exist isomorphisms such that $x \otimes \mathbf{1} \cong \mathbf{1} \otimes x \cong x$. Also, for an object x which has i tensor product factors of e and j factors of m in any order, there exists an isomorphism such that $x \cong W_{i,j}$.

The fusion product rule is then

$$W_{i,j} \otimes W_{k,l} \cong W_{i+k,j+l}. \tag{3.2.5}$$

Here and below the subscripts are to be taken modulo N. It is straightforward to check that this description is consistent with the one for $N = 2$ in Section 2.6. This result in particular implies that the *object dual* (or conjugate) to $W_{i,j}$, written as $W_{i,j}^\dagger$, satisfies

$$W_{i,j}^\dagger = W_{-i,-j}. \tag{3.2.6}$$

Then it also follows that

$$W_{i,j} \otimes W_{i,j}^\dagger = \mathbf{1}. \tag{3.2.7}$$

Since when N is even we have $\frac{N}{2} = -\frac{N}{2} \pmod N$, then we have the following

Lemma 3.5. *If N is even, there exist exactly 4 self-dual classes of simple objects. For such N the representatives for the self-dual isomorphism class are*

$$W_{0,0},\ W_{0,N/2},\ W_{N/2,0} \text{ and } W_{N/2,N/2}. \tag{3.2.8}$$

Lemma 3.6. *If N is odd, there exists exactly one self-dual class of simple objects. For such N the representative for the self-dual isomorphism class is*

$$W_{0,0}. \tag{3.2.9}$$

Thus, since $W_{0,0}$ is the representative for the "no charge" isomorphism class, only for even N we have non-trivial self-conjugate charges and that these charges are

$$e^{\frac{N}{2}},\ m^{\frac{N}{2}},\ \text{and}\ \epsilon^{\frac{N}{2}}. \tag{3.2.10}$$

3.3 Braiding of charges

The identity morphism $\mathrm{id}_{W_{i,j}}$ associated with a simple object $W_{i,j}$ is depicted as

$\mathrm{id}_{W_{i,j}} =$  . (3.3.1)

In the case of the objects $W_{i,0}$ and $W_{0,j}$ we use the coloring of red and blue of such lines as before. In particular, for $i = 1$ or $j = 1$ we denote the identity morphisms by id_e and id_m, and depict them as

$\mathrm{id}_e =$  , $\mathrm{id}_m =$  . (3.3.2)

We only consider lines which are upwards oriented since, according to (3.2.6), we have

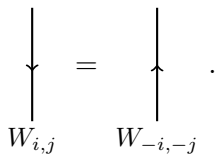 . (3.3.3)

By abuse of notation we drop the arrows marking the orientation for the rest of this section.

Denote the braiding morphisms of $W_{i,j}$ with $W_{k,l}$ by

$$c_{i,k}^{j,l} = \quad . \tag{3.3.4}$$

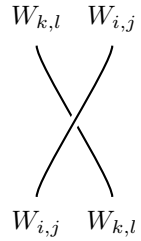

For the special case $i = k = 1$ and $j = l = 0$ we have the self-braiding

$$c_{1,1}^{0,0} = c_{ee} = \quad . \tag{3.3.5}$$

Since $e \otimes e \mapsto e \otimes e$ is simply a number R_{ee} times the identity morphism $\mathrm{id}_e \otimes \mathrm{id}_e$, by the same reasoning as for $N = 2$, we get

$$R_{ee}\,\mathrm{id}_e \otimes \mathrm{id}_e = c_{ee} = \quad = \quad = \quad , \tag{3.3.6}$$

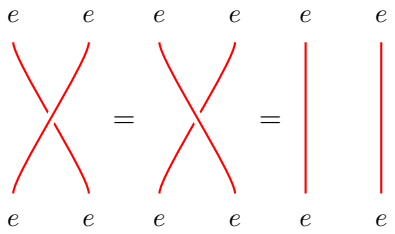

which shows that $R_{ee} = 1$. The same reasoning leads to $R_{mm} = 1$.

Proposition 3.7. *For $i \in \{1, 2, ..., N-1\}$, the self-braiding morphism $c_{i,i}^{0,0}$ satisfies*

$$c_{i,i}^{0,0} = R_{i,i}^{0,0}\ \mathrm{id}_{W_{i,0}} \otimes \mathrm{id}_{W_{i,0}} \tag{3.3.7}$$

with

$$R_{i,i}^{0,0} = 1. \tag{3.3.8}$$

Thus, for a purely electric simple object the self-braiding is trivial.

Proof. For $i = 1$ we have (3.3.6). Let $i > 1$ and make the induction assumption

$$c_{i-1,i-1}^{0,0} = \mathrm{id}_{W_{i-1,0}} \otimes \mathrm{id}_{W_{i-1,0}}. \tag{3.3.9}$$

But

$$c_{i,i}^{0,0} \cong c_{1,1}^{0,0} \otimes c_{i-1,i-1}^{0,0} = c_{1,1}^{0,0} \otimes \mathrm{id}_{W_{i-1,0}} \otimes \mathrm{id}_{W_{i-1,0}} \tag{3.3.10}$$

and by (3.3.6) we have

$$c_{1,1}^{0,0} = \mathrm{id}_{W_{1,0}} \otimes \mathrm{id}_{W_{1,0}}. \tag{3.3.11}$$

Thus

$$c_{i,i}^{0,0} \cong \left(\mathrm{id}_{W_{1,0}} \otimes \mathrm{id}_{W_{1,0}}\right) \otimes \left(\mathrm{id}_{W_{i-1,0}} \otimes \mathrm{id}_{W_{i-1,0}}\right) \cong \mathrm{id}_{W_{i,0}} \otimes \mathrm{id}_{W_{i,0}}. \tag{3.3.12}$$

By induction the proof is completed for $i \in \{1, 2, ..., N-1\}$. □

By the same reasoning, a similar statement for the "magnetic" case can be made:

Proposition 3.8. *For $j \in \{1, 2, ..., N-1\}$, the self-braiding morphism $c^{j,j}_{0,0}$ satisfies*

$$c^{j,j}_{0,0} = R^{j,j}_{0,0}\ \mathrm{id}_{W_{0,j}} \otimes \mathrm{id}_{W_{0,j}} \tag{3.3.13}$$

with

$$R^{j,j}_{0,0} = 1. \tag{3.3.14}$$

Thus, for a purely magnetic simple object the self-braiding is trivial.

The self-braiding of $W_{1,1}$, which in the $N = 2$ case was called ϵ, is

$$R^{1,1}_{1,1}\left(\mathrm{id}_{W_{1,1}} \otimes \mathrm{id}_{W_{1,1}}\right) = c^{1,1}_{1,1} =$$

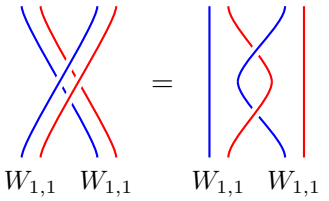

$$\overset{(3.1.12)}{=} \zeta$$

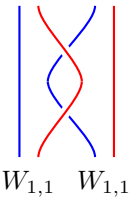

$$= \zeta$$

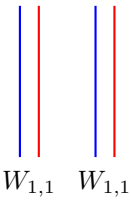

, (3.3.15)

so we have

$$R^{1,1}_{1,1} = \zeta. \tag{3.3.16}$$

By induction it is not hard to prove the following generalization of Proposition 3.7 and 3.8:

Proposition 3.9. *For $i, j \in \{0, 1, ..., N-1\}$, the self-braiding morphism $c^{j,j}_{i,i}$ satisfies*

$$c^{j,j}_{i,i} = R^{j,j}_{i,i}\ \mathrm{id}_{W_{i,j}} \otimes \mathrm{id}_{W_{i,j}} \tag{3.3.17}$$

with

$$R^{j,j}_{i,i} = \zeta^{ij}. \tag{3.3.18}$$

The general braiding morphism $W_{i,j} \otimes W_{k,l} \to W_{k,l} \otimes W_{j,k}$ is also characterized by a number $R^{j,l}_{i,k}$ since both $W_{i,j} \otimes W_{k,l}$ and $W_{k,l} \otimes W_{j,k}$ are isomorphic to the simple object $W_{i+k,j+l}$. As in the $N = 2$ case, the number depends on a choice of basis in the respective isomorphism spaces. Only for self-braidings ($i = k$ and $j = l$) do we have the same isomorphism space before and after braiding and are able to calculate basis independent numbers $R^{j,l}_{i,k}$. By applying the braid twice, however, first $c^{j,l}_{i,k}$ and then $c^{l,j}_{k,i}$, we can find the basis independent number $\left(R^{l,j}_{k,i}\, R^{j,l}_{i,k}\right)$. Consider the case of $c^{1,0}_{0,1}\, c^{0,1}_{1,0}$, in which we have

$$\left(R^{1,0}_{0,1}\, R^{0,1}_{1,0}\right)\ \mathrm{id}_{W_{1,0}} \otimes \mathrm{id}_{W_{0,1}} = c^{1,0}_{0,1}\, c^{0,1}_{1,0} =$$

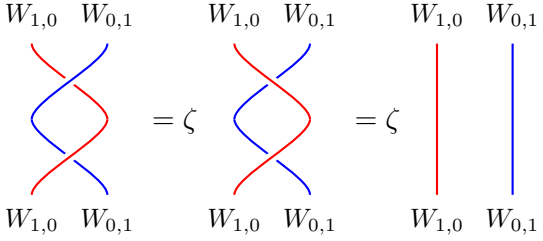

. (3.3.19)

Thus we have $R^{1,0}_{0,1}\, R^{0,1}_{1,0} = \zeta$. By iterating this process we can finally derive the following proposition:

Proposition 3.10. *For $i,j,k,l \in \{0,1,...,N-1\}$, the braiding morphism $c^{l,j}_{k,i}\, c^{j,l}_{i,k}$ satisfies*

$$c^{l,j}_{k,i}\, c^{j,l}_{i,k} = R^{l,j}_{k,i}\, R^{j,l}_{i,k}\ \mathrm{id}_{W_{i,j}} \otimes \mathrm{id}_{W_{k,l}} \tag{3.3.20}$$

with

$$R^{l,j}_{k,i}\, R^{j,l}_{i,k} = \zeta^{il+jk}. \tag{3.3.21}$$

We also note two distinct duality symmetries of the braiding rules (3.3.21). First we have invariance under the outer automorphism

$$W_{i,j} \longleftrightarrow W_{j,i}, \tag{3.3.22}$$

which is the generalization of the e-m duality for $N = 2$ seen in Section 2. The second symmetry is invariance under the outer automorphism

$$W_{i,j} \otimes W_{k,l} \longleftrightarrow W_{-i,-j} \otimes W_{-k,-l}, \tag{3.3.23}$$

where all objects go to their conjugate or dual. This symmetry is referred to as the *charge conjugate duality*, and was not considered in the $\mathbb{Z}_2$ case because for the special case of $N = 2$ the charges are self-conjugate. Further on in this section we shall see that the e-m duality is realized by the same class of dislocations as in Section 2.9. We shall also see that charge conjugation can be realized by a different class of dislocations.

3.4 Ground state degeneracy and *e*-*m* duality dislocations

The ground state degeneracy of the $\mathbb{Z}_N$ toric plaquette model without dislocations is calculated in the same way as was done for $N = 2$ in Section 2.8, with the exception that now, each site contributes with a dimension of N to the full state space giving a total dimension of $N^{\otimes|M|}$, and that each independent constraint equation reduces the dimension by a factor of $|M|$. The constraint equations are

$$O_p = 1, \quad \forall p \in \mathrm{P}. \tag{3.4.1}$$

The charges are created in conjugate pairs, one at each end point of an open string, so we have zero charge globally. For a lattice with even periods we have two equations of charge neutrality, namely

$$\prod_{p\in \mathrm{P}_e} O_p = 1 \tag{3.4.2}$$

and

$$\prod_{p\in \mathrm{P}_m} O_p = 1, \tag{3.4.3}$$

where P_e is the subset of P containing only the electric plaquettes, and P_m is the subset of P containing only the magnetic plaquettes. For a lattice with at least one odd period we instead have

$$\prod_{p\in \mathrm{P}} O_p = 1. \tag{3.4.4}$$

So, since on a lattice with periodic boundary conditions we have $|P| = |M|$, the number of independent constraint equations is $|M| - 2$ for an even lattice and $|M| - 1$ for a lattice with at least one odd period.

In conclusion we have the following:

Theorem 3.11. *(i) For a lattice with periodic boundary conditions and with even periods, the ground state degeneracy with $n = 0$ dislocations is*

$$\bar{D}^0_\Omega = N^2. \tag{3.4.5}$$

(ii) For a lattice with periodic boundary conditions and with at least one odd period, the ground state degeneracy with $n = 0$ dislocations is

$$\tilde{D}^0_\Omega = N. \tag{3.4.6}$$

We now consider lattice dislocations of the type described in Section 2.9. Again, with a pair of dislocations and defect line $\mathcal{C}$, as illustrated by (2.9.1) it is now natural to introduce double plaquette operators. Again there are two types of double plaquettes: let $\mathrm{P}_\mathcal{C} \subset \mathrm{P}$ be the set of all double plaquettes in the "interior' of the defect line and let $\partial\mathrm{P}_\mathcal{C} \subset \mathrm{P}_\mathcal{C}$ be the set of the two double plaquettes around the dislocations at the ends of the defect line. The definition of the double plaquette operators in the $\mathbb{Z}_N$ model is

$P_q =$ 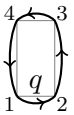 $= Z_1\, X_2\, Z_3^\dagger\, X_4^\dagger \quad \text{for } q \in \mathrm{P}_\mathcal{C} \setminus \partial\mathrm{P}_\mathcal{C},$ (3.4.7)

and the pentagonal plaquette operators at the edges are defined for $q \in \partial\mathrm{P}_\mathcal{C}$ by

$P_q = -\zeta^{-\frac{1}{2}}$ 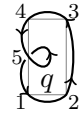 $= -\zeta^{-\frac{1}{2}}\, Z_1\, X_2\, Z_3^\dagger\, X_4^\dagger\, Z_5 X_5^\dagger = Z_1\, X_2\, Z_3^\dagger\, X_4^\dagger\, Y_5 \quad \text{(left dislocation)},$ (3.4.8)

and

$P_q = -\zeta^{-\frac{1}{2}}$ 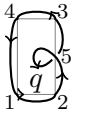 $= -\zeta^{-\frac{1}{2}}\, Z_1\, X_2\, Z_3^\dagger\, X_4^\dagger\, Z_5^\dagger X_5 = Z_1\, X_2\, Z_3^\dagger\, X_4^\dagger\, Y_5^\dagger \quad \text{(right dislocation)}.$ (3.4.9)

Here, as was done in (3.1.14), when defining the operator Y_i, the phase factor $-\zeta^{-\frac{1}{2}}$ is present to ensure that $P_q^N = 1$, just as for the remaining plaquette operators O_p. It is straightforward to check that these definitions reduce to those of Section 2.9 for the $N = 2$ case.

The new double plaquette operators are closed strings, so according to Theorem 3.4 we have

$$[O_p, P_q] = 0, \quad \forall p \in \mathrm{P} \setminus \mathrm{P}_\mathcal{C},\, q \in \mathrm{P}_\mathcal{C}, \tag{3.4.10}$$

ensuring the mutual commutativity among plaquette operators. Just like in Example 2.6, the defect line realizes the *e-m* duality, which is a $\mathbb{Z}_2$ symmetry of the $\mathbb{Z}_N$ model.

The new Hamiltonian $H_0^\mathcal{C}$ (the superscript $\mathcal{C}$ indicates the branch cut) is then, as before, the sum of the plaquette operators and their hermitian adjoints:

$$H_0^\mathcal{C} = -\frac{1}{2} \sum_{p \in \mathrm{P} \setminus \mathrm{P}_\mathcal{C}} \left(O_p + O_p^\dagger \right) - \frac{1}{2} \sum_{q \in \mathrm{P}_\mathcal{C}} \left(P_q + P_q^\dagger \right). \tag{3.4.11}$$

The constraint equations are now

$$O_p = 1, \quad \forall p \in \mathrm{P} \setminus \mathrm{P}_\mathcal{C} \tag{3.4.12}$$

and

$$P_q = 1, \quad \forall q \in \mathrm{P}_\mathcal{C}. \tag{3.4.13}$$

The reader is referred to Section 2.9 for a discussion about how dislocations affect the degeneracy of the ground state. In the $\mathbb{Z}_N$ case the results are similar, with the only difference of changing the base from 2 to N, as can be seen in the following theorems:

Theorem 3.12. *(i) For a $\mathbb{Z}_N$ lattice with even periods, with periodic boundary conditions and with n pairs of e-m duality dislocations, the ground state degeneracy is given by*

$$\bar{D}_\Omega^n = \begin{cases} N^2 & \text{for } n = 0, \\ N^{n+1} & \text{for } n = 1, 2, ... \end{cases} \tag{3.4.14}$$

(ii) For a $\mathbb{Z}_N$ lattice with at least one odd period, with periodic boundary conditions and with n pairs of e-m duality dislocations, the ground state degeneracy is given by

$$\tilde{D}_\Omega^n = N^{n+1} \quad \text{for } n = 0, 1, ... \tag{3.4.15}$$

For this reason one may formally attribute each e-m duality dislocation a quantum dimension $\sqrt{N}$.

3.5 A basis for the space of ground states with *e-m* duality dislocations

As was seen in Section 2.10, a basis for the ground state can be found by choosing loops that are not contractible. These non-contractible loops are closed strings that cannot be written as a product of plaquette operators, as stated by Proposition 2.4. The process of loop contraction was also shown in Example 2.7, and is still valid for general N, with the modification of now using the hermitian adjoint plaquette operator to contract the loop.

In the $\mathbb{Z}_N$ model, any ground state without defects can be written as

$$|\Omega\rangle = \prod_{p \in \mathrm{P}} \sum_{k=0}^{N-1} (O_p)^k \, |\omega\rangle \,, \tag{3.5.1}$$

where $|\omega\rangle$ is any linear combination of states chosen from the basis $\mathcal{B}_p$. To see that $|\Omega\rangle$ is a ground state, notice that for all $p \in \mathrm{P}$ we have

$$\begin{aligned} O_p \sum_{k=0}^{N-1} (O_p)^k &= O_p \left(\mathbf{1} + O_p + \cdots + (O_p)^{N-1} \right) \\ &= \left(O_p + (O_p)^2 + \cdots + (O_p)^{N-1} + (O_p)^N \right) \\ &= \left(O_p + (O_p)^2 + \cdots + (O_p)^{N-1} + \mathbf{1} \right) = \sum_{k=0}^{N-1} (O_p)^k \,, \end{aligned} \tag{3.5.2}$$

together with the fact that

$$\left[\sum_{k=0}^{N-1} (O_p)^k \,, \sum_{k=0}^{N-1} \left(O_{p'}\right)^k \right] = 0, \quad \forall p, p' \in \mathrm{P}. \tag{3.5.3}$$

The discussion in Section 2.10 about finding non-contractible loops to characterize the different ground states is, in all points that matter here, independent of the fact that $N = 2$. For the special case $N = 2$ we have seen that the electric and magnetic loops anti-commute, and using the same arguments for the general N case we get

$$E_y \, M_x = \zeta \, M_x \, E_y, \tag{3.5.4}$$

and

$$M_y \, E_x = \zeta \, E_x \, M_y. \tag{3.5.5}$$

These two independent algebras both require an N-dimensional representation space, which is consistent with the N^2 degeneracy for even period lattices in Theorem 3.12 (i). For the case of an odd period lattice there is no distinction between electric and magnetic loops (at least in

the direction of the odd period) and so there is only one such independent algebra requiring an N-dimensional representation space. This is consistent with Theorem 3.12 (ii).

When adding e-m duality dislocations to the lattice we also add independent non-contractible loops and we choose these according to the homology basis developed in [5], as discussed in Section 2.12. For $n \geq 2$ pairs of defects, the degeneracy is increased by a factor of N^{n-1} so we need to choose $2(n-1)$ classes of non-contractible loops such that every loop only crosses one other loop once and none of the others. The process for each added pair of dislocations is the same as before, namely:

1. Add one loop encircling the new pair.

2. Add one loop that goes through the defect line between the new pair and the defect line of the first pair.

The operators corresponding to these loops are labeled as suggested in Section 2.12. Then, from the braiding relations given in Proposition 3.9 and 3.10 it follows that the commutation rules are

$$\mathcal{O}_{ij}\,\mathcal{O}_{kl} = \begin{cases} \mathcal{O}_{kl}\,\mathcal{O}_{ij}, & j \neq k \\ \zeta\,\mathcal{O}_{kl}\,\mathcal{O}_{ij}, & j = k. \end{cases} \tag{3.5.6}$$

Thus for $n \geq 2$ there exists an orthogonal basis

$$\mathcal{B}_D = \left\{ |r_1 \otimes \cdots \otimes r_{n-1}\rangle \;\middle|\; r_i \in \{0,1,...,N-1\}, i \in \{1,2,...,n-1\} \right\} \tag{3.5.7}$$

such that for $k \in \{1,2,...,n-1\}$, $i = 2k-1$ and $j = 2k$ we have

$$\mathcal{O}_{ij}\ |r_1 \otimes \cdots \otimes r_k \otimes \cdots \otimes r_{n-1}\rangle = \zeta^{r_k}\ |r_1 \otimes \cdots \otimes r_k \otimes \cdots \otimes r_{n-1}\rangle \tag{3.5.8}$$

and for $k \in \{1,2,...,n-1\}$, $i = 2k$ and $j = 2n-1$ we have

$$\mathcal{O}_{ij}\ |r_1 \otimes \cdots \otimes r_k \otimes \cdots \otimes r_{n-1}\rangle = |r_1 \otimes \cdots \otimes (r_k - 1)_{\text{mod } N} \otimes \cdots \otimes r_{n-1}\rangle\,. \tag{3.5.9}$$

3.6 Braiding properties for e-m duality dislocations

We the braiding properties of e-m duality dislocations by considering the case of $n = 2$ dislocations. Loop operators are chosen according to a similar process as in Section 2.12:

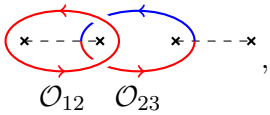

, (3.6.1)

where again we are using the macroscopic picture. Orientation arrows are now added when representing the non-contractible loops. We have

$$\mathcal{O}_{12}\ |r\rangle = \zeta^r\ |r\rangle\,, \quad r \in \{0,1,...,N-1\} \tag{3.6.2}$$

and

$$\mathcal{O}_{23}\ |r\rangle = |r-1\rangle\,, \tag{3.6.3}$$

where here and below r should be taken modulo N. The operators $\mathcal{O}_{12}$ and $\mathcal{O}_{23}$ commute according to

$$\mathcal{O}_{23}\,\mathcal{O}_{12} = \zeta\,\mathcal{O}_{12}\,\mathcal{O}_{23}. \tag{3.6.4}$$

Let B_{12} denote the braiding of dislocations 1 and 2, and let B_{23} denote the braiding of dislocations 2 and 3 by rotating them 180° counter-clockwise, as is shown in the pictures (2.13.7) and (2.13.9) respectively. We can then calculate the braiding properties of the dislocations. It

is obvious that the braiding B_{12} leaves the operator $\mathcal{O}_{12}$ invariant, and the same holds for B_{23} with $\mathcal{O}_{23}$, similar to what can be seen in (2.13.11) and (2.13.12). Now we consider the effect of braiding B_{12} on the operator $\mathcal{O}_{23}$ by proceeding as follows:

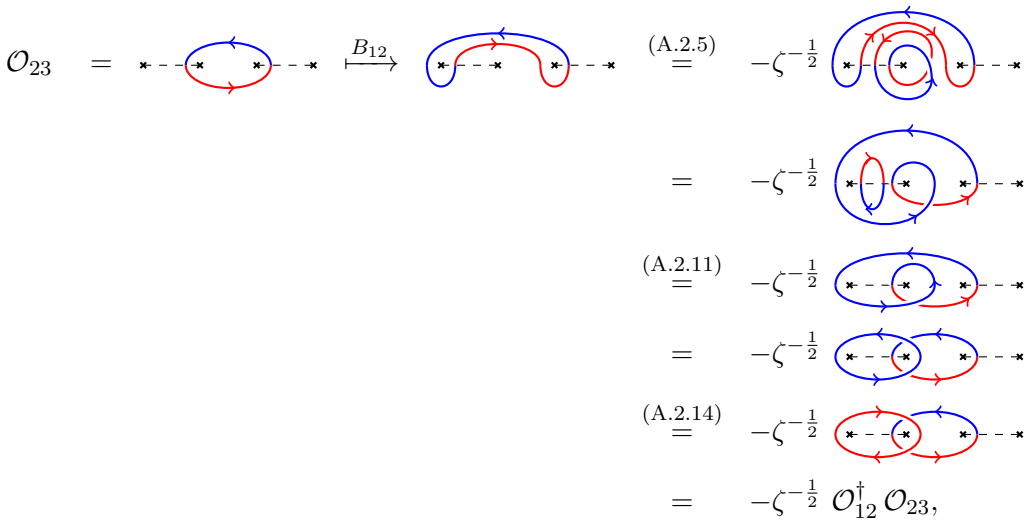

(3.6.5)

where we have fused and unfused both the electric and magnetic lines according to (3.2.5) and used the braiding rules from equation (3.3.21).

Next, consider the effect of braiding B_{23} on the operator $\mathcal{O}_{12}$:

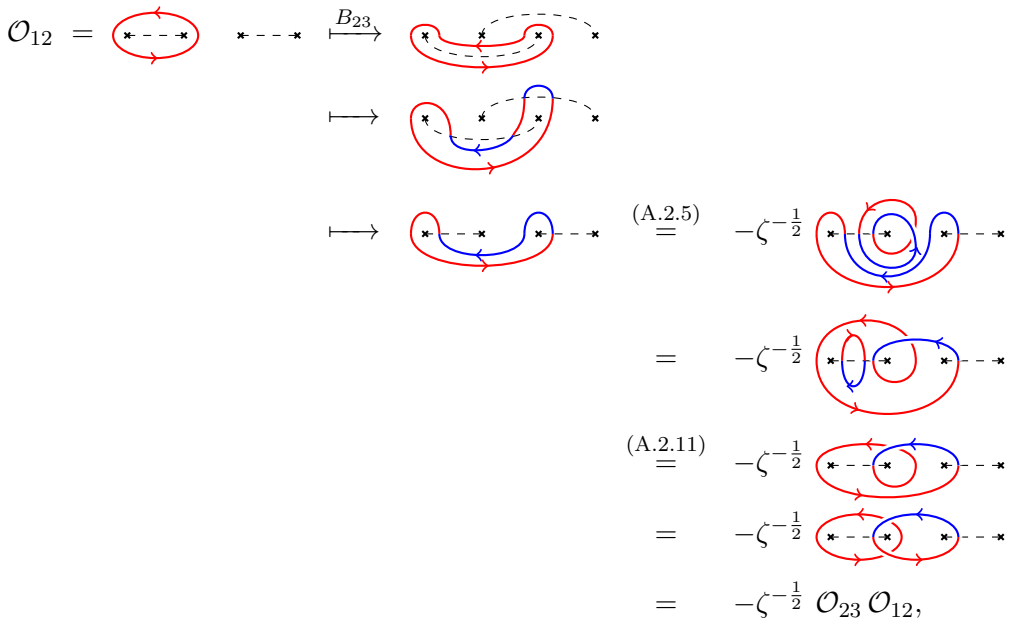

(3.6.6)

where again we have fused and unfused both the electric and magnetic lines.

We conclude that the braiding transformations satisfy

$$B_{12}: \begin{cases} \mathcal{O}_{12} \mapsto \mathcal{O}_{12} \\ \mathcal{O}_{23} \mapsto -\zeta^{-\frac{1}{2}}\,\mathcal{O}_{12}^{\dagger}\,\mathcal{O}_{23} \end{cases} \tag{3.6.7}$$

and

$$B_{23}: \begin{cases} \mathcal{O}_{12} \mapsto -\zeta^{-\frac{1}{2}}\,\mathcal{O}_{23}\,\mathcal{O}_{12} \\ \mathcal{O}_{23} \mapsto \mathcal{O}_{23}. \end{cases} \tag{3.6.8}$$

As in Section 2.13 we want to find two unitary operators T_{12} and T_{23}, acting on the ground state subspace that satisfy

$$T_{12}^{\dagger}\,\mathcal{O}_{12}\,T_{12} = \mathcal{O}_{12}, \tag{3.6.9}$$

$$T_{12}^\dagger \, \mathcal{O}_{23} \, T_{12} = -\zeta^{-\frac{1}{2}} \, \mathcal{O}_{12}^\dagger \, \mathcal{O}_{23}, \tag{3.6.10}$$

$$T_{23}^\dagger \, \mathcal{O}_{12} \, T_{23} = -\zeta^{-\frac{1}{2}} \, \mathcal{O}_{23} \, \mathcal{O}_{12}, \tag{3.6.11}$$

and

$$T_{23}^\dagger \, \mathcal{O}_{23} \, T_{23} = \mathcal{O}_{23}. \tag{3.6.12}$$

According to Theorem A.4 (see Appendix A.3 for the proof) the following two operators solve equations (3.6.9) - (3.6.12):

$$T_{12} := \mathrm{e}^{\mathrm{i}\psi_{12}} \sum_r \zeta^{\frac{r(N-r)}{2}} \, |r\rangle\langle r| \tag{3.6.13}$$

and

$$T_{23} := \frac{\mathrm{e}^{\mathrm{i}\psi_{23}}}{\sqrt{N}} \sum_{r,r'} \zeta^{\frac{1}{2}(r-r'-N/2)^2} \, |r\rangle\langle r'| \,, \tag{3.6.14}$$

where $\sum_{r,r'}$ denotes the double sum over $r, r' \in \{0, 1, ..., N-1\}$ and where $\psi_{12}, \psi_{23} \in \mathbb{R}$ are arbitrary phases. Furthermore, if we choose ψ_{12} and ψ_{23} such that

$$\psi_{12} - \psi_{23} = \frac{\pi}{4}, \tag{3.6.15}$$

then, by Theorem A.5, the braid group equation

$$T_{12} \, T_{23} \, T_{12} = T_{23} \, T_{12} \, T_{23} \tag{3.6.16}$$

is satisfied as well [25, p. 5]. By choosing the phases accordingly, we see that the space of ground states carries a genuine representation of the braid group. For other choices of phase, the braid group equation is only satisfied up to a phase. In the latter case we have a *projective* representation of the braid group.

In conclusion, we have seen that we can find non-contractible loops that label different ground states which are induced by the addition of dislocation pairs. The braiding of these dislocations deform the loops into each other and thus transforms one ground state into another. The operators T_{ij} represent the non-abelian Berry phase that is acquired over the course of braiding defects i and j.

3.7 Charge conjugate duality dislocations

As implied by the braiding rule (3.3.21) and the discussion thereafter, the $\mathbb{Z}_N$ plaquette model has an intrinsic charge conjugate duality. We have already seen how the e-m duality can be realized with dislocations, so it is natural to ask whether there is another type of dislocation that realizes the charge conjugate duality. The answer to this question is yes.

To avoid realizing the e-m duality simultaneously we now consider lattice dislocations for which 3 rows of plaquettes are removed instead of 2, as shown in the following picture:

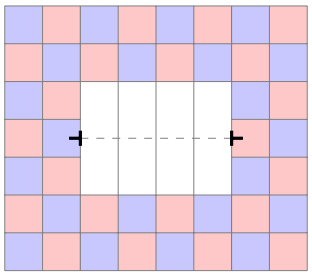

(3.7.1)

The symbol ⊣ denotes edge dislocations connected by a dashed defect line, which is denoted by $\mathcal{C}$. The *triple plaquettes* are colored in white. A natural choice of new plaquette operators would

be to again have counter-clockwise loops going around each triple plaquette. However, we shall see that there is another choice that we can make and still have all new plaquette operators commute with all the original ones.

Let $\mathrm{P}_{\mathcal{C}} \subset \mathrm{P}$ be the set of all triple plaquettes in the "interior' of the defect line and let $\partial\mathrm{P}_{\mathcal{C}} \subset \mathrm{P}_{\mathcal{C}}$ be the set of the two triple plaquettes located at the ends of the defect line. Then the definition of the triple plaquette operators on the interior of the defect line is

$$P_q = \quad = Z_1\, X_2\, Z_3\, X_4 \quad \text{for } q \in \mathrm{P}_{\mathcal{C}} \setminus \partial\mathrm{P}_{\mathcal{C}} \tag{3.7.2}$$

and the plaquette operators at the edges are defined, for $q \in \partial\mathrm{P}_{\mathcal{C}}$, by

$$P_q = \quad = Z_1\, X_2\, Z_3\, X_4\, Z_5^\dagger\, X_6^\dagger \quad \text{(left dislocation)} \tag{3.7.3}$$

and

$$P_q = \quad = Z_1\, X_2\, Z_3\, X_4\, Z_5^\dagger\, X_6^\dagger \quad \text{(right dislocation).} \tag{3.7.4}$$

These operators effectively realize the charge conjugate duality, as can be seen in the following example:

Example 3.3. Consider the following string S which creates positive charges on both plaquettes p_1 and p_2:

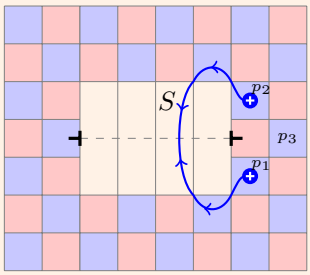

(3.7.5)

In order to be compatible with orientation, we have to require that the orientation of a string gets reversed when passing the defect line. Also note that should both ends continue into plaquette p_3 they would not cancel out, thus not closing the string, unless the charge on p_1 were the conjugate of the charge on p_2.

Apparently, the new plaquette operators measure charge differently than the plaquette operators in the absence of dislocations. On the bottom side they measure a positive charge from an exiting string and a negative charge from an entering string, just as in Proposition 3.1. On the top side, however, it is the other way around, positive charges are created by entering strings and negative charges by exiting strings. Thus, closed strings crossing the defect line are possible only when passing the defect line twice (or an even number of times). This is similar to the e-m duality for which we obviously cannot close a string crossing the defect line once, since the two ends then have different colors. The reason in the case of charge conjugation is that the ends of the strings have opposite orientation, as can be seen in Example 3.3. For e-m duality defects these closed loops were generated by the P_q operators defined at the edges of the defect line by equations (3.4.8) and (3.4.9), and in the case of charge conjugation the loops are generated by the operators P_q both in the interior and on the edges of the defect line.

Example 3.4. The following picture illustrates a closed string S crossing the defect line twice:

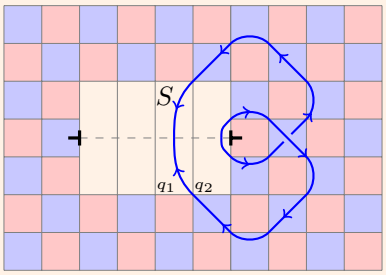

(3.7.6)

Here, P_{q_1} measures neutral charge since S enters at the top and bottom, creating conjugate charges. The same is true for P_{q_2} except here S exits on both places.

As could be seen in Example 3.3, a string crossing the defect line once creates identical charges on both end points. Therefore, should they meet on the same plaquette, they will only neutralize if they are self-conjugate. Having in mind Lemma 3.5 and the discussion following it, we see that a $\mathbb{Z}_N$ plaquette model includes a self-conjugate charge if and only if N is even. Such a charge can be created with $\frac{N}{2}$ multiples of the same string operator.

Example 3.5. Here the Z_i operator acts $N/2$ times. Since $-N/2 = N/2$ (modulo N) when N is even, the string is unoriented and the charges are self-conjugate:

$$\left(Z_i\right)^{\frac{N}{2}} = \left(Z_i^\dagger\right)^{\frac{N}{2}} = \quad \text{i} \tag{3.7.7}$$

By taking $N/2$ multiples of the same string we could in this was create a closed string passing the defect line only once, as can be seen in the following example:

Example 3.6. The closed string S is a product of plaquette operators.

$$S = -P_q^{\frac{N}{2}} O_p^{\frac{N}{2}} = \quad \text{S} \,, \tag{3.7.8}$$

where the sign factor is due to the commutation rules of the involved operators.

The class of closed strings represented by S in Example 3.6 is generated by the triple plaquette operators already introduced. However, there is another class of such strings that can not be generated by operators already introduced, namely closed strings that go around either dislocation as tightly as possible, as can be seen in the following example:

Example 3.7. The operator

$$\left(Z_1\right)^{\frac{N}{2}}\left(X_2\right)^{\frac{N}{2}} = \quad , \tag{3.7.9}$$

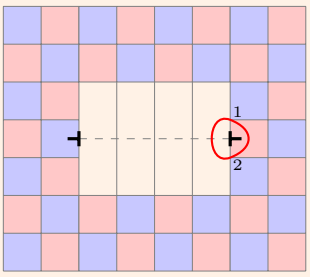

is a closed string passing the defect line only once.

The above discussion and Example 3.7 motivates us to define, for even N, *dislocation loop operators*, for $q \in \partial \mathrm{P}_{\mathcal{C}}$, by

$$C_q = \quad = \left(-Z_1\, X_2\right)^{\frac{N}{2}} \quad \text{(left dislocation)} \tag{3.7.10}$$

and

$$C_q = \quad = \left(-X_1\, Z_2\right)^{\frac{N}{2}} \quad \text{,(right dislocation)} \tag{3.7.11}$$

where $q \in \partial \mathrm{P}_{\mathcal{C}}$ now indicates that the operator involves sites in the plaquette in either edge of the defect line $\mathcal{C}$. The factor of -1 is, for now, an unimportant choice included for later convenience. We see that

$$\left(C_q\right)^2 = \left(-Z_1\, X_2\right)^{\frac{N}{2}} \left(-Z_1\, X_2\right)^{\frac{N}{2}} = (-1)^N \left(Z_1\right)^N \left(X_2\right)^N = \mathbf{1}, \tag{3.7.12}$$

since N is even and $[Z_1, X_2] = 0$. Equation (3.7.12) means in particular that the operator C_q has two eigenvalues, ± 1. For convenience, we say that C_q are plaquette operators.

It is not hard to show that the new operators P_q and C_q all commute with each other and with the old plaquette operators. The new operators are not closed strings in the same sense as before since they have end points according to the previous definition. At these end points no charges are created, however, because of the orientation reversal at the defect line, and so in this sense the new operators are also closed strings without end points.

We redefine the Hamiltonian $H_0^{\mathcal{C}}$ as the sum of the new set of plaquette operators and their hermitian adjoints,

$$H_0^{\mathcal{C}} = \begin{cases} -\frac{1}{2} \sum\limits_{p \in \mathrm{P} \setminus \mathrm{P}_{\mathcal{C}}} \left(O_p + O_p^\dagger\right) - \frac{1}{2} \sum\limits_{q \in \overline{\mathrm{P}}_{\mathcal{C}}} \left(P_q + P_q^\dagger\right), & N \text{ odd}, \\ -\frac{1}{2} \sum\limits_{p \in \mathrm{P} \setminus \mathrm{P}_{\mathcal{C}}} \left(O_p + O_p^\dagger\right) - \frac{1}{2} \sum\limits_{q \in \overline{\mathrm{P}}_{\mathcal{C}}} \left(P_q + P_q^\dagger + 2C_q\right), & N \text{ even}. \end{cases} \tag{3.7.13}$$

The constraint equations for N odd are

$$O_p = 1 \quad \forall p \in \mathrm{P} \setminus \mathrm{P}_{\mathcal{C}} \tag{3.7.14}$$

and

$$P_q = 1 \quad \forall q \in \mathrm{P}_{\mathcal{C}}, \tag{3.7.15}$$

with the addition for N even of

$$C_q = 1 \quad \forall q \in \partial \mathrm{P}_{\mathcal{C}}. \tag{3.7.16}$$

Thus there are $|P|$ constraint equations for odd N and $|P|+2$ for even N.

First we calculate the effects of charge conjugate dislocations on ground state degeneracy for odd N. For every pair of dislocations removing k sites, $3\left(\frac{k}{2}+1\right)$ plaquette operators are also removed. We then redefine $\frac{k}{2}+1$ triple plaquette operators for a total loss of

$$3\left(\frac{k}{2}+1\right)-\left(\frac{k}{2}+1\right)=k+2, \tag{3.7.17}$$

which then also is the total loss of constraint equations. Each independent equation reduces the ground state space dimension with a factor of N^{-1}. After the loss of $k+2$ equations, the total constraint factor becomes reduced by a factor of N^{k+2}. Each site contributes with dimension N, so the total space dimension is reduced by a factor of N^{-k}. The resulting factor on the ground state space dimension for N odd, by adding one pair of charge conjugate dislocations, is

$$\frac{1}{N^k}\cdot\frac{1}{N^{-(k+2)}}=N^2. \tag{3.7.18}$$

For even N we have two extra constraint equations, each reducing the ground state space by a factor of $1/2$. Thus we get the resulting factor on the ground state space dimension for N even, when adding one pair of charge conjugate dislocations, by taking

$$\frac{1}{N^k}\cdot\frac{1}{N^{-(k+2)}}\cdot\frac{1}{2^2}=\left(\frac{N}{2}\right)^2. \tag{3.7.19}$$

Similar to what was done before, we formally attribute each charge conjugate duality dislocation a quantum dimension N for odd N and quantum dimension $N/2$ for even N. In particular we see that for $N=2$ the degeneracy of the ground state is unaltered, each dislocation having quantum dimension 1.

The first pair of defects is, however, special, just like in the case of e-m duality dislocations. Recall that the degeneracies in Theorem 3.11 were calculated using the fact that charges were created in conjugate pairs and thus we could expect global charge neutrality. In Example 3.3 we can clearly see that charges no longer necessarily cancel each other out. Furthermore, with the charge conjugate duality defect, charge creation can now be achieved singularly, as can be seen in the following example:

Example 3.8. Consider the open string S defined by

$$S=X_6^\dagger=$$

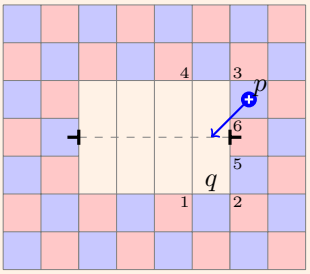

. (3.7.20)

S creates a positive charge on plaquette p, measurable by the operator O_p. However, S commutes with $P_q=Z_1\,X_2\,Z_3\,X_4\,Z_5^\dagger\,X_6^\dagger$ from (3.7.4), so no charge is created on the triple plaquette q.

For even N there is a partial remedy in the form of the operator $C_q=(-X_5\,Z_6)^{\frac{N}{2}}$ from (3.7.11). Here, by using (3.1.13) $N/2$ times, we have

$$C_q\,S=(-X_5\,Z_6)^{\frac{N}{2}}\;X_6^\dagger=\zeta^{\frac{N}{2}}\,X_6^\dagger\,(-X_5\,Z_6)^{\frac{N}{2}}=-S\,C_q, \tag{3.7.21}$$

thus measuring a charge with the dislocation loop operator. For an even number charge however, for example the open string $S' = X_6^\dagger X_6^\dagger$, creating a $+2$ charge on plaquette p, the same reasoning would lead to no charge being measured with the dislocation loop operator.

Example 3.9. Another example of charges not being created in pairs is the string S'' given in the following picture by

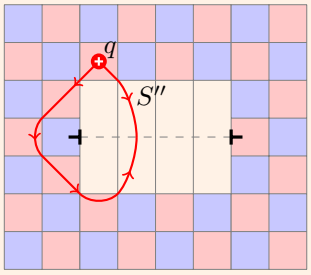

. (3.7.22)

The charge q is two copies of the same positive charge, and thus it is always an even number charge. In particular this means that for even N, q can only take on half of the possible charge values. For odd N, however, we have $N+1$ an even number, and with $q = (N+1)_{\mathrm{mod}\, N} = 1$ it is obvious that all the possible charge values are possible.

We consider the ground state degeneracy for an odd period lattice. As seen in Examples 3.8 and 3.9, the charges are no longer required to be created in pairs, so we can no longer impose equation (3.4.4), which previously had made one of the constraint equations obsolete. Except for the first pair, for odd N, each pair of dislocations affects the ground state degeneracy by a factor N^2. When adding the first pair, equation (3.4.4) is removed, so another constraint equation is added, affecting the ground state degeneracy by a factor N^{-1}. The resulting factor becomes

$$\frac{1}{N^k} \cdot \frac{1}{N^{-(k+2)}} \cdot \frac{1}{N} = N, \quad \text{for odd } N \text{ and odd period lattice.} \tag{3.7.23}$$

For even N, we first impose the constraint equations of the two extra plaquette operators C_q, which affect degeneracy by a factor 2^{-1} each. Thus we know that charges cannot be created as in Example 3.8. The remaining possibility to create a charge on a single plaquette alone is the one seen in Example 3.9. There we saw that such a string can only create an even valued charge. Thus we can impose constraint equations in the usual way on all plaquettes except one, but the final plaquette can then only take on even charge values, so the last constraint only affects the ground state degeneracy by a factor $2/N$. The resulting factor becomes

$$\frac{1}{N^k} \cdot \frac{1}{N^{-(k+2)}} \cdot \frac{1}{2} \cdot \frac{1}{2} \cdot \frac{2}{N} = \frac{N}{2}, \quad \text{for even } N \text{ and odd period lattice.} \tag{3.7.24}$$

Now consider an even period lattice. The difference from odd period lattices is that now we have two equations that no longer hold, namely (3.4.2) and (3.4.3). We get the resulting factors

$$\frac{1}{N^k} \cdot \frac{1}{N^{-(k+2)}} \cdot \frac{1}{N} \cdot \frac{1}{N} = 1, \quad \text{for odd } N \text{ and even period lattice,} \tag{3.7.25}$$

and

$$\frac{1}{N^k} \cdot \frac{1}{N^{-(k+2)}} \cdot \frac{1}{2} \cdot \frac{1}{2} \cdot \frac{2}{N} \cdot \frac{2}{N} = 1, \quad \text{for even } N \text{ and even period lattice.} \tag{3.7.26}$$

In conclusion, for n pairs of charge conjugate dislocations we state the following theorem:

Theorem 3.13. *For a $\mathbb{Z}_N$ lattice with*

(i) odd N, at least one odd period, periodic boundary conditions and with n pairs of charge conjugate duality dislocations, the ground state degeneracy is given by

$$\tilde{\tilde{D}}^n_\Omega = \begin{cases} N & \text{for } n = 0 \\ N^{2n} & \text{for } n = 1, 2, ... \end{cases} \tag{3.7.27}$$

(ii) even N, at least one odd period, periodic boundary conditions and with n pairs of charge conjugate duality dislocations, the ground state degeneracy is given by

$$\tilde{\tilde{D}}^n_\Omega = \begin{cases} N & \text{for } n = 0 \\ \dfrac{N^{2n}}{2^{2n-1}} & \text{for } n = 1, 2, ... \end{cases} \tag{3.7.28}$$

(iii) odd N, even periods, periodic boundary conditions and with n pairs of charge conjugate duality dislocations, the ground state degeneracy is given by

$$\tilde{\tilde{D}}^n_\Omega = \begin{cases} N^2 & \text{for } n = 0 \\ N^{2n} & \text{for } n = 1, 2, ... \end{cases} \tag{3.7.29}$$

(iv) even N, even periods, periodic boundary conditions and with n pairs of charge conjugate duality dislocations, the ground state degeneracy is given by

$$\tilde{\tilde{D}}^n_\Omega = \begin{cases} N^2 & \text{for } n = 0 \\ \dfrac{N^{2n}}{2^{2n-2}} & \text{for } n = 1, 2, ... \end{cases} \tag{3.7.30}$$

3.8 A basis for the space of ground states with charge conjugate duality dislocations

We can find a basis for the space of ground states by finding non-contractible loop operators. For convenience we consider the case of $n = 2$ pairs of dislocations, so that the degeneracy has increased by a factor of N^2 for even N and $(N/2)^2$ for odd N. To span this additional ground state space we need the four loops $\mathcal{O}^e_{12}$,$\mathcal{O}^m_{12}$,$\mathcal{O}^e_{23}$ and $\mathcal{O}^m_{23}$, given by the following picture:

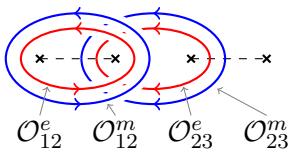

. (3.8.1)

The superscripts e and m indicate whether the loop is electric or magnetic.

By the braiding rules of (3.3.21) it is easily checked that

$$\mathcal{O}^m_{23}\,\mathcal{O}^e_{12} = \zeta^2\,\mathcal{O}^e_{12}\,\mathcal{O}^m_{23}, \tag{3.8.2}$$

$$\mathcal{O}^e_{23}\,\mathcal{O}^m_{12} = \zeta^2\,\mathcal{O}^m_{12}\,\mathcal{O}^e_{23}, \tag{3.8.3}$$

and

$$[\mathcal{O}^e_{12}, \mathcal{O}^e_{23}] = [\mathcal{O}^m_{12}, \mathcal{O}^m_{23}] = [\mathcal{O}^e_{12}, \mathcal{O}^m_{12}] = [\mathcal{O}^e_{23}, \mathcal{O}^m_{23}] = 0. \tag{3.8.4}$$

Let $|r_e, r_m\rangle := |r_e\rangle \otimes |r_m\rangle$ denote the common eigenstates of $\mathcal{O}^e_{12}$ and $\mathcal{O}^m_{12}$, where r_e and r_m are to be taken as modulo N throughout, such that

$$\mathcal{O}^e_{12}\ |r_e, r_m\rangle = \zeta^{r_e}\ |r_e, r_m\rangle \tag{3.8.5}$$

and

$$\mathcal{O}^m_{12}\ |r_e, r_m\rangle = \zeta^{r_m}\ |r_e, r_m\rangle\,. \tag{3.8.6}$$

Then, by (3.8.2) and (3.8.3), we have

$$\mathcal{O}^e_{23}\ |r_e, r_m\rangle = \ |r_e, (r_m - 2)\rangle \tag{3.8.7}$$

and

$$\mathcal{O}^m_{23}\ |r_e, r_m\rangle = \ |(r_e - 2), r_m\rangle\,. \tag{3.8.8}$$

Explicitly we have

$$\mathcal{O}^e_{12} = \sum_{r_e, r_m} \zeta^{r_e}\, |r_e, r_m\rangle\langle r_e, r_m|\,, \tag{3.8.9}$$

$$\mathcal{O}^m_{12} = \sum_{r_e, r_m} \zeta^{r_m}\, |r_e, r_m\rangle\langle r_e, r_m|\,, \tag{3.8.10}$$

$$\mathcal{O}^e_{23} = \sum_{r_e, r_m} |r_e, (r_m - 2)\rangle\langle r_e, r_m| \tag{3.8.11}$$

and

$$\mathcal{O}^m_{23} = \sum_{r_e, r_m} |(r_e - 2), r_m\rangle\langle r_e, r_m|\,, \tag{3.8.12}$$

where the sum $\sum_{r_e, r_m}$ denotes the double sum over all $r_e, r_m \in \{0, 1, ..., N-1\}$.

From (3.8.2) we also see that for even N we have

$$\mathcal{O}^m_{23}\ (\mathcal{O}^e_{12})^{N/2} = \zeta^N\ (\mathcal{O}^e_{12})^{N/2}\ \mathcal{O}^m_{23} = (\mathcal{O}^e_{12})^{N/2}\ \mathcal{O}^m_{23}, \tag{3.8.13}$$

which shows that this set of operators can only generate $N/2$ orthogonal states and thus the algebra only requires an $N/2$ dimensional representation space. A similar statement can be proved using equation (3.8.3). For odd N however, $N/2$ is not an integer so equation (3.8.13) does not hold. This illustrates the difference in degeneracy depending on the parity of N, found in (3.7.18) and (3.7.19). For convenience we introduce the notation

$$\mathcal{N} = \begin{cases} N/2 & \text{for even } N, \\ N & \text{for odd } N, \end{cases} \tag{3.8.14}$$

so that the quantum dimension of each charge conjugate dislocation is simply $\mathcal{N}$ [25, p. 6].

3.9 Braiding properties of charge conjugate duality dislocations

To determine the braiding properties we first note that when restricted to the space of ground states we have

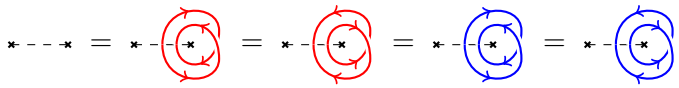

(3.9.1)

which is evident from the macroscopic picture illustrated in (3.7.6), and can also be seen from Proposition 3.8 stating the trivial fusion rules for purely electric or magnetic objects. Also we have

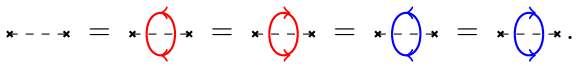

(3.9.2)

We consider the braiding for the case of $n = 2$ dislocations, again assuming that the rule of paired charges has been broken, so that the degeneracy has increased by a factor of $\mathcal{N}$. The counter-clockwise braiding of dislocation i and j is denoted B_{ij} as described in Section 2.13. We only consider the effects of braiding on the electric operators $\mathcal{O}^e_{12}$ and $\mathcal{O}^e_{23}$, the results being analogous for their magnetic counterparts.

Similarly to what was already discussed, it is obvious that B_{12} does nothing to $\mathcal{O}^e_{12}$, and the same holds for B_{23} with $\mathcal{O}^e_{23}$. Now take

$\mathcal{O}^e_{23} =$ 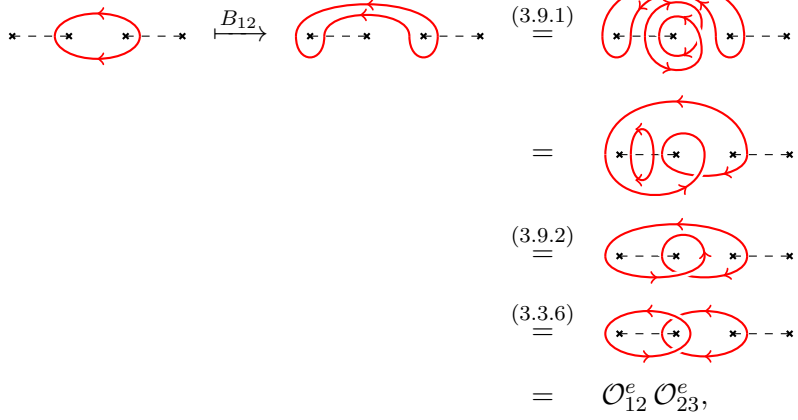

$= \mathcal{O}^e_{12}\,\mathcal{O}^e_{23},$ (3.9.3)

where we have fused and unfused strings. We also consider

$\mathcal{O}^e_{12} =$ 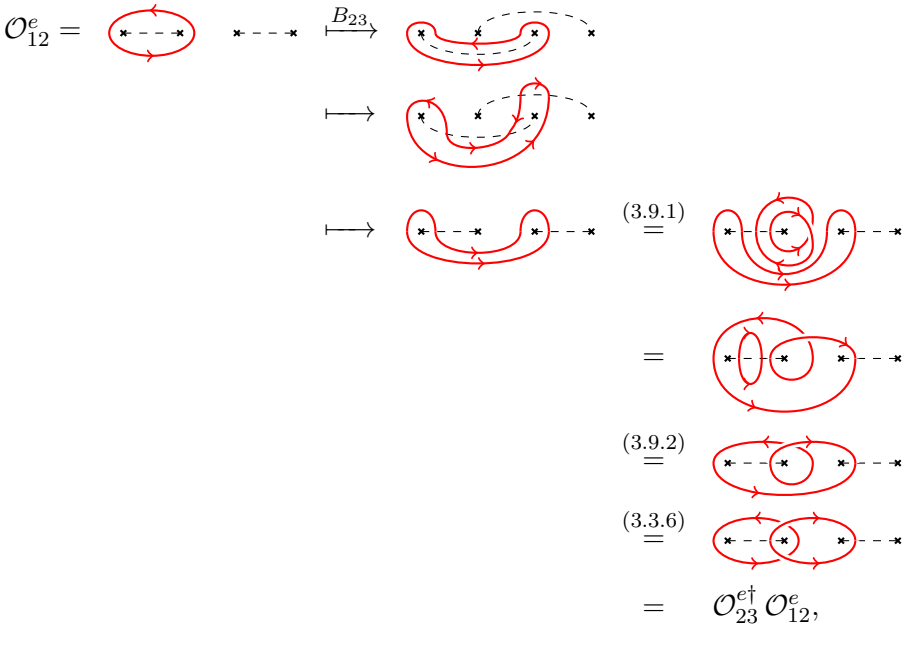

$= \mathcal{O}^{e\dagger}_{23}\,\mathcal{O}^e_{12},$ (3.9.4)

where we have rearranged the defect lines after the braiding. We summarize the results as follows:

$$B_{12} : \begin{cases} \mathcal{O}^{e(m)}_{12} \mapsto \mathcal{O}^{e(m)}_{12} \\ \mathcal{O}^{e(m)}_{23} \mapsto \mathcal{O}^{e(m)}_{12}\,\mathcal{O}^{e(m)}_{23} \end{cases} \tag{3.9.5}$$

and

$$B_{23} : \begin{cases} \mathcal{O}^{e(m)}_{12} \mapsto \mathcal{O}^{e(m)\dagger}_{23}\,\mathcal{O}^{e(m)}_{12} \\ \mathcal{O}^{e(m)}_{23} \mapsto \mathcal{O}^{e(m)}_{23}. \end{cases} \tag{3.9.6}$$

Similarly as before we search for two unitary operators T_{12} and T_{23}, acting on the ground state subspace and satisfying the 8 equations

$$T^\dagger_{12}\,\mathcal{O}^{e(m)}_{12}\,T_{12} = \mathcal{O}^{e(m)}_{12}, \tag{3.9.7}$$

$$T^\dagger_{12}\,\mathcal{O}^{e(m)}_{23}\,T_{12} = \mathcal{O}^{e(m)}_{12}\,\mathcal{O}^{e(m)}_{23}, \tag{3.9.8}$$

$$T^\dagger_{23}\,\mathcal{O}^{e(m)}_{12}\,T_{23} = \mathcal{O}^{e(m)\dagger}_{23}\,\mathcal{O}^{e(m)}_{12}, \tag{3.9.9}$$

and

$$T_{23}^{\dagger}\,\mathcal{O}_{23}^{e(m)}\,T_{23} = \mathcal{O}_{23}^{e(m)}. \tag{3.9.10}$$

The two unitary operators given by

$$T_{12} = \mathrm{e}^{\mathrm{i}\psi_{12}} \sum_{r_e, r_m} \zeta^{\frac{1}{2} r_e r_m} \, |r_e, r_m\rangle\langle r_e, r_m| \,, \tag{3.9.11}$$

and

$$T_{23} = \frac{\mathrm{e}^{\mathrm{i}\psi_{23}}}{\mathcal{N}} \sum_{\substack{r_e, r_m \\ r'_e, r'_m}} \zeta^{-\frac{1}{2}(r_e - r'_e)(r_m - r'_m)} \, |r_e, r_m\rangle\langle r'_e, r'_m| \,, \tag{3.9.12}$$

with $\mathcal{N}$ as in (3.8.14), ψ_{12} and ψ_{23} are arbitrary phases and where

$$r_e, r_m, r'_e, r'_m \in \{0, 2, ..., 2(\mathcal{N} - 1)\}, \tag{3.9.13}$$

solve these equations by Theorem A.6, as first suggested by You, Jian and Wen in [25, p. 6]. Furthermore, by Theorem A.7, if we choose ψ_{12} and ψ_{23} such that

$$\psi_{12} = \psi_{23}, \tag{3.9.14}$$

then the braid group equation

$$T_{12}\,T_{23}\,T_{12} = T_{23}\,T_{12}\,T_{23} \tag{3.9.15}$$

is also satisfied. Thus, the space of ground states with charge conjugate dislocations also carries a genuine representation of the braid group. For other choices of phase we have a projective representation of the braid group. The dislocations can be seen as a kind of quasi-particle with non-commutative braiding properties, which is why sometimes in the literature they are referred to as *projective non-abelian anyons* and also sometimes as *genons* [2].

4 Synthetic dislocations

In the previous sections we have seen how both the e-m and charge conjugate dualities can be realized by the introduction of defects and how the dislocations expand the ground state subspace dimension in different ways. Furthermore, we have found a basis for the extra dimensions of the ground state subspace and derived braiding properties for the dislocations. We found that by braiding two dislocations counter-clockwise we can transform one ground state into another. But can these dislocations be created in a controlled manner? And how would you go about moving a physical dislocation in a lattice? This question is addressed in [25] for the same type of lattice dislocations that we have been considering. Other types of synthetic dislocations have also been considered, for example in [4]. The proposal is that it may be possible to emulate lattice dislocations by external fields that can be moved or switched on and off at will, and that these fields can be described by a perturbation to the Hamiltonian.

In this section we review the suggestions on how to realize such synthetic dislocations given in [25]. The connection and similarity between this type of dislocations and the lattice dislocations of Section 2 and 3 is illustrated mainly by examples for the $N = 2$ case.

4.1 Synthetic e-m dislocations

We start with the lattice model described in Section 2.1-2.8 for the case of $N = 2$, with the unperturbed Hamiltonian given by

$$H_0 = -\sum_{p\in \mathrm{P}} O_p, \tag{4.1.1}$$

where O_p are the plaquette operators (2.2.3). The full Hamiltonian is then

$$H = H_0 + g\, H_{\mathcal{C}}, \tag{4.1.2}$$

where g is a coupling constant, $\mathcal{C}$ denotes the defect line and where

$$H_{\mathcal{C}} = \sum_{i\in \mathrm{M}_{\mathcal{C}}} \sigma_i^y. \tag{4.1.3}$$

Here $\mathrm{M}_{\mathcal{C}}$ is the set of sites which should be "removed" in order to create the defect line.

It is clear from our previous considerations that $\sigma_i^y = \mathrm{i}$  acts on the site i as two open strings, creating two pairs of excitations diagonally:

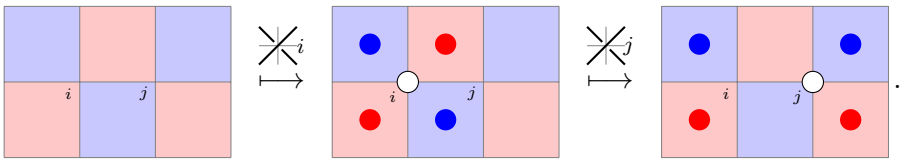

. (4.1.4)

Here the second step shows that acting on a consecutive line of sites $\mathrm{M}_{\mathcal{C}}$ with σ^y, first creates two pairs and then moves them apart from each other and along the defect line $\mathcal{C}$. The pairs of charges on each side of $\mathcal{C}$ correspond to the class ϵ of simple objects, or what we have previously referred to as dyons. We may also translate this action in terms of dyon creation and annihilation operators, $d_q^\dagger$ and d_q, where q is the label of the "double plaquette" at which the dyon is to be created. Then we have

$$\sigma_i^y = d_q^\dagger\, d_{q+1}^\dagger + d_q^\dagger\, d_{q+1} + d_{q+1}\, d_q + d_{q+1}^\dagger\, d_q; \tag{4.1.5}$$

A proof of this identity can be found in Appendix A.7.

For small values of the coupling constant g the ground state degeneracy is unchanged, but for values above some critical value $g = g_c$, it is evident by inspection of the Hamiltonian in (4.1.3) that, in the ground state, the sites in $\mathrm{M}_{\mathcal{C}}$ must be polarized to the state for which

$$\sigma_i^y = -\mathbf{1}, \quad \forall i \in \mathcal{C}. \tag{4.1.6}$$

The sites involved are effectively "frozen" in their degrees of freedom; we say that the intrinsic dyons are *condensed* at the edges of the branch cut. The critical value for g turns out to be $g_c = 2$, for which You, Jian and Wen [25, p. 2] state that the system is driven into the weak pairing phase. To learn more about weak pairing, see for instance Read and Green in [18].

In [25, p. 2] the authors state that it is possible to replace the Hamiltonian with an *effective Hamiltonian* acting only on the low energy subspace, or the space of ground states for H_0. The specific calculations leading to the effective Hamiltonian are not covered by this text, but the idea is briefly described in [25]. For more information on the theory of effective Hamiltonians the reader is referred to for example [20] and [19].

Instead of going into the exact process of finding the effective Hamiltonian, we try to appreciate its emergence by considering a few examples.

For convenience we label all operators that overlap with $\mathcal{C}$ in exactly 2 sites as O_u (below $\mathcal{C}$) or $O_{\hat{u}}$ (above $\mathcal{C}$) to distinguish them from the non-overlapping ones. Operators that overlap with $\mathcal{C}$ in exactly 1 site we label as O_v and $O_{\hat{v}}$.

Example 4.1. Consider a synthetic defect line $\mathcal{C}$ with 4 sites. Plaquette operators overlapping $\mathcal{C}$ are labelled v, $\hat{v}$, u and $\hat{u}$.

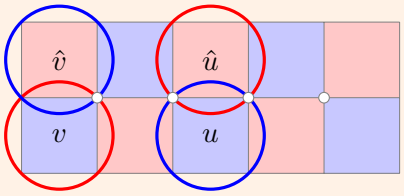

(4.1.7)

All O_p commute with H_0, so all O_p that do not overlap with $\mathcal{C}$ commute with the Hamiltonian. It is also clear that none of the operators O_r (with $r \in \{u, \hat{u}, v, \hat{v}\}$) commute with $H_{\mathcal{C}}$. In fact, they anti-commute.

However, a product of two operators O_u and $O_{\hat{u}}$, where u and $\hat{u}$ overlap at both sites in $\mathrm{M}_{\mathcal{C}}$, also commutes with $H_{\mathcal{C}}$. This is also the case for a combination of two operators O_v and $O_{\hat{v}}$, where v and $\hat{v}$ overlap on $\mathcal{C}$.

Example 4.2. Consider the case where there are only two sites in $\mathrm{M}_{\mathcal{C}}$, as seen below:

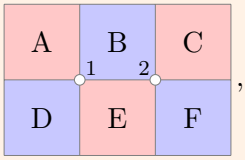

(4.1.8)

with the labels 1 and 2 for the sites in $\mathrm{M}_{\mathcal{C}}$ and the labels A through F for the plaquettes involved.

First consider $O_u O_{\hat{u}}$, which in this example is $O_B O_E$, as shown below with relabelled nodes:

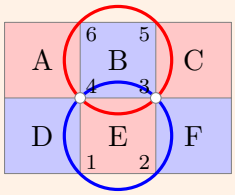

(4.1.9)

The operators are

$$O_E = \sigma_1^z \sigma_2^x \sigma_3^z \sigma_4^x \tag{4.1.10}$$

and

$$O_B = \sigma_4^z \sigma_3^x \sigma_5^z \sigma_6^x, \tag{4.1.11}$$

so

$$O_B\, O_E = (\sigma_4^z \sigma_3^x \sigma_5^z \sigma_6^x)\,(\sigma_1^z \sigma_2^x \sigma_3^z \sigma_4^x) = \sigma_1^z \sigma_2^x (-\mathrm{i}\sigma_3^y)(\mathrm{i}\sigma_4^y)\sigma_5^z \sigma_6^x = \sigma_1^z \sigma_2^x \sigma_3^y \sigma_4^y \sigma_5^z \sigma_6^x. \tag{4.1.12}$$

The defect line consists of the sites 3 and 4, so we have

$$H_{\mathcal{C}} = \sigma_3^y + \sigma_4^y, \tag{4.1.13}$$

which means that

$$[H, O_B\, O_E] = [H_{\mathcal{C}}, O_B\, O_E] = [\sigma_3^y + \sigma_4^y, \sigma_1^z \sigma_2^x \sigma_3^y \sigma_4^y \sigma_5^z \sigma_6^x] = 0. \tag{4.1.14}$$

The next case is the edge of $\mathcal{C}$ or in terms of operators, $O_v\, O_{\hat{v}}$, as shown below:

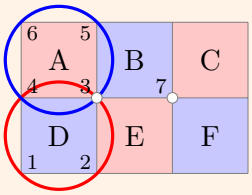

(4.1.15)

In this case, after relabelling the nodes according to the picture, we have

$$O_A\, O_D = (\sigma_4^z \sigma_3^x \sigma_5^z \sigma_6^x)\,(\sigma_1^z \sigma_2^x \sigma_3^z \sigma_4^x) = \sigma_1^z \sigma_2^x (-\mathrm{i}\sigma_3^y)(\mathrm{i}\sigma_4^y)\sigma_5^z \sigma_6^x = \sigma_1^z \sigma_2^x \sigma_3^y \sigma_4^y \sigma_5^z \sigma_6^x \tag{4.1.16}$$

and

$$H_{\mathcal{C}} = \sigma_3^y + \sigma_7^y. \tag{4.1.17}$$

By the same reasoning we get

$$[H, O_A\, O_D] = 0. \tag{4.1.18}$$

Finally, when comparing the operator $O_B\, O_E$ in (4.1.12) to the double plaquette operator P_q defined in (2.9.2), for for $g \geq g_c$, in the ground state subspace where $\sigma^y = 1$, we see that the operators are equivalent. The same comparison can be made between (4.1.16) and (2.9.4).

Example 4.2 shows that the original plaquette operators that overlap the branch cut no longer commute, but it is possible to find new such operators. The operators found are equivalent to the double plaquette operators of the *e*-*m* lattice dislocations, when acting in the ground state subspace. In fact, the second order perturbation effective Hamiltonian given in [25] is

$$H_{\text{eff}} = -\sum_{p \in \mathrm{P} \setminus \mathrm{P}_{\mathcal{C}}} O_p - \frac{1}{2g} \sum_{q \in \mathrm{P}_{\mathcal{C}} \setminus \partial \mathrm{P}_{\mathcal{C}}} P_q - \frac{1}{g} \sum_{q \in \partial \mathrm{P}_{\mathcal{C}}} P_q, \tag{4.1.19}$$

where $\mathrm{P}_{\mathcal{C}}$ is the set of all double plaquettes in $\mathcal{C}$ and $\partial \mathrm{P}_{\mathcal{C}}$ is the subset of $\mathrm{P}_{\mathcal{C}}$ containing the operators on the edges of the defect line. The effective Hamiltonian in (4.1.19) contains the same operators as the Hamiltonian from (2.9.11), and only differs by some constants. Thus, the results following equation (2.9.11) in Section 2 can also be applied to this case, showing that the *e*-*m* duality dislocations for $N = 2$ can be synthetically created by an external field.

4.2 Synthetic *e-m* dislocations for arbitrary N

To generalize the previous result to arbitrary N we use the generalized definitions of the plaquette operators from (3.1.31) and define the unperturbed Hamiltonian as

$$H_0 = -\frac{1}{2}\sum_{p\in \mathrm{P}} \left(O_p + O_p^\dagger\right), \tag{4.2.1}$$

and $H_{\mathcal{C}}$ as

$$H_{\mathcal{C}} = -\frac{1}{2}\sum_{i\in \mathrm{M}_{\mathcal{C}}} \left(Y_i + Y_i^\dagger\right), \tag{4.2.2}$$

where O_p and Y_i are the operators defined in (3.1.31) and (3.1.14) respectively. Then the Hamiltonian has the form

$$H = H_0 + g\, H_{\mathcal{C}}, \tag{4.2.3}$$

as before. For $g \geq g_c$, the second order perturbation effective Hamiltonian given in [25] is

$$H_{\text{eff}} = -\frac{1}{2}\sum_{p\in \mathrm{P}\setminus \mathrm{P}_{\mathcal{C}}} O_p - \frac{1}{4g\sin^2\left(\frac{\pi}{N}\right)}\left(\sum_{q\in \mathrm{P}_{\mathcal{C}}\setminus \partial \mathrm{P}_{\mathcal{C}}} P_q + 2\sum_{q\in \partial \mathrm{P}_{\mathcal{C}}} P_q\right) + h.c., \tag{4.2.4}$$

where the operators P_q coincide with the double plaquettes given in (3.4.7), (3.4.8) and (3.4.9) and where *h.c.* denotes the hermitian conjugate. In this case a strong g field polarizes the sites in $\mathcal{C}$ to the $Y_i = +1$ state. The difference in sign from the $N = 2$ case can be accounted for by noting that for $N = 2$ we have $Y_i = -\sigma_i^y$. The effective Hamiltonian (4.2.4) can now be compared to the one given in (3.4.11) to see that the synthetization of *e-m* dislocations is generalized to arbitrary N.

4.3 Charge conjugate dislocations

To synthetically emulate the charge conjugate dislocations we start by defining the operator

$$I_l = \frac{1}{2}\left(\begin{array}{|c|c|}\hline & 2\nearrow \\ \hline & 1\searrow \\ \hline\end{array} + \begin{array}{|c|c|}\hline & 2\searrow \\ \hline & 1\nearrow \\ \hline\end{array}\right) = \frac{1}{2}\left(Z_1\, X_2 + X_1\, Z_2\right), \tag{4.3.1}$$

where the index $l \subset \mathrm{M}_{\mathcal{C}}$ denotes a set of "linked" pair of sites 1 and 2, in the desired branch cut region $\mathcal{C}$. For this reason we refer to I_l as the *link operator*. We then define the Hamiltonian according to

$$H = H_0 + g\, H_{\mathcal{C}}, \tag{4.3.2}$$

where now

$$H_0 = -\frac{1}{2}\sum_{p\in \mathrm{P}} \left(O_p + O_p^\dagger\right), \tag{4.3.3}$$

$$H_{\mathcal{C}} = -\frac{1}{2}\sum_{l\subset \mathrm{M}_{\mathcal{C}}} \left(I_l + I_l^\dagger\right), \tag{4.3.4}$$

and g is a coupling constant as before.

By (3.1.10) we see that

$$\begin{aligned}(Z_1\, X_2)\,(X_1\, Z_2) &= Z_1\, X_1\, X_2\, Z_2 = \zeta^{-1}\, X_1\, Z_1\, X_2\, Z_2 \\ &= \zeta\,\zeta^{-1}\, X_1\, Z_1\, Z_2\, X_2 = (X_1\, Z_2)\,(Z_1\, X_2),\end{aligned} \tag{4.3.5}$$

so that

$$[Z_1\, X_2,\, X_1\, Z_2] = 0, \tag{4.3.6}$$

which means that we can find a simultaneous eigenstate of $Z_1\,X_2$ and $X_1\,Z_2$ for which $X_1\,Z_2 = Z_1\,X_2 = 1$. Thus, for strong enough g, in the ground state the link operators get polarized to a state for which

$$I_l = \mathbf{1},\ \ \forall l \subset \mathrm{M}_{\mathcal{C}}. \tag{4.3.7}$$

The second order effective Hamiltonian given in [25] is

$$H_{\text{eff}} = -\frac{1}{2}\sum_{p\in \mathrm{P}\setminus \mathrm{P}_{\mathcal{C}}} O_p - \frac{1}{4g\sin^2\left(\frac{\pi}{N}\right)}\left(\sum_{q\in \mathrm{P}_{\mathcal{C}}\setminus \partial \mathrm{P}_{\mathcal{C}}} P_q + 2\sum_{q\in \partial \mathrm{P}_{\mathcal{C}}} P_q\right) + h.c., \tag{4.3.8}$$

where P_q coincides with the triple plaquettes defined in (3.7.2), (3.7.3) and (3.7.4). It is also stated that for even N there is an $\frac{N}{2}$th order perturbation term in the effective Hamiltonian given by

$$-\,\alpha \sum_{p\in \partial \mathrm{P}_{\mathcal{C}}} C_q = -\left(\frac{g}{2}\right)^{1-N/2}\left(\frac{N}{2}\right)^{-2}\sum_{p\in \partial \mathrm{P}_{\mathcal{C}}} C_q \tag{4.3.9}$$

where C_q coincides with the dislocation loop operators from equations (3.7.10) and (3.7.11). We also note that, for $g \geq 2$, this term gets weaker with increasing N.

With the inclusion of this last term for even N we once again have an effective Hamiltonian with the same operators (except for constant coefficients) as in the case of a "physical" defect. Thus it is possible to emulate the charge conjugate dislocations with an external field.

5 Summary

In this section we summarize the previous sections, repeating important results and equations to provide an accessible overview of what has been done.

In Section 2 we started with a square lattice with periodic boundary conditions (topologically a torus) and with a 2-dimensional state space assigned to each site. The Hamiltonian defined by

$$H_0 = -\sum_{p\in \mathrm{P}} O_p, \tag{5.1}$$

where

$$O_p = \sigma_1^z\,\sigma_2^x\,\sigma_3^z\,\sigma_4^x = \quad , \tag{5.2}$$

gives rise to topological ground state degeneracy. The ground state degeneracy depends on the parity of the periodicity of the lattice, and is given by

$$\bar{D}_\Omega = 4, \tag{5.3}$$

when both periods of the lattice are even and by

$$\tilde{D}_\Omega = 2, \tag{5.4}$$

when at least one period of the lattice is odd.

The end points of open strings can be seen as quasi-particle excitations which are labeled by e and m. The fusion rules are

$$\begin{aligned} &e\otimes m \cong m\otimes e \cong \epsilon, && e\otimes e \cong \mathbf{1},\\ &m\otimes m \cong \mathbf{1}, && \epsilon\otimes\epsilon \cong \mathbf{1},\\ &\epsilon\otimes e \cong e\otimes\epsilon \cong m, && \epsilon\otimes m \cong m\otimes\epsilon \cong e. \end{aligned} \tag{5.5}$$

The braiding rules are given by

$$R_{ee} = R_{mm} = 1, \quad R_{\epsilon\epsilon} = -1, \quad R_{em}R_{me} = -1, \tag{5.6}$$

where R_{ij} characterizes the braiding of objects i over j. Since the fusion and braiding rules are invariant under the exchange of e and m, there is an e-m duality.

We introduced dislocations to the lattice by removing sites from a row and altering the Hamiltonian to become

$$H_0^{\mathcal{C}} = -\sum_{p\in \mathrm{P}\setminus \mathrm{P}_{\mathcal{C}}} O_p - \sum_{q\in \mathrm{P}_{\mathcal{C}}} P_q, \tag{5.7}$$

where $\mathcal{C}$ denotes the branch cut, $\mathrm{P}_{\mathcal{C}}$ denotes the set of new plaquettes along $\mathcal{C}$ and where P_q are products of Pauli operators as given by (2.9.2), (2.9.3) and (2.9.4). We saw that an e-charge crossing the defect line turns into an m-charge and vice versa. The introduction of n pair(s) of dislocations also altered the ground state degeneracy according to

$$\bar{D}_\Omega^n = \begin{cases} 2^2 & \text{for } n = 0,\\ 2^{n+1} & \text{for } n = 1, 2, \ldots \end{cases} \tag{5.8}$$

for even period lattices and

$$\tilde{D}_\Omega^n = 2^{n+1} \quad \text{for } n = 0, 1, \ldots \tag{5.9}$$

for odd period lattices. In particular we noted that for $n > 0$ the ground state degeneracy does no longer depend on the parity of the lattice periods. Adding the first pair of dislocations breaks any global distinction between e and m charges.

Strings without end points (closed strings, or loops) were found to commute with the Hamiltonian, thus leaving energy eigenstates invariant under their operation. Non-contractible loops, closed strings that cannot continuously be deformed to a point by basic operations, could then be used to characterize different degenerate states. In Section 2.10, a basis for the space of ground states was found by identifying the proper set of non-contractible loops. In Section 2.12 we saw how this basis can be expanded with the introduction of dislocation pairs. Then, using the new set of non-contractible loops represented by the operator $\mathcal{O}_{ij}$, denoting a loop going around dislocations i and j, braiding properties of the dislocations themselves were calculated, given by

$$\begin{aligned} T_{12}^\dagger \mathcal{O}_{12} T_{12} &= \mathcal{O}_{12}, & T_{12}^\dagger \mathcal{O}_{23} T_{12} &= \mathrm{i}\, \mathcal{O}_{12} \mathcal{O}_{23}, \\ T_{23}^\dagger \mathcal{O}_{12} T_{23} &= \mathrm{i}\, \mathcal{O}_{23} \mathcal{O}_{12}, & T_{23}^\dagger \mathcal{O}_{23} T_{23} &= \mathcal{O}_{23}. \end{aligned} \tag{5.10}$$

It was also proved that the unitary operators T_{12} and T_{23} given in (2.13.19) and (2.13.20) solve these equations. We noted that also the braid group relation is satisfied by T_{12} and T_{23}, concluding that the space of ground states carries a representation of the braid group. The braiding properties of the dislocations resemble those of non-abelian anyons, even though they are extrinsic defects of the lattice for a Hamiltonian describing abelian anyons.

In Section 3 we performed a generalization of Section 2 to a lattice with an N-dimensional state space assigned to each site. The Hamiltonian was defined in the same way as before, with the exception that strings were now oriented, as can be seen when considering the plaquette operator

$$O_p = Z_1 X_2 Z_3^\dagger X_4^\dagger = \tag{5.11}$$

where Z and X are generalizations of the Pauli operators σ^z and σ^x, with more general commutation rules.

The e-m duality was realised in a similar way for general N, and the ground state degeneracy for n pair(s) of dislocations was given by

$$\bar{D}_\Omega^n = \begin{cases} N^2 & \text{for } n = 0, \\ N^{n+1} & \text{for } n = 1, 2, ... \end{cases} \tag{5.12}$$

for even period lattices and

$$\tilde{D}_\Omega^n = N^{n+1} \quad \text{for } n = 0, 1, ... \tag{5.13}$$

for odd period lattices.

The generalized equations determining the unitary braiding operators for e-m duality dislocations were given by (3.6.9)-(3.6.12), and their solutions by (3.6.13) and (3.6.14). Also for general N it was confirmed that the braiding properties of the dislocations resembled those of non-abelian anyons.

The isomorphism classes of simple objects were represented by W_{ij}, labelling an object with an i-fold electric charge and j-fold magnetic charge. The fusion rules were given by

$$W_{i,j} \otimes W_{k,l} \cong W_{i+k,j+l}, \tag{5.14}$$

and the braiding rules by

$$R_{i,i}^{j,j} = \zeta^{ij}. \tag{5.15}$$

and

$$R_{k,i}^{l,j} R_{i,k}^{j,l} = \zeta^{il+jk}, \tag{5.16}$$

where $R_{i,k}^{j,l}$ characterizes the braiding of objects $W_{i,j}$ over $W_{k,l}$. In particular $R_{i,i}^{j,j}$ characterizes the self-braiding of $W_{i,j}$. The fusion and braiding are not only invariant under the e-m duality automorphism

$$W_{i,j} \longleftrightarrow W_{j,i}, \tag{5.17}$$

but also under the charge conjugate; an automorphism given by

$$W_{i,j} \longleftrightarrow W_{-i,-j}. \tag{5.18}$$

The latter duality symmetry was realised by a new type of dislocations removing two rows of sites from a branch cut region and altering the Hamiltonian according to

$$H_0^{\mathcal{C}} = \begin{cases} -\frac{1}{2} \sum\limits_{p \in \mathrm{P} \setminus \mathrm{P}_{\mathcal{C}}} \left(O_p + O_p^\dagger \right) - \frac{1}{2} \sum\limits_{q \in \mathrm{P}_{\mathcal{C}}} \left(P_q + P_q^\dagger \right), & N \text{ odd}, \\ -\frac{1}{2} \sum\limits_{p \in \mathrm{P} \setminus \mathrm{P}_{\mathcal{C}}} \left(O_p + O_p^\dagger \right) - \frac{1}{2} \sum\limits_{q \in \mathrm{P}_{\mathcal{C}}} \left(P_q + P_q^\dagger + 2C_q \right), & N \text{ even}. \end{cases} \tag{5.19}$$

Here, P_q and C_q were given by (3.7.2), (3.7.3), (3.7.4), (3.7.10) and (3.7.11), respectively. The Hamiltonian was defined differently depending on the parity of N, and together with differences depending on the parity of the lattice periods this led to four different cases of ground state degeneracy for n dislocation pairs, namely

$$\tilde{\tilde{D}}_\Omega^n = \begin{cases} N & \text{for } n = 0 \\ N^{2n} & \text{for } n = 1, 2, ... \end{cases} \tag{5.20}$$

for odd N, odd period,

$$\bar{\tilde{D}}_\Omega^n = \begin{cases} N & \text{for } n = 0 \\ \dfrac{N^{2n}}{2^{2n-1}} & \text{for } n = 1, 2, ... \end{cases} \tag{5.21}$$

for even N, odd period,

$$\bar{\tilde{D}}_\Omega^n = \begin{cases} N^2 & \text{for } n = 0 \\ N^{2n} & \text{for } n = 1, 2, ... \end{cases} \tag{5.22}$$

for odd N, even period and

$$\bar{\bar{D}}_\Omega^n = \begin{cases} N^2 & \text{for } n = 0 \\ \dfrac{N^{2n}}{2^{2n-2}} & \text{for } n = 1, 2, ... \end{cases} \tag{5.23}$$

for even N, even period.

Again using non-contractible loops, whose corresponding operators are given by equations (3.8.9)-(3.8.12), the braiding properties of the dislocations were determined. The unitary braiding operators should satisfy

$$\begin{aligned} T_{12}^\dagger \, \mathcal{O}_{12}^{e(m)} \, T_{12} &= \mathcal{O}_{12}^{e(m)}, & T_{12}^\dagger \, \mathcal{O}_{23}^{e(m)} \, T_{12} &= \mathcal{O}_{12}^{e(m)} \, \mathcal{O}_{23}^{e(m)}, \\ T_{23}^\dagger \, \mathcal{O}_{12}^{e(m)} \, T_{23} &= \mathcal{O}_{23}^{e(m)\dagger} \, \mathcal{O}_{12}^{e(m)}, & T_{23}^\dagger \, \mathcal{O}_{23}^{e(m)} \, T_{23} &= \mathcal{O}_{23}^{e(m)}. \end{aligned} \tag{5.24}$$

Solutions were given by (3.9.11) and (3.9.12), and by choosing phase factors according to (3.9.14) these operators also satisfied the braid group equation, showing that the dislocations resemble non-abelian anyons.

In Section 4 we saw that the e-m branch cuts considered previously could be emulated synthetically by the addition of an external field. The Hamiltonian was given by

$$H = H_0 - \frac{1}{2} \, g \sum_{i \in \mathrm{M}_{\mathcal{C}}} \left(Y_i + Y_i^\dagger \right), \tag{5.25}$$

where H_0 was the original Hamiltonian without dislocations and g a coupling constant. For g large enough the effective Hamiltonian became similar to the dislocated Hamiltonian from

adding lattice dislocations, and similar conclusions could be drawn. Theoretically, the dislocations could now be activated and moved in a controlled manner, giving control of the ground state degeneracy and of the Berry phase from the braiding operations.

By instead adding an external field perturbing the Hamiltonian according to

$$H = H_0 - \frac{1}{2}\, g \sum_{l \subset \mathrm{M}_\mathcal{C}} \left(I_l + I_l^\dagger \right), \tag{5.26}$$

where I_l is given by (4.3.1), we saw that in a similar fashion the charge conjugate dislocations could be synthetically implemented, with the conclusions from lattice dislocations applying also to the synthetical case.

In conclusion we have seen that two-dimensional square lattice models together with the plaquette model Hamiltonian give rise to two intrinsic symmetries, the e-m duality and the charge conjugate duality. These symmetries can be realised by introducing dislocations, both extrinsic (physical lattice dislocations) and intrinsic (synthetical dislocations by external field), which also affect ground state degeneracy. The braiding of dislocations lead to a non-abelian Berry phase, a measurable quantity which can be used to track different ground states. The non-abelian anyons discussed in this thesis do not allow for a complete set of logical quantum gates, although there are suggestions on how to circumvent this problem, opening up the possibility for fault-tolerant quantum computations in the future. As stated in the introduction of this thesis, there are presently several experimental proposals and some actual experiments on obtaining topological ground state degeneracy and non-abelian anyons from abelian anyon models, such as bilayer FQH states. Most notably, in [14] an experimental proposal has been suggested that realizes the square plaquette toric code Hamiltonian from [12], a Hamiltonian that is similar to the one presented in this thesis.

A Appendix

A.1 Commutation relations of Pauli operators

Looking at the unabbreviated notation (2.1.7) of the state space, it is obvious that

$$\left[\sigma_i^a, \sigma_j^a\right] = 0, \quad \forall i, j \text{ and } a \in \{x, y, z\}, \tag{A.1.1}$$

where [,] denotes the commutator of two operators. We also have the known Pauli operator relations

$$(\sigma_i^x)^2 = (\sigma_i^y)^2 = (\sigma_i^z)^2 = 1, \tag{A.1.2}$$

and

$$\left[\sigma_i^a, \sigma_i^b\right] = 2\mathrm{i} \sum_c \epsilon_{abc} \sigma_i^c \tag{A.1.3}$$

where

$$\epsilon_{abc} = \begin{cases} +1 & \text{if } (abc) \text{ is } (x,y,z),(y,z,x),(z,x,y) \\ -1 & \text{if } (abc) \text{ is } (x,z,y),(z,y,x),(y,x,z) \\ 0 & \text{if } a=b,\ a=c \text{ or } b=c. \end{cases} \tag{A.1.4}$$

The above relations can be summarized as

$$\left\{\sigma_i^a, \sigma_i^b\right\} = 2\delta_{ab} \tag{A.1.5}$$

where { , } denotes the anti-commutator. This is simply to say that σ_i^a commutes with σ_i^b if $a = b$ and anti-commutes if $a \neq b$.

A.2 Proofs concerning loop-operators

Theorem A.1. *When restricted to the ground state subspace of the $\mathbb{Z}_N$ model we have the following identities:*

(i)

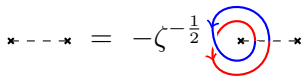

(A.2.1)

(ii)

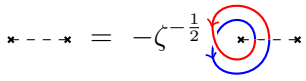

(A.2.2)

(iii)

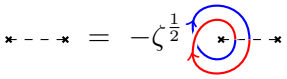

(A.2.3)

(iv)

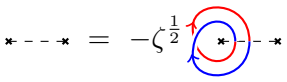

(A.2.4)

(v)

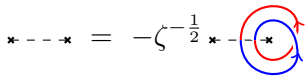

(A.2.5)

(vi)

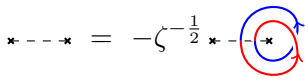

(A.2.6)

(vii)

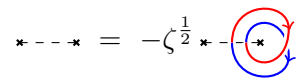

(A.2.7)

(viii)

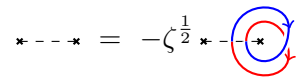

(A.2.8)

(ix)

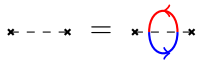

(A.2.9)

(x)

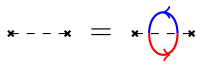

(A.2.10)

(xi)

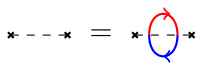

(A.2.11)

(xii)

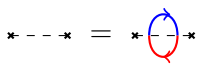

(A.2.12)

Proof. The proof is elementary. The right hand side of (A.2.1) is simply the macroscopic representation of the pentagonal plaquette operator P_q around the left dislocation defined by (3.4.8) and since the constraints on the ground state stipulate that $P_q = \mathbf{1}$ for all q, we have the equality (A.2.1). In the same way, the right hand side of (A.2.5) is the corresponding pentagonal plaquette operator around the right dislocation. To prove (A.2.2) we proceed as follows:

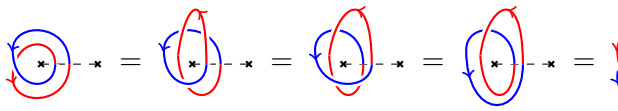

(A.2.13)

Similar manipulations prove (A.2.6). Moreover, the right hand sides of (A.2.3), (A.2.4), (A.2.7) and (A.2.8) are simply the corresponding hermitian adjoints of the right hand sides of (A.2.1), (A.2.2), (A.2.5) and (A.2.6) respectively. Also, the right hand side of (A.2.9) is the macroscopic representation of the defect line plaquette operator P_q defined by (3.4.7), and the right hand side of (A.2.10) is the other possible choice in coloring this operator. In this case, having in mind the microscopic picture, it is obvious that both these coloring choices are equivalent. Finally, the right hand sides of (A.2.11) and (A.2.12) are the hermitian adjoints of the right hand sides of (A.2.9) and (A.2.10) respectively. □

Theorem A.2. *When restricted to the ground state subspace of the $\mathbb{Z}_N$ model we have*

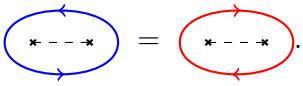

(A.2.14)

Proof. Proceed as follows:

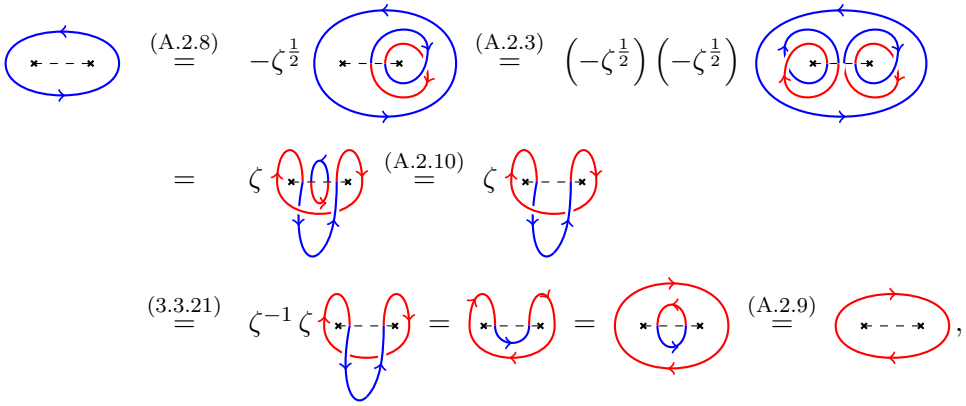

(A.2.15)

where, when using equation (3.3.21) we get the factor

$$R^{l,j}_{k,i}\, R^{j,l}_{i,k} = \zeta^{il+jk} \tag{A.2.16}$$

with

$$i = 0,\ j = N-1,\ k = 1,\ l = 0, \tag{A.2.17}$$

which is the number representing the braiding of a $q_m = N-1$ magnetic charge with a $q_e = 1$ electric charge. The number $N-1$ is due to the fact that the orientation arrow of the magnetic string is in the conjugate direction. The resulting factor is then

$$\zeta^{0\times 0 + (N-1)\times 1} = \zeta^{N-1} = \zeta^{-1}. \tag{A.2.18}$$

In the proof, we have also fused and unfused both the electric and magnetic lines according to the fusion rules of Section 3.2. □

Theorem A.3. *When restricted to the ground state subspace of the $\mathbb{Z}_N$ model we have*

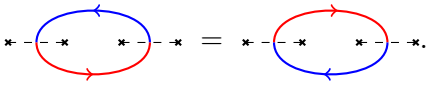

(A.2.19)

Proof. Proceed as follows:

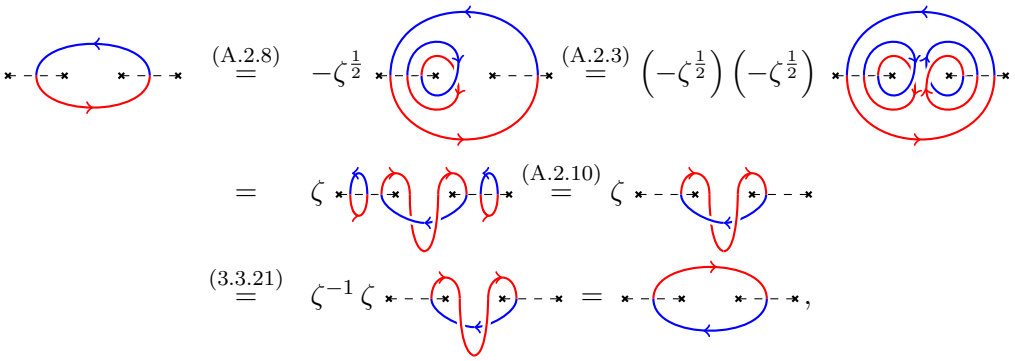

(A.2.20)

where the factor ζ^{-1} from the braiding rule (3.3.21) is calculated in the same way as in the proof for Theorem A.2. We have also fused and unfused both the electric and magnetic lines according to the fusion rules of Section 3.2. □

A.3 Solutions to the defect braiding relations of the *e-m* duality

The solutions given in the following theorem are taken from [25, p. 5]. Let

$$\zeta := \mathrm{e}^{\mathrm{i}\frac{2\pi}{N}}, \qquad N \in \mathbb{Z}, \tag{A.3.1}$$

and let

$$\mathcal{O}_{12} = \sum_r \zeta^r \, |r\rangle\langle r| \tag{A.3.2}$$

and

$$\mathcal{O}_{23} = \sum_r |r-1\rangle\langle r| \,, \tag{A.3.3}$$

where the sum $\sum_r$ denotes the sum over all $r \in \{0, 1, ..., N-1\}$ and the number r is to be read as modulo N throughout this section. Let $\sum_{r,r'}$ denote the double sum over $r, r' \in \{0, 1, ..., N-1\}$ and let $\psi_{12}, \psi_{23} \in \mathbb{R}$ be arbitrary phases. Finally let

$$\langle r|r'\rangle = \delta_{r,r'}. \tag{A.3.4}$$

Theorem A.4. *The two operators*

$$T_{12} := \mathrm{e}^{\mathrm{i}\psi_{12}} \sum_r \zeta^{\frac{r(N-r)}{2}} \, |r\rangle\langle r| \tag{A.3.5}$$

and

$$T_{23} := \frac{\mathrm{e}^{\mathrm{i}\psi_{23}}}{\sqrt{N}} \sum_{r,r'} \zeta^{\frac{1}{2}(r-r'-N/2)^2} \, |r\rangle\langle r'| \,, \tag{A.3.6}$$

(i) are unitary operators;

(ii) satisfy the four equations

$$T_{12}^\dagger \, \mathcal{O}_{12} \, T_{12} = \mathcal{O}_{12}, \tag{A.3.7}$$

$$T_{12}^\dagger \, \mathcal{O}_{23} \, T_{12} = -\zeta^{-\frac{1}{2}} \, \mathcal{O}_{12}^\dagger \, \mathcal{O}_{23}, \tag{A.3.8}$$

$$T_{23}^\dagger \, \mathcal{O}_{23} \, T_{23} = \mathcal{O}_{23}, \tag{A.3.9}$$

and

$$T_{23}^\dagger \, \mathcal{O}_{12} \, T_{23} = -\zeta^{-\frac{1}{2}} \, \mathcal{O}_{23} \, \mathcal{O}_{12}. \tag{A.3.10}$$

Proof of Theorem A.4 (i). We have

$$T_{12}^\dagger = \mathrm{e}^{-\mathrm{i}\psi_{12}} \sum_r \zeta^{-\frac{r(N-r)}{2}} \, |r\rangle\langle r| \tag{A.3.11}$$

so that

$$T_{12}^\dagger \, T_{12} = \sum_r \zeta^{-\frac{r(N-r)}{2}} \zeta^{\frac{r(N-r)}{2}} \, |r\rangle\langle r| = \sum_r |r\rangle\langle r| = \mathbf{1}, \tag{A.3.12}$$

proving that T_{12} is unitary.

For T_{23} we have

$$T_{23}^\dagger = \frac{\mathrm{e}^{-\mathrm{i}\psi_{23}}}{\sqrt{N}} \sum_{r,r'} \zeta^{-\frac{1}{2}(r-r'-N/2)^2} \, |r'\rangle\langle r| \,, \tag{A.3.13}$$

so that

$$\begin{aligned} T_{23}^\dagger T_{23} &= \left(\frac{\mathrm{e}^{-\mathrm{i}\psi_{23}}}{\sqrt{N}}\sum_{r,r'}\zeta^{-\frac{1}{2}(r-r'-N/2)^2}\,|r''\rangle\langle r|\right)\left(\frac{\mathrm{e}^{\mathrm{i}\psi_{23}}}{\sqrt{N}}\sum_{r,r''}\zeta^{\frac{1}{2}(r-r''-N/2)^2}\,|r\rangle\langle r''|\right) \\ &= \frac{1}{N}\sum_{\substack{r,r'\\r''}}\zeta^{\frac{1}{2}\left[(r-r'-N/2)^2-(r-r''-N/2)^2\right]}\,|r'\rangle\langle r''| \\ &= \frac{1}{N}\sum_{\substack{r,r'\\r''}}\zeta^{\frac{1}{2}\left[(r'')^2-(r')^2+N(r''-r')-2n(r''-r')\right]}\,|r'\rangle\langle r''| \\ &= \frac{1}{N}\sum_{r',r''}\left(\sum_{r=0}^{N-1}\zeta^{r(r'-r'')}\right)\zeta^{\frac{1}{2}\left[(r'')^2-(r')^2+N(r''-r')\right]}\,|r'\rangle\langle r''|\,. \end{aligned} \tag{A.3.14}$$

For all terms with $r'' \neq r'$ we have a factor depending only on r namely

$$\sum_{r=0}^{N-1}\zeta^{r(r'-r'')} = \sum_{r=0}^{N-1}\mathrm{e}^{\mathrm{i}\frac{2\pi r(r'-r'')}{N}}. \tag{A.3.15}$$

This is a sum over the Nth roots of unity, with the property that

$$\sum_{r=0}^{N-1}\zeta^{r(r'-r'')} = \sum_{r=0}^{N-1}\left(\zeta^{r'-r''}\right)^r = \begin{cases} N & \text{for } \zeta^{r'-r''}=1 \\ \frac{1-\left(\zeta^{r'-r''}\right)^N}{1-\zeta^{r'-r''}} & \text{for } \zeta^{r'-r''}\neq 1. \end{cases} \tag{A.3.16}$$

Thus for $\zeta^{r'-r''} \neq 1$ we have

$$\begin{aligned} \sum_{r=0}^{N-1}\zeta^{r(r'-r'')} &= \frac{1-\left(\zeta^{r'-r''}\right)^N}{1-\zeta^{r'-r''}} = \frac{1-\left(\zeta^N\right)^{r'-r''}}{1-\zeta^{r'-r''}} \\ &= \frac{1-\left(\mathrm{e}^{\mathrm{i}\frac{2\pi N}{N}}\right)^{r'-r''}}{1-\zeta^{r'-r''}} = \frac{1-1^{r'-r''}}{1-\zeta^{r'-r''}} = 0. \end{aligned} \tag{A.3.17}$$

Since $r'-r'' \in \{0,\pm1,\pm2,...,\pm(N-1)\}$ we do indeed have $\zeta^{r'-r''} \neq 1$ for any occurring combination of r' and r'' except $r'=r''$ and thus this factor is equal to zero for $r'' \neq r'$ or N for $r''=r'$. The remaining sum is then

$$T_{23}^\dagger T_{23} = \frac{N}{N}\sum_{r'}|r'\rangle\langle r'| = \sum_{r'}|r'\rangle\langle r'| = \mathbf{1}, \tag{A.3.18}$$

proving that T_{23} is unitary. □

Proof of equation (A.3.7). Both T_{12} and $\mathcal{O}_{12}$ are diagonal. Hence they commute, so that

$$T_{12}^\dagger\,\mathcal{O}_{12}\,T_{12} = T_{12}^\dagger\,T_{12}\,\mathcal{O}_{12} = \mathcal{O}_{12}. \tag{A.3.19}$$

□

Proof of equation (A.3.8). Take the left hand side of (A.3.8), and begin with

$$\mathcal{O}_{23}\,T_{12} = \mathrm{e}^{\mathrm{i}\psi_{12}}\sum_{n}\zeta^{\frac{r(N-r)}{2}}\,|r-1\rangle\langle r|\,. \tag{A.3.20}$$

Then, noting that by shifting $r \mapsto (r-1)$ we have

$$T_{12}^\dagger = \mathrm{e}^{-\mathrm{i}\psi_{12}}\sum_{r}\zeta^{-\frac{r(N-r)}{2}}\,|r\rangle\langle r| = \sum_{n}\zeta^{-\frac{(r-1)(N-r+1)}{2}}\,|r-1\rangle\langle r-1|\,, \tag{A.3.21}$$

we get

$$\begin{aligned} T_{12}^\dagger \mathcal{O}_{23} T_{12} &= \sum_r \zeta^{-\frac{(r-1)(N-r+1)}{2}} \zeta^{\frac{r(N-r)}{2}} |r-1\rangle\langle r| \\ &= \sum_r \zeta^{\frac{r(N-r)-(r-1)(N-r+1)}{2}} |r-1\rangle\langle r| \\ &= \sum_r \zeta^{\frac{N+1-2n}{2}} |r-1\rangle\langle r| . \end{aligned} \tag{A.3.22}$$

Now take the right hand side of (A.3.8) and first note that

$$-\zeta^{-\frac{1}{2}} = -\mathrm{e}^{-\mathrm{i}\frac{\pi}{N}} = \mathrm{e}^{\mathrm{i}\pi}\mathrm{e}^{-\mathrm{i}\frac{\pi}{N}} = \mathrm{e}^{\mathrm{i}\pi-\frac{\pi}{N}} = \mathrm{e}^{\mathrm{i}\frac{\pi}{N}(N-1)} = \zeta^{\frac{N-1}{2}}. \tag{A.3.23}$$

Then we have

$$\begin{aligned} -\zeta^{-\frac{1}{2}} \mathcal{O}_{12}^\dagger \mathcal{O}_{23} &= \zeta^{\frac{N-1}{2}} \mathcal{O}_{12}^\dagger \mathcal{O}_{23} \\ &= \zeta^{\frac{N-1}{2}} \mathcal{O}_{12}^\dagger \sum_r |r-1\rangle\langle r| \\ &= \zeta^{\frac{N-1}{2}} \sum_r \zeta^{-(r-1)} |r-1\rangle\langle r| = \sum_r \zeta^{\frac{N-1-2n+2}{2}} |r-1\rangle\langle r| \\ &= \sum_r \zeta^{\frac{N+1-2n}{2}} |r-1\rangle\langle r| . \end{aligned} \tag{A.3.24}$$

This is equal to the left hand side of the equation and thus completes the proof. □

Proof of equation (A.3.9). Take

$$\begin{aligned} \mathcal{O}_{23} T_{23} &= \frac{\mathrm{e}^{\mathrm{i}\psi_{23}}}{\sqrt{N}} \sum_{r,r'} \zeta^{\frac{(r-r'-N/2)^2}{2}} |r-1\rangle\langle r'| \\ &= \frac{\mathrm{e}^{\mathrm{i}\psi_{23}}}{\sqrt{N}} \sum_{r,r'} \zeta^{\frac{(r+1-r'-N/2)^2}{2}} |r\rangle\langle r'| , \end{aligned} \tag{A.3.25}$$

where in the last step we shift $r \mapsto (r+1)$. Then

$$\begin{aligned} T_{23}^\dagger \mathcal{O}_{23} T_{23} &= \frac{1}{N} \sum_{\substack{r,r' \\ r''}} \zeta^{\frac{(r+1-r'-N/2)^2-(r-r''-N/2)^2}{2}} |r''\rangle\langle r'| \\ &= \frac{1}{N} \sum_{\substack{r,r' \\ r''}} \zeta^{\frac{(r+1-r'-N/2)^2-(r+1-r''-N/2)^2}{2}} |r''-1\rangle\langle r'| , \end{aligned} \tag{A.3.26}$$

where we now have shifted $r'' \mapsto (r''-1)$ in the last step. Looking at the exponent of ζ we see that for all terms with $r' = r''$ the triple sum becomes

$$\sum_r \zeta^{\frac{(r+1-r'-N/2)^2-(r+1-r'-N/2)^2}{2}} = \sum_r \zeta^0 = N. \tag{A.3.27}$$

It is not hard to show that

$$(r+1-r'-N/2)^2 - (r+1-r''-N/2)^2 = 2n(r''-r') + C, \tag{A.3.28}$$

where $C = C(r', r'')$, so for each fixed combination of r' and r'' with $r' \neq r''$ we get the sum over r given by

$$\frac{1}{N} \zeta^C \sum_r \zeta^{r(r''-r')} |r''-1\rangle\langle r'| . \tag{A.3.29}$$

By (A.3.17) this sum is zero, and thus we have

$$T_{23}^\dagger \mathcal{O}_{23} T_{23} = \sum_{r'} |r'-1\rangle\langle r'| = \mathcal{O}_{23}, \tag{A.3.30}$$

which completes the proof. □

Proof of equation (A.3.10). Consider the right hand side of (A.3.10) to get

$$\begin{aligned} -\zeta^{-\frac{1}{2}}\,\mathcal{O}_{23}\,\mathcal{O}_{12} &= \zeta^{\frac{N-1}{2}}\,\mathcal{O}_{23}\,\mathcal{O}_{12} \\ &= \zeta^{\frac{N-1}{2}}\,\mathcal{O}_{23}\sum_r \zeta^r\,|r\rangle\langle r| \\ &= \sum_r \zeta^{\frac{N-1+2n}{2}}\,\mathcal{O}_{23}\,|r\rangle\langle r| \\ &= \sum_r \zeta^{\frac{N-1+2n}{2}}\,|r-1\rangle\langle r|\,. \end{aligned} \tag{A.3.31}$$

Now we note that

$$T_{23}^\dagger = \frac{\mathrm{e}^{-\mathrm{i}\psi_{23}}}{\sqrt{N}}\sum_{r,r'} \zeta^{-\frac{(r-r'-N/2)^2}{2}}\,|r'\rangle\langle r|\,, \tag{A.3.32}$$

and then take

$$\mathcal{O}_{12}\,T_{23} = \frac{\mathrm{e}^{\mathrm{i}\psi_{23}}}{\sqrt{N}}\sum_{r,r''} \zeta^{\frac{(r-r''-N/2)^2}{2}}\,\zeta^r\,|r\rangle\langle r''| = \frac{\mathrm{e}^{\mathrm{i}\psi_{23}}}{\sqrt{N}}\sum_{r,r''} \zeta^{\frac{(r-r''-N/2)^2+2n}{2}}\,|r\rangle\langle r''|\,. \tag{A.3.33}$$

Then we get

$$\begin{aligned} T_{23}^\dagger\,\mathcal{O}_{12}\,T_{23} &= \frac{1}{N}\sum_{\substack{r,r'\\r''}} \zeta^{-\frac{(r-r'-N/2)^2}{2}}\zeta^{\frac{(r-r''-N/2)^2+2n}{2}}\,|r'\rangle\langle r''| \\ &= \frac{1}{N}\sum_{\substack{r,r'\\r''}} \zeta^{\frac{2n+(r-r''-N/2)^2-(r-r'-N/2)^2}{2}}\,|r'\rangle\langle r''| \\ &= \frac{1}{N}\sum_{\substack{r,r'\\r''}} \zeta^{\frac{2n+(r-r''-N/2)^2-(r+1-r'-N/2)^2}{2}}\,|r'-1\rangle\langle r''|\,, \end{aligned} \tag{A.3.34}$$

where the last step is due to shifting $r' \mapsto (r'-1)$. Focusing only on the exponent of ζ it is not hard to show that

$$2n+(r-r''-N/2)^2-(r+1-r'-N/2)^2 = (r'')^2-(r')^2+(r'-r'')(2n-N)+N-1+2r', \tag{A.3.35}$$

showing that for all terms where $r'=r''$ we have

$$T_{23}^\dagger\,\mathcal{O}_{12}\,T_{23}\frac{1}{N}\sum_{r,r'} \zeta^{\frac{N-1+2r'}{2}}\,|r'-1\rangle\langle r'| = \sum_{r'} \zeta^{\frac{N-1+2r'}{2}}\,|r'-1\rangle\langle r'|\,. \tag{A.3.36}$$

It is also easy to show that

$$2n+(r-r''-N/2)^2-(r+1-r'-N/2)^2 = 2n(r'-r'')+C, \tag{A.3.37}$$

where $C=C(r',r'')$ is a constant for each sum over r. Thus, if we separate the terms where $r'=r''$ from the rest, we have

$$T_{23}^\dagger\,\mathcal{O}_{12}\,T_{23} = \sum_{r'} \zeta^{\frac{N-1+2n'}{2}}\,|r'-1\rangle\langle r'| + \frac{1}{N}\sum_{\substack{r,r',r''\\r'\neq r''}} \zeta^{r(r'-r'')}\,|r'-1\rangle\langle r''|\,. \tag{A.3.38}$$

In the last term of (A.3.38) we have a triple sum, and for each r',r'' held fixed we have

$$\sum_{r=0}^{N-1} \zeta^{r(r'-r'')} = 0, \tag{A.3.39}$$

since $\zeta^{r'-r''}\neq 1$, as was shown in equation (A.3.17), and thus the triple sum in (A.3.38) is zero. Comparing (A.3.38) to the right hand side of (A.3.31) completes the proof. □

A.4 The braid group equation for *e-m* duality solutions

Theorem A.5. *For*

$$\psi_{12} - \psi_{23} = \frac{\pi}{4} \pm 2\pi k, \;\; k \in \{0, 1, 2, ...\}, \tag{A.4.1}$$

the two operators

$$T_{12} := \mathrm{e}^{\mathrm{i}\psi_{12}} \sum_r \zeta^{\frac{r(N-r)}{2}} \, |r\rangle\langle r| \tag{A.4.2}$$

and

$$T_{23} := \frac{\mathrm{e}^{\mathrm{i}\psi_{23}}}{\sqrt{N}} \sum_{r,r'} \zeta^{\frac{1}{2}(r-r'-N/2)^2} \, |r\rangle\langle r'| \,, \tag{A.4.3}$$

satisfy the braid group equation

$$T_{12}\, T_{23}\, T_{12} = T_{23}\, T_{12}\, T_{23}. \tag{A.4.4}$$

We need a few equations in preparation for the proof. Let $a, N \in \mathbb{Z}$. Then, if the product aN is even, we have

$$S(a, N) = \sqrt{\frac{N}{a}} \mathrm{e}^{\mathrm{i}\frac{\pi}{4}} S^*(N, a), \tag{A.4.5}$$

where S^* denotes the complex conjugate of S and

$$S(a, N) := \sum_{c=0}^{N-1} \mathrm{e}^{\mathrm{i}\frac{\pi}{N}ac^2}. \tag{A.4.6}$$

The sum $S(a, N)$ is called a quadratic Gauss sum and a proof of equation (A.4.5) can be found in [1, p. 196]. We now introduce the two separate notations

$$S(a, N, k) := \sum_{c=0}^{N-1} \mathrm{e}^{\mathrm{i}\frac{\pi}{N}a(c+k)^2}, \tag{A.4.7}$$

and

$$S'(a, N, k) := \sum_{c=0}^{N-1} \mathrm{e}^{\mathrm{i}\frac{\pi}{N}a(c+k+\frac{1}{2})^2}, \tag{A.4.8}$$

where $a, N, k \in \mathbb{Z}$. By (A.4.5) we see that

$$S(1, N, 0) = \sqrt{N} \mathrm{e}^{\mathrm{i}\frac{\pi}{4}}. \tag{A.4.9}$$

We also note that

$$S(a, N, k+1) - S(a, N, k) = \mathrm{e}^{\mathrm{i}\frac{\pi}{N}(N+k)^2} - \mathrm{e}^{\mathrm{i}\frac{\pi}{N}k^2} = \mathrm{e}^{\mathrm{i}\frac{\pi}{N}k^2} \left(\mathrm{e}^{\mathrm{i}\pi N} - 1\right), \tag{A.4.10}$$

which implies that for even N we have

$$S(a, N, k+1) = S(a, N, k), \tag{A.4.11}$$

which leads to the result

$$S(1, N, k) = \sqrt{N} \mathrm{e}^{\mathrm{i}\frac{\pi}{4}}, \;\; \forall N, k \in \mathbb{Z}, N \text{ even}. \tag{A.4.12}$$

Next we note that

$$S'(a, N, k+1) - S'(a, N, k) = \mathrm{e}^{\mathrm{i}\frac{\pi}{N}(N+k+\frac{1}{2})^2} - \mathrm{e}^{\mathrm{i}\frac{\pi}{N}(k+\frac{1}{2})^2} = \mathrm{e}^{\mathrm{i}\frac{\pi}{N}(k+\frac{1}{2})^2} \left(\mathrm{e}^{\mathrm{i}\pi(N+1)} - 1\right), \tag{A.4.13}$$

which implies that for odd N we have

$$S'(a,N,k+1) = S'(a,N,k), \quad \forall k \in \mathbb{Z}. \tag{A.4.14}$$

In particular we have

$$S(1,N,N) = \begin{cases} S(1,N,0) & N \text{ even} \\ -S(1,N,0) & N \text{ odd}, \end{cases} \tag{A.4.15}$$

and

$$S'(1,N,N) = \begin{cases} S'(1,N,0) & N \text{ odd} \\ -S'(1,N,0) & N \text{ even}. \end{cases} \tag{A.4.16}$$

Now, assume N is odd. Then we have

$$\begin{aligned} S(1,4N,0) &= \sum_{c=0}^{4N-1} \mathrm{e}^{\mathrm{i}\frac{\pi}{4N}c^2} = \sum_{\substack{c=0 \\ c \text{ even}}}^{4N-2} \mathrm{e}^{\mathrm{i}\frac{\pi}{4N}c^2} + \sum_{\substack{c=1 \\ c \text{ odd}}}^{4N-1} \mathrm{e}^{\mathrm{i}\frac{\pi}{4N}c^2} \\ &= \sum_{c=0}^{2N-1} \mathrm{e}^{\mathrm{i}\frac{\pi}{4N}(2c)^2} + \sum_{c=0}^{2N-1} \mathrm{e}^{\mathrm{i}\frac{\pi}{4N}(2c+1)^2} \\ &= \sum_{c=0}^{2N-1} \mathrm{e}^{\mathrm{i}\frac{\pi}{N}(c)^2} + \sum_{c=0}^{2N-1} \mathrm{e}^{\mathrm{i}\frac{\pi}{N}(c+\frac{1}{2})^2} \\ &= \sum_{c=0}^{N-1} \mathrm{e}^{\mathrm{i}\frac{\pi}{N}(c)^2} + \sum_{c=0}^{N-1} \mathrm{e}^{\mathrm{i}\frac{\pi}{N}(c+N)^2} + \sum_{c=0}^{N-1} \mathrm{e}^{\mathrm{i}\frac{\pi}{N}(c+\frac{1}{2})^2} + \sum_{c=0}^{N-1} \mathrm{e}^{\mathrm{i}\frac{\pi}{N}(c+\frac{1}{2}+N)^2} \\ &= S(1,N,0) + S(1,N,N) + S'(1,N,0) + S'(1,N,N) = 2S'(1,N,0), \end{aligned} \tag{A.4.17}$$

where in the last step we have used (A.4.15) and (A.4.16) for N odd. We also note that by (A.4.12) we have

$$S(1,4N,0) = \sqrt{4N}\mathrm{e}^{\mathrm{i}\frac{\pi}{4}} = 2\sqrt{N}\mathrm{e}^{\mathrm{i}\frac{\pi}{4}}. \tag{A.4.18}$$

Putting (A.4.17) and (A.4.18) together we get

$$S'(1,N,0) = \sqrt{N}\mathrm{e}^{\mathrm{i}\frac{\pi}{4}}, \tag{A.4.19}$$

and by (A.4.14) we get the final result

$$S'(1,N,k) = \sqrt{N}\mathrm{e}^{\mathrm{i}\frac{\pi}{4}}, \quad \forall N,k \in \mathbb{Z}, N \text{ odd}. \tag{A.4.20}$$

While equation (A.4.12) was certainly a known result, the result given by equation (A.4.20) was not found in the literature, however it was most probably known from before by experts on the subject.

Proof of Theorem A.5. First we take

$$T_{12}\,T_{23} = \frac{\mathrm{e}^{\mathrm{i}(\psi_{12}+\psi_{23})}}{\sqrt{N}} \sum_{a,b} \zeta^{\frac{1}{2}\left[(a-b-N/2)^2+a(N-a)\right]} |a\rangle\langle b|\,. \tag{A.4.21}$$

To calculate the left hand side of (A.4.4) we act on $T_{12}\,T_{23}$ with T_{12} from the right. Then we get

$$\begin{aligned} T_{12}\,T_{23}\,T_{12} &= \frac{\mathrm{e}^{\mathrm{i}(2\psi_{12}+\psi_{23})}}{\sqrt{N}} \sum_{a,b} \zeta^{\frac{1}{2}\left[(a-b-N/2)^2+a(N-a)+b(N-b)\right]} |a\rangle\langle b| \\ &= \frac{\mathrm{e}^{\mathrm{i}(2\psi_{12}+\psi_{23})}}{\sqrt{N}} \sum_{a,b} \zeta^{\frac{1}{2}\left[(N/2)^2-2aN-2ab)\right]} |a\rangle\langle b| \\ &= \frac{\mathrm{e}^{\mathrm{i}(2\psi_{12}+\psi_{23})}}{\sqrt{N}} \zeta^{\frac{N^2}{8}} \sum_{a,b} \zeta^{-aN}\zeta^{-ab} |a\rangle\langle b| \\ &= \frac{\mathrm{e}^{\mathrm{i}(2\psi_{12}+\psi_{23}+\frac{\pi}{4}N)}}{\sqrt{N}} \sum_{a,b} \zeta^{-ab} |a\rangle\langle b|\,. \end{aligned} \tag{A.4.22}$$

Now consider the right hand side of (A.4.4). By acting on $T_{12}\,T_{23}$ from the left with T_{23} we get

$$\begin{aligned} T_{23}\,T_{12}\,T_{23} &= \frac{\mathrm{e}^{\mathrm{i}(\psi_{12}+2\psi_{23})}}{N}\sum_{a,b,c}\zeta^{\frac{1}{2}\left[(c-b-N/2)^2+c(N-c)+(a-c-N/2)^2\right]}\,|a\rangle\langle b| \\ &= \frac{\mathrm{e}^{\mathrm{i}(\psi_{12}+2\psi_{23})}}{N}\zeta^{\frac{N^2}{4}}\sum_{a,b,c}\zeta^{\frac{1}{2}\left[a^2+b^2+c^2-N(a-b+c)-2c(a+b)\right]}\,|a\rangle\langle b| \\ &= \frac{\mathrm{e}^{\mathrm{i}(\psi_{12}+2\psi_{23}+\frac{\pi}{2}N)}}{N}\sum_{a,b,c}\zeta^{\frac{1}{2}c(c-2a-2b-N)}\zeta^{\frac{1}{2}\left(a^2-aN\right)}\zeta^{\frac{1}{2}\left(b^2+bN\right)}\,|a\rangle\langle b| \\ &= \frac{\mathrm{e}^{\mathrm{i}(\psi_{12}+2\psi_{23}+\frac{\pi}{2}N)}}{N}\sum_{a,b,c}\zeta^{\frac{1}{2}\left(c-a-b-\frac{N}{2}\right)^2}\zeta^{-\frac{N^2}{8}}\zeta^{-ab}\zeta^{-aN}\,|a\rangle\langle b| \\ &= \frac{\mathrm{e}^{\mathrm{i}(\psi_{12}+2\psi_{23}+\frac{\pi}{4}N)}}{N}\sum_{a,b,c}\zeta^{\frac{1}{2}\left(c-a-b-\frac{N}{2}\right)^2}\zeta^{-ab}\,|a\rangle\langle b| \end{aligned} \tag{A.4.23}$$

Thus equating (A.4.22) with (A.4.23) implies that for all $a, b \in \{0, 1, ..., N-1\}$ we have

$$\frac{\mathrm{e}^{\mathrm{i}(2\psi_{12}+\psi_{23}+\frac{\pi}{4}N)}}{\sqrt{N}} = \frac{\mathrm{e}^{\mathrm{i}(\psi_{12}+2\psi_{23}+\frac{\pi}{4}N)}}{N}\sum_{c=0}^{N-1}\zeta^{\frac{1}{2}\left(c-a-b-\frac{N}{2}\right)^2}, \tag{A.4.24}$$

which is equivalent to

$$\sum_{c=0}^{N-1}\zeta^{\frac{1}{2}\left(c-a-b-\frac{N}{2}\right)^2} = \sqrt{N}\mathrm{e}^{\mathrm{i}(\psi_{12}-\psi_{23})}. \tag{A.4.25}$$

Recall that by assumption we have

$$\psi_{12} - \psi_{23} = \frac{\pi}{4} \pm 2\pi k, \;\; k \in \{0, 1, 2, ...\}. \tag{A.4.26}$$

Then equation (A.4.4) is true if and only if for all $a, b \in \{0, 1, ..., N-1\}$ we have

$$\sum_{c=0}^{N-1}\zeta^{\frac{1}{2}\left(c-a-b-\frac{N}{2}\right)^2} = \sum_{c=0}^{N-1}\mathrm{e}^{\mathrm{i}\frac{\pi}{N}\left(c-a-b-\frac{N}{2}\right)^2} = \sqrt{N}\mathrm{e}^{\mathrm{i}\frac{\pi}{4}}. \tag{A.4.27}$$

For even N we can write,

$$-a-b-\frac{N}{2} = k, \quad k \in \mathbb{Z}, \tag{A.4.28}$$

and for odd N we can write

$$-a-b-\frac{N}{2} = k+\frac{1}{2}, \quad k \in \mathbb{Z}. \tag{A.4.29}$$

Thus, by (A.4.12) and (A.4.20), equation (A.4.4) holds for all a and b, both for even and odd N. □

A.5 Solutions to the defect braiding relations of the charge conjugate duality

The solutions given in the following theorem are taken from [25, p. 5]. Let

$$\zeta := \mathrm{e}^{\mathrm{i}\frac{2\pi}{N}}, \qquad N \in \mathbb{Z}, \tag{A.5.1}$$

and let

$$\mathcal{O}^e_{12} = \sum_{r_e,r_m} \zeta^{r_e} \left|r_e, r_m\right\rangle\!\left\langle r_e, r_m\right|, \tag{A.5.2}$$

$$\mathcal{O}^m_{12} = \sum_{r_e,r_m} \zeta^{r_m} \left|r_e, r_m\right\rangle\!\left\langle r_e, r_m\right|, \tag{A.5.3}$$

$$\mathcal{O}^e_{23} = \sum_{r_e,r_m} \left|r_e, r_m - 2\right\rangle\!\left\langle r_e, r_m\right|, \tag{A.5.4}$$

and

$$\mathcal{O}^m_{23} = \sum_{r_e,r_m} \left|r_e - 2, r_m\right\rangle\!\left\langle r_e, r_m\right|, \tag{A.5.5}$$

where the sum $\sum_{r_e,r_m}$ denotes the double sum over all $r_e, r_m \in \{0, 1, ..., N-1\}$ and the numbers r_e and r_m are to be read as modulo N throughout this section. Let $\psi_{12}, \psi_{23} \in \mathbb{R}$ be arbitrary phases and

$$\langle r_e, r_m | r'_e, r'_m \rangle = \delta_{r_e,r'_e}\, \delta_{r_m,r'_m}. \tag{A.5.6}$$

Then we have the following:

Theorem A.6. *The two operators*

$$T_{12} = \mathrm{e}^{\mathrm{i}\psi_{12}} \sum_{r_e,r_m} \zeta^{\frac{1}{2}r_e r_m} \left|r_e, r_m\right\rangle\!\left\langle r_e, r_m\right|, \tag{A.5.7}$$

and

$$T_{23} = \frac{\mathrm{e}^{\mathrm{i}\psi_{23}}}{\mathcal{N}} \sum_{\substack{r_e,r_m \\ r'_e,r'_m}} \zeta^{-\frac{1}{2}(r_e - r'_e)(r_m - r'_m)} \left|r_e, r_m\right\rangle\!\left\langle r'_e, r'_m\right|, \tag{A.5.8}$$

where

$$\mathcal{N} = \begin{cases} \frac{N}{2}, & \text{if } N \text{ is even,} \\ N, & \text{if } N \text{ is odd,} \end{cases} \tag{A.5.9}$$

and where

$$r_e, r_m, r'_e, r'_m \in \{0, 2, ..., 2(\mathcal{N}-1)\} \tag{A.5.10}$$

(i) are unitary.

(ii) satisfy the equations

$$T^\dagger_{12}\, \mathcal{O}^{e(m)}_{12}\, T_{12} = \mathcal{O}^{e(m)}_{12}, \tag{A.5.11}$$

$$T^\dagger_{12}\, \mathcal{O}^{e(m)}_{23}\, T_{12} = \mathcal{O}^{e(m)}_{12}\, \mathcal{O}^{e(m)}_{23}, \tag{A.5.12}$$

$$T^\dagger_{23}\, \mathcal{O}^{e(m)}_{23}\, T_{23} = \mathcal{O}^{e(m)}_{23}, \tag{A.5.13}$$

and

$$T^\dagger_{23}\, \mathcal{O}^{e(m)}_{12}\, T_{23} = \mathcal{O}^{e(m)\dagger}_{23}\, \mathcal{O}^{e(m)}_{12}. \tag{A.5.14}$$

(There are actually eight equations as they hold for $\mathcal{O}^e_{ij}$ and $\mathcal{O}^m_{ij}$ individually.)

Proof of Theorem A.6 (i). From (A.5.7) it is obvious that T_{12} is unitary.

For T_{23} we have

$$T_{23}^\dagger T_{23} = \frac{1}{\mathcal{N}^2} \sum_{\substack{r_e, r_m \\ r'_e, r'_m \\ r''_e, r''_m}} \zeta^{\frac{1}{2}[(r''_e - r_e)(r''_m - r_m) - (r'_e - r_e)(r'_m - r_m)]} \, |r''_e, r''_m\rangle\langle r'_e, r'_m| \,, \tag{A.5.15}$$

and to see that this is unity we first note that putting $r''_{e(m)} = r'_{e(m)}$ we get

$$\zeta^{\frac{1}{2}[(r'_e - r_e)(r'_m - r_m) - (r'_e - r_e)(r'_m - r_m)]} \, |r'_e, r'_m\rangle\langle r'_e, r'_m| = 1. \tag{A.5.16}$$

For each pair of $r'_{e(m)}$ there are $\mathcal{N}^2$ terms (one for each r_e and r_m), so we can write equation (A.5.15) as

$$\begin{aligned} T_{23}^\dagger T_{23} &= \frac{\mathcal{N}^2}{\mathcal{N}^2} + \frac{1}{\mathcal{N}^2} \sum_{\substack{r_e, r_m \\ r'_e, r'_m \\ r''_e, r''_m \\ r''_{e(m)} \neq r'_{e(m)}}} \zeta^{\frac{1}{2}[(r''_e - r_e)(r''_m - r_m) - (r'_e - r_e)(r'_m - r_m)]} \, |r''_e, r''_m\rangle\langle r'_e, r'_m| \\ &= 1 + \frac{1}{\mathcal{N}^2} \sum_{\substack{r_e, r_m \\ r'_e, r'_m \\ r''_e, r''_m \\ r''_{e(m)} \neq r'_{e(m)}}} \zeta^{\frac{1}{2}[(r''_e - r_e)(r''_m - r_m) - (r'_e - r_e)(r'_m - r_m)]} \, |r''_e, r''_m\rangle\langle r'_e, r'_m| \,. \end{aligned} \tag{A.5.17}$$

To see that the last sum is zero we first note that for each r_e with $r_m, r'_{e(m)}, r''_{e(m)}$ fixed we get

$$(r''_e - r_e)(r''_m - r_m) - (r'_e - r_e)(r'_m - r_m) = r_e(r'_m - r''_m) + C, \tag{A.5.18}$$

where C is a constant term depending on the fixed r's. So the above sum of all r_e with the others fixed is

$$\frac{1}{\mathcal{N}^2} \sum_{r_e} \zeta^{\frac{1}{2}[r_e(r'_m - r''_m) + C]} \, |r''_e, r''_m\rangle\langle r'_e, r'_m| = \frac{\zeta^{\frac{C}{2}}}{\mathcal{N}^2} \sum_{r_e} \zeta^{\frac{1}{2} r_e (r'_m - r''_m)} \, |r''_e, r''_m\rangle\langle r'_e, r'_m| \,. \tag{A.5.19}$$

From now on we remove everything that is constant from the calculations and focus on all terms involving r_e.

First we take the case of N odd, so $\mathcal{N} = N$. Recall that $r_{e(m)} \in \{0, 2, ..., 2(\mathcal{N}-1)\}$ so we can put $k = \frac{r_e}{2}$ with $k \in \{0, 1, ..., (N-1)\}$ and $m = r'_m - r''_m$ with $m \in \{\pm 2, \pm 4, ..., \pm 2(N-1)\}$. The sum involving r_e from (A.5.19) becomes

$$\sum_{r_e} \zeta^{\frac{1}{2} r_e (r'_m - r''_m)} = \sum_{k=0}^{N-1} \zeta^{km} = \sum_{k=0}^{N-1} (\zeta^m)^k = \frac{1 - (\zeta^m)^N}{1 - \zeta^m}, \tag{A.5.20}$$

and since

$$(\zeta^m)^N = \left(\zeta^N\right)^m = \left(\mathrm{e}^{\mathrm{i}\frac{2\pi N}{N}}\right)^m = 1^m = 1, \tag{A.5.21}$$

the above sum is zero, and thus we have proved that T_{23} is indeed unitary if N is odd.

For N even we have $\mathcal{N} = \frac{N}{2}$ so again we let $k = \frac{r_e}{2}$ with $k \in \{0, 1, ..., (\mathcal{N}-1)\}$ but instead let $m = \frac{r'_m - r''_m}{2}$ with $m \in \{\pm 1, \pm 2, ..., \pm(\mathcal{N}-1)\}$. Then

$$\sum_{r_e} \zeta^{\frac{1}{2} r_e (r'_m - r''_m)} = \sum_{k=0}^{\mathcal{N}-1} \mathrm{e}^{\mathrm{i}\frac{\pi}{N} r_e (r'_m - r''_m)} = \sum_{k=0}^{\mathcal{N}-1} \mathrm{e}^{\mathrm{i}\frac{\pi}{(2\mathcal{N})}(2k)(2m)} = \sum_{k=0}^{\mathcal{N}-1} \mathrm{e}^{\mathrm{i}\frac{2\pi}{\mathcal{N}} km}, \tag{A.5.22}$$

and then we have the same situation as for N odd, which proves that, for all N we have

$$T_{23}^\dagger T_{23} = 1. \tag{A.5.23}$$

□

Proof of equation (A.5.11). Combining (A.5.2) and (A.5.7) we have

$$\mathcal{O}^e_{12}\, T_{12} = \mathrm{e}^{\mathrm{i}\psi_{12}} \sum_{r_e, r_m} \zeta^{(r_e + \frac{r_e r_m}{2})} \, |r_e, r_m\rangle\langle r_e, r_m| \tag{A.5.24}$$

so

$$T^\dagger_{12}\, \mathcal{O}^e_{12}\, T_{12} = \sum_{r_e, r_m} \zeta^{r_e} \, |r_e, r_m\rangle\langle r_e, r_m| = \mathcal{O}^e_{12}, \tag{A.5.25}$$

so the proof is complete. The same argument applies to $\mathcal{O}^m_{12}$. □

Proof of equation (A.5.12). Note that

$$\mathcal{O}^e_{23}\, T_{12} = \mathrm{e}^{\mathrm{i}\psi_{12}} \sum_{r_e, r_m} \zeta^{\frac{r_e r_m}{2}} \, |r_e, r_m - 2\rangle\langle r_e, r_m| \,, \tag{A.5.26}$$

and then

$$\begin{aligned} T^\dagger_{12}\, \mathcal{O}^e_{23}\, T_{12} &= \sum_{r_e, r_m} \zeta^{\frac{1}{2}[r_e r_m - r_e(r_m - 2)]} \, |r_e, r_m - 2\rangle\langle r_e, r_m| \\ &= \sum_{r_e, r_m} \zeta^{r_e} \, |r_e, r_m - 2\rangle\langle r_e, r_m| \,. \end{aligned} \tag{A.5.27}$$

Considering the right hand side of (A.5.27), combining (A.5.2) and (A.5.4) gives

$$\begin{aligned} \mathcal{O}^e_{12}\, \mathcal{O}^e_{23}\, |r_e, r_m\rangle &= \left(\sum_{r_e, r_m} \zeta^{r_e} \, |r_e, r_m\rangle\langle r_e, r_m| \right) \left(\sum_{r_e, r_m} |r_e, r_m - 2\rangle\langle r_e, r_m| \right) \\ &= \left(\sum_{r_e, r_m} \zeta^{r_e} \, |r_e, r_m - 2\rangle\langle r_e, r_m - 2| \right) \left(\sum_{r_e, r_m} |r_e, r_m - 2\rangle\langle r_e, r_m| \right) \\ &= \sum_{r_e, r_m} \zeta^{r_e} \, |r_e, r_m - 2\rangle\langle r_e, r_m| \,, \end{aligned} \tag{A.5.28}$$

which when comparing to the left hand side completes the proof. The same proof can be made for $\mathcal{O}^m_{23}$. □

Proof of equation (A.5.13). Note that $[\, T_{23},\, \mathcal{O}^e_{23}] = 0$ by first taking the action

$$\begin{aligned} \mathcal{O}^e_{23}\, T_{23}\, |r'_e, r'_m\rangle &= \mathcal{O}^e_{23}\, \frac{\mathrm{e}^{\mathrm{i}\psi_{23}}}{\mathcal{N}} \sum_{r_e, r_m} \zeta^{-\frac{1}{2}(r_e - r'_e)(r_m - r'_m)} \, |r_e, r_m\rangle \\ &= \frac{\mathrm{e}^{\mathrm{i}\psi_{23}}}{\mathcal{N}} \sum_{r_e, r_m} \zeta^{-\frac{1}{2}(r_e - r'_e)(r_m - r'_m)} \, |r_e, r_m - 2\rangle \,, \end{aligned} \tag{A.5.29}$$

and then in the reverse order,

$$\begin{aligned} T_{23}\, \mathcal{O}^e_{23}\, |r'_e, r'_m\rangle &= T_{23}\, |r'_e, r'_m - 2\rangle \\ &= \frac{\mathrm{e}^{\mathrm{i}\psi_{23}}}{\mathcal{N}} \sum_{r_e, r_m} \zeta^{-\frac{1}{2}(r_e - r'_e)(r_m - r'_m + 2)} \, |r_e, r_m\rangle \\ &= \frac{\mathrm{e}^{\mathrm{i}\psi_{23}}}{\mathcal{N}} \sum_{r_e, r_m} \zeta^{-\frac{1}{2}(r_e - r'_e)(r_m - r'_m)} \, |r_e, r_m - 2\rangle \,, \end{aligned} \tag{A.5.30}$$

where the last step is to shift $r_m \mapsto (r_m - 2)$ which makes no difference when summing all r_m. The unitary property of T_{23} and the commutativity of T_{23} and $\mathcal{O}^e_{23}$ completes the proof of equation (A.5.13). The proof for $\mathcal{O}^m_{23}$ is identical. □

Proof of equation (A.5.14). Combine (A.5.2) and (A.5.8) and act on an arbitrary state $|r'_e, r'_m\rangle$, so that we get

$$\begin{aligned} \mathcal{O}^e_{12}\, T_{23}\, |r'_e, r'_m\rangle &= \mathcal{O}^e_{12}\, \frac{\mathrm{e}^{\mathrm{i}\psi_{23}}}{\mathcal{N}} \sum_{r_e, r_m} \zeta^{-\frac{1}{2}(r_e - r'_e)(r_m - r'_m)}\, |r_e, r_m\rangle \\ &= \frac{\mathrm{e}^{\mathrm{i}\psi_{23}}}{\mathcal{N}} \sum_{r_e, r_m} \zeta^{-\frac{1}{2}[(r_e - r'_e)(r_m - r'_m) - 2r_e]}\, |r_e, r_m\rangle\,. \end{aligned} \tag{A.5.31}$$

Now we take them in the opposite order, so we get

$$\begin{aligned} T_{23}\, \mathcal{O}^e_{12}\, |r'_e, r'_m\rangle &= T_{23}\, \zeta^{r'_e}\, |r'_e, r'_m\rangle \\ &= \frac{\mathrm{e}^{\mathrm{i}\psi_{23}}}{\mathcal{N}} \sum_{r_e, r_m} \zeta^{-\frac{1}{2}[(r_e - r'_e)(r_m - r'_m) - 2r'_e]}\, |r_e, r_m\rangle\,, \end{aligned} \tag{A.5.32}$$

the difference of the two being that $2r_e$ is exchanged by $2r'_e$ in the exponential function. Now we act on equation (A.5.32) with $\mathcal{O}^{e\dagger}_{23}$, so we get

$$\begin{aligned} \mathcal{O}^{e\dagger}_{23}\, T_{23}\, \mathcal{O}^e_{12}\, |r'_e, r'_m\rangle &= \frac{\mathrm{e}^{\mathrm{i}\psi_{23}}}{\mathcal{N}} \sum_{r_e, r_m} \zeta^{-\frac{1}{2}[(r_e - r'_e)(r_m - r'_m) - 2r'_e]}\, |r_e, r_m + 2\rangle \\ &= \frac{\mathrm{e}^{\mathrm{i}\psi_{23}}}{\mathcal{N}} \sum_{r_e, r_m} \zeta^{-\frac{1}{2}[(r_e - r'_e)(r_m - 2 - r'_m) - 2r'_e]}\, |r_e, r_m\rangle\,, \end{aligned} \tag{A.5.33}$$

where in the last step r_m was shifted to $(r_m - 2)$. Now we compare the differing parts of the arguments in the exponential function between (A.5.31), which is

$$(r_e - r'_e)(r_m - r'_m) - 2r_e = r_e(r_m - r'_m - 2) - r'_e(r_m - r'_m), \tag{A.5.34}$$

and (A.5.33), which is

$$\begin{aligned} (r_e - r'_e)(r_m - 2 - r'_m) - 2r'_e &= r_e(r_m - 2 - r'_m) - r'_e(r_m - 2 + r'_m + 2) \\ &= r_e(r_m - r'_m - 2) - r'_e(r_m - r'_m). \end{aligned} \tag{A.5.35}$$

Since $|r'_e, r'_m\rangle$ was arbitrary, we have proved that

$$\mathcal{O}^e_{12}\, T_{23} = \mathcal{O}^{e\dagger}_{23}\, T_{23}\, \mathcal{O}^e_{12}, \tag{A.5.36}$$

and since $[T_{23}, \mathcal{O}_{23}] = 0$ then $\mathcal{O}^{e\dagger}_{23}$ commutes with T_{23}, which leads us to the final result, namely that

$$T^\dagger_{23}\, \mathcal{O}^e_{12}\, T_{23} = T^\dagger_{23}\, \mathcal{O}^{e\dagger}_{23}\, T_{23}\, \mathcal{O}^e_{12} = T^\dagger_{23}\, T_{23}\, \mathcal{O}^{e\dagger}_{23}\, \mathcal{O}^e_{12} = \mathcal{O}^{e\dagger}_{23}\, \mathcal{O}^e_{12}, \tag{A.5.37}$$

and the proof is complete. The proof involving $\mathcal{O}^m_{12}$ and $\mathcal{O}^{m\dagger}_{23}$ is done in the same way. □

A.6 The braid group equation for charge conjugate duality solutions

Theorem A.7. *For*

$$\psi_{12} - \psi_{23} = 2\pi k, \;\; k \in \{0, 1, 2, ...\}, \tag{A.6.1}$$

the two operators

$$T_{12} = \mathrm{e}^{\mathrm{i}\psi_{12}} \sum_{r_e, r_m} \zeta^{\frac{1}{2} r_e r_m} \left| r_e, r_m \right\rangle \left\langle r_e, r_m \right|, \tag{A.6.2}$$

and

$$T_{23} = \frac{\mathrm{e}^{\mathrm{i}\psi_{23}}}{\mathcal{N}} \sum_{\substack{r_e, r_m \\ r'_e, r'_m}} \zeta^{-\frac{1}{2}(r_e - r'_e)(r_m - r'_m)} \left| r_e, r_m \right\rangle \left\langle r'_e, r'_m \right|, \tag{A.6.3}$$

where

$$\mathcal{N} = \begin{cases} \frac{N}{2}, & \text{if } N \text{ is even,} \\ N, & \text{if } N \text{ is odd,} \end{cases} \tag{A.6.4}$$

ψ_{12} and ψ_{23} are arbitrary phases and where

$$r_e, r_m, r'_e, r'_m \in \{0, 2, ..., 2(\mathcal{N} - 1)\}, \tag{A.6.5}$$

satisfy the braid group equation

$$T_{12}\, T_{23}\, T_{12} = T_{23}\, T_{12}\, T_{23}. \tag{A.6.6}$$

Proof. Assume N is odd. Then for

$$a_e, a_m, b_e, b_m \in \{0, 1, ..., N - 1\}, \tag{A.6.7}$$

we have

$$T_{12} = \mathrm{e}^{\mathrm{i}\psi_{12}} \sum_{a_e, a_m} \zeta^{2 a_e a_m} \left| a_e, a_m \right\rangle \left\langle a_e, a_m \right|, \tag{A.6.8}$$

and

$$T_{23} = \frac{\mathrm{e}^{\mathrm{i}\psi_{23}}}{N} \sum_{\substack{a_e, a_m \\ b_e, b_m}} \zeta^{-2(a_e - b_e)(a_m - b_m)} \left| a_e, a_m \right\rangle \left\langle b_e, b_m \right|. \tag{A.6.9}$$

Then

$$\begin{aligned} T_{12}\, T_{23} &= \frac{\mathrm{e}^{\mathrm{i}(\psi_{12} + \psi_{23})}}{N} \sum_{\substack{a_e, a_m \\ b_e, b_m}} \zeta^{2 a_e a_m - 2(a_e - b_e)(a_m - b_m)} \left| a_e, a_m \right\rangle \left\langle b_e, b_m \right| \\ &= \frac{\mathrm{e}^{\mathrm{i}(\psi_{12} + \psi_{23})}}{N} \sum_{\substack{a_e, a_m \\ b_e, b_m}} \zeta^{2(a_e b_m + a_m b_e - b_e b_m)} \left| a_e, a_m \right\rangle \left\langle b_e, b_m \right|. \end{aligned} \tag{A.6.10}$$

Furthermore, we have

$$\begin{aligned} T_{12}\, T_{23}\, T_{12} &= \frac{\mathrm{e}^{\mathrm{i}(2\psi_{12} + \psi_{23})}}{N} \sum_{\substack{a_e, a_m \\ b_e, b_m}} \zeta^{2(a_e b_m + a_m b_e - b_e b_m) + 2 b_e b_m} \left| a_e, a_m \right\rangle \left\langle b_e, b_m \right| \\ &= \frac{\mathrm{e}^{\mathrm{i}(2\psi_{12} + \psi_{23})}}{N} \sum_{\substack{a_e, a_m \\ b_e, b_m}} \zeta^{2(a_e b_m + a_m b_e)} \left| a_e, a_m \right\rangle \left\langle b_e, b_m \right|. \end{aligned} \tag{A.6.11}$$

We also have

$$\begin{aligned} T_{23}\,T_{12}\,T_{23} &= \frac{\mathrm{e}^{\mathrm{i}(\psi_{12}+2\psi_{23})}}{N^2}\sum_{\substack{a_e,a_m\\ b_e,b_m\\ c_e,c_m}} \zeta^{2(c_e b_m+c_m b_e-b_e b_m)-2(a_e-c_e)(a_m-c_m)}\,|a_e,a_m\rangle\langle b_e,b_m| \\ &= \frac{\mathrm{e}^{\mathrm{i}(\psi_{12}+2\psi_{23})}}{N^2}\sum_{\substack{a_e,a_m\\ b_e,b_m\\ c_e,c_m}} \zeta^{2(c_e b_m+c_m b_e-b_e b_m+a_e c_m+a_m c_e-a_e a_m-c_e c_m)}\,|a_e,a_m\rangle\langle b_e,b_m| \\ &= \frac{\mathrm{e}^{\mathrm{i}(\psi_{12}+2\psi_{23})}}{N^2}\sum_{\substack{a_e,a_m\\ b_e,b_m\\ c_e,c_m}} \zeta^{2c_e(a_m+b_m-c_m)}\zeta^{2(c_m b_e+c_m a_e-a_e a_m-b_e b_m)}\,|a_e,a_m\rangle\langle b_e,b_m|\,. \end{aligned} \tag{A.6.12}$$

For each value of a_e,a_m,b_e,b_m and c_m we have the inner sum

$$\sum_{c_e=0}^{N-1}\zeta^{2c_e(a_m+b_m-c_m)} = \begin{cases} N & \text{for } c_m = a_m+b_m, \\ 0 & \text{otherwise.} \end{cases} \tag{A.6.13}$$

Thus (A.6.12) becomes

$$\begin{aligned} T_{23}\,T_{12}\,T_{23} &= N\frac{\mathrm{e}^{\mathrm{i}(\psi_{12}+2\psi_{23})}}{N^2}\sum_{\substack{a_e,a_m\\ b_e,b_m}} \zeta^{2[(a_m+b_m)b_e+(a_m+b_m)a_e-a_e a_m-b_e b_m]}\,|a_e,a_m\rangle\langle b_e,b_m| \\ &= \frac{\mathrm{e}^{\mathrm{i}(\psi_{12}+2\psi_{23})}}{N}\sum_{\substack{a_e,a_m\\ b_e,b_m}} \zeta^{2(a_m b_e+b_e b_m+a_e a_m+a_e b_m-a_e a_m-b_e b_m)}\,|a_e,a_m\rangle\langle b_e,b_m| \\ &= \frac{\mathrm{e}^{\mathrm{i}(\psi_{12}+2\psi_{23})}}{N}\sum_{\substack{a_e,a_m\\ b_e,b_m}} \zeta^{2(a_m b_e+a_e b_m)}\,|a_e,a_m\rangle\langle b_e,b_m|\,. \end{aligned} \tag{A.6.14}$$

By comparing (A.6.11) and (A.6.14) we see that (A.6.6) holds if and only if

$$\mathrm{e}^{\mathrm{i}2\psi_{12}+\psi_{23}} = \mathrm{e}^{\mathrm{i}\psi_{12}+2\psi_{23}}, \tag{A.6.15}$$

or

$$\psi_{12}-\psi_{23} = 2\pi k, \quad k\in 0,1,2,..., \tag{A.6.16}$$

which completes the proof for odd N.

Now assume N is even. Then for

$$a_e,a_m,b_e,b_m \in \left\{0,1,...,\frac{N}{2}-1\right\}, \tag{A.6.17}$$

we have

$$T_{12} = \mathrm{e}^{\mathrm{i}\psi_{12}}\sum_{a_e,a_m}\zeta^{2a_e a_m}\,|a_e,a_m\rangle\langle a_e,a_m|\,, \tag{A.6.18}$$

and

$$T_{23} = \frac{2\mathrm{e}^{\mathrm{i}\psi_{23}}}{N}\sum_{\substack{a_e,a_m\\ b_e,b_m}}\zeta^{-2(a_e-b_e)(a_m-b_m)}\,|a_e,a_m\rangle\langle b_e,b_m|\,. \tag{A.6.19}$$

We have

$$T_{12}\,T_{23} = \frac{2\mathrm{e}^{\mathrm{i}(\psi_{12}+\psi_{23})}}{N}\sum_{\substack{a_e,a_m\\ b_e,b_m}}\zeta^{2(a_e b_m+a_m b_e-b_e b_m)}\,|a_e,a_m\rangle\langle b_e,b_m|\,, \tag{A.6.20}$$

and so

$$T_{12}\,T_{23}\,T_{12}\frac{2\mathrm{e}^{\mathrm{i}(2\psi_{12}+\psi_{23})}}{N}\sum_{\substack{a_e,a_m\\ b_e,b_m}}\zeta^{2(a_e b_m+a_m b_e)}\,|a_e,a_m\rangle\langle b_e,b_m|\,. \tag{A.6.21}$$

For the right hand side we have

$$\begin{aligned} T_{23}\,T_{12}\,T_{23} &= \tfrac{4\mathrm{e}^{\mathrm{i}(\psi_{12}+2\psi_{23})}}{N^2} \sum_{\substack{a_e,a_m\\ b_e,b_m\\ c_e,c_m}} \zeta^{2(c_e b_m + c_m b_e - b_e b_m) - 2(a_e - c_e)(a_m - c_m)} \,|a_e, a_m\rangle\langle b_e, b_m| \\ &= \frac{4\mathrm{e}^{\mathrm{i}(\psi_{12}+2\psi_{23})}}{N^2} \sum_{\substack{a_e,a_m\\ b_e,b_m\\ c_e,c_m}} \zeta^{2c_e(a_m+b_m-c_m)} \zeta^{2(c_m b_e + c_m a_e - a_e a_m - b_e b_m)} \,|a_e, a_m\rangle\langle b_e, b_m|\,. \end{aligned} \tag{A.6.22}$$

Similar to before, for each value of a_e,a_m,b_e,b_m and c_m we have the inner sum

$$\sum_{c_e=0}^{N/2-1} \zeta^{2c_e(a_m+b_m-c_m)} = \sum_{c_e=0}^{N/2-1} \mathrm{e}^{\mathrm{i}\frac{2\pi}{N/2}c_e(a_m+b_m-c_m)} = \begin{cases} \frac{N}{2} & \text{for } c_m = a_m + b_m, \\ 0 & \text{otherwise.} \end{cases} \tag{A.6.23}$$

Thus (A.6.22) becomes

$$\begin{aligned} T_{23}\,T_{12}\,T_{23} &= \frac{N}{2} \cdot \frac{4\mathrm{e}^{\mathrm{i}(\psi_{12}+2\psi_{23})}}{N^2} \sum_{\substack{a_e,a_m\\ b_e,b_m}} \zeta^{2[(a_m+b_m)b_e + (a_m+b_m)a_e - a_e a_m - b_e b_m]} \,|a_e, a_m\rangle\langle b_e, b_m| \\ &= \frac{2\mathrm{e}^{\mathrm{i}(\psi_{12}+2\psi_{23})}}{N} \sum_{\substack{a_e,a_m\\ b_e,b_m}} \zeta^{2(a_m b_e + b_e b_m + a_e a_m + a_e b_m - a_e a_m - b_e b_m)} \,|a_e, a_m\rangle\langle b_e, b_m| \\ &= \frac{2\mathrm{e}^{\mathrm{i}(\psi_{12}+2\psi_{23})}}{N} \sum_{\substack{a_e,a_m\\ b_e,b_m}} \zeta^{2(a_m b_e + a_e b_m)} \,|a_e, a_m\rangle\langle b_e, b_m|\,. \end{aligned} \tag{A.6.24}$$

The proof is concluded by comparing (A.6.21) and (A.6.24) and applying the same reasoning as for odd N. □

A.7 Proof of translation from Pauli operators to dyon creation operators

In this section of the appendix we prove the equation

$$\sigma_i^y = d_q^\dagger\, d_{q+1}^\dagger + d_q^\dagger\, d_{q+1} + H.c. = d_q^\dagger\, d_{q+1}^\dagger + d_q^\dagger\, d_{q+1} + d_{q+1}\, d_q + d_{q+1}^\dagger\, d_q, \tag{A.7.1}$$

where q is the label of the double plaquette "to the left" of site i.

It is known that σ_i^y squares to 1 and that acting with σ^y on i creates a dyon on plaquettes q and $q+1$ (if double plaquettes are numbered consecutively from left to right). Also, acting with σ^y on $i+1$ when the two dyons are already present moves the rightmost dyon one step to the right, to plaquette $q+2$. These three behaviours of σ_i^y will be shown for the right hand side of (A.7.1).

According to the braiding rule (2.7.14), dyons for $N=2$ have "fermionic" statistics, hence the creation operators follow the anti-commutator algebra

$$\{d_i\,,\, d_j\} = \{d_i^\dagger\,,\, d_j^\dagger\} = 0 \tag{A.7.2}$$

and

$$\{d_i\,,\, d_j^\dagger\} = \delta_{ij}, \tag{A.7.3}$$

which imply that changing the places of any two disjoint ($i \neq j$) operators reverses the sign, that

$$d_i\, d_i = d_i^\dagger\, d_i^\dagger = 0, \tag{A.7.4}$$

and finally that

$$N_i = d_i^\dagger\, d_i = 1 - d_i\, d_i^\dagger, \tag{A.7.5}$$

where N_i is the number operator, which in this case can take values 0 for a non-excited double plaquette and 1 for a double plaquette excited with a dyon.

Acting with σ_i^y twice on the vertex i sitting between the two double plaquettes $q=1$ and $q+1=2$ gives the operator

$$\begin{aligned}
&\left(d_1^\dagger\, d_2^\dagger + d_1^\dagger\, d_2 + d_2\, d_1 + d_2^\dagger\, d_1\right)\left(d_1^\dagger\, d_2^\dagger + d_1^\dagger\, d_2 + d_2\, d_1 + d_2^\dagger\, d_1\right) \\
&= d_1^\dagger\, d_2^\dagger\, d_1^\dagger\, d_2^\dagger + d_1^\dagger\, d_2^\dagger\, d_1^\dagger\, d_2 + d_1^\dagger\, d_2^\dagger\, d_2\, d_1 + d_1^\dagger\, d_2^\dagger\, d_2^\dagger\, d_1 \\
&\quad + \; d_1^\dagger\, d_2\, d_1^\dagger\, d_2^\dagger + d_1^\dagger\, d_2\, d_1^\dagger\, d_2 + d_1^\dagger\, d_2\, d_2\, d_1 + d_1^\dagger\, d_2\, d_2^\dagger\, d_1 \\
&\quad + \; d_2\, d_1\, d_1^\dagger\, d_2^\dagger + d_2\, d_1\, d_1^\dagger\, d_2 + d_2\, d_1\, d_2\, d_1 + d_2\, d_1\, d_2^\dagger\, d_1 \\
&\quad + \; d_2^\dagger\, d_1\, d_1^\dagger\, d_2^\dagger + d_2^\dagger\, d_1\, d_1^\dagger\, d_2 + d_2^\dagger\, d_1\, d_2\, d_1 + d_2^\dagger\, d_1\, d_2^\dagger\, d_1 \\
&= 0 + 0 + d_1^\dagger\, d_2^\dagger\, d_2\, d_1 + 0 \\
&\quad + \; 0 + 0 + 0 + d_1^\dagger\, d_2\, d_2^\dagger\, d_1 \\
&\quad + \; d_2\, d_1\, d_1^\dagger\, d_2^\dagger + 0 + 0 + 0 \\
&\quad + \; 0 + d_2^\dagger\, d_1\, d_1^\dagger\, d_2 + 0 + 0 \\
&= N_1\, N_2 + N_1\,(1 - N_2) + (1 - N_1)\,(1 - N_2) + (1 - N_1)\, N_2 \\
&= 1.
\end{aligned} \tag{A.7.6}$$

This proves that the operator squares to identity, just as $(\sigma_i^y)^2 = \mathbf{1}$.

To see that operating first with σ_i^y between the double plaquettes 1 and 2 and then with σ_{i+1}^y between the double plaquettes 2 and 3, moves the rightmost excitation one step to the

right (when beginning from the unexcited state) and labelling the double plaquettes $1, 2$ and 3 from left to right, we calculate

$$\begin{aligned}
&\Big(d_2^\dagger\, d_3^\dagger + d_2^\dagger\, d_3 + d_3\, d_2 + d_3^\dagger\, d_2\Big)\Big(d_1^\dagger\, d_2^\dagger + d_1^\dagger\, d_2 + d_2\, d_1 + d_2^\dagger\, d_1\Big) \\
&\quad = d_2^\dagger\, d_3^\dagger\, d_1^\dagger\, d_2 + d_2^\dagger\, d_3^\dagger\, d_2\, d_1 + d_2^\dagger\, d_3\, d_1^\dagger\, d_2 + d_2^\dagger\, d_3\, d_2\, d_1 \\
&\qquad +\ \ d_3\, d_2\, d_1^\dagger\, d_2^\dagger + d_3\, d_2\, d_2^\dagger\, d_1 + d_3^\dagger\, d_2\, d_1^\dagger\, d_2^\dagger + d_3^\dagger\, d_2\, d_2^\dagger\, d_1 \\
&\quad = N_2\Big(d_3^\dagger\, d_1^\dagger - d_3^\dagger\, d_1 + d_3\, d_1^\dagger - d_3\, d_1\Big) \\
&\qquad +\ \ \Big(1 - N_2\Big)\Big(d_3\, d_1 - d_3\, d_1^\dagger + d_3^\dagger\, d_1 - d_3^\dagger\, d_1^\dagger\Big) \\
&\quad = \Big(1 - 2N_2\Big)\Big(d_1^\dagger\, d_3^\dagger + d_1^\dagger\, d_3 + d_3^\dagger\, d_1 + d_3\, d_1\Big) \\
&\quad = \Big(-1\Big)^{N_2}\Big(d_1^\dagger\, d_3^\dagger + d_1^\dagger\, d_3 + H.c.\Big).
\end{aligned} \tag{A.7.7}$$

This proves that this operation is equivalent to having plaquettes 1 and 3 excited when starting from the ground state, with an additional factor of -1 if plaquette 2 is already excited. This sign factor can be accounted for by the fact that the excitations are fermions, so the order of creation should indeed differ by a sign.

References

[1] T.M. Apostol. *Introduction to Analytic Number Theory.* Number v. 1 in Introduction to Analytic Number Theory. Springer, 1976.

[2] Maissam Barkeshli, Chao-Ming Jian, and Xiao-Liang Qi. Twist defects and projective non-Abelian braiding statistics. *Phys. Rev. B*, 87:045130, Jan 2013.

[3] Maissam Barkeshli, Yuval Oreg, and Xiao-Liang Qi. Experimental Proposal to Detect Topological Ground State Degeneracy, 2014.

[4] Maissam Barkeshli and Xiao-Liang Qi. Synthetic Topological Qubits in Conventional Bilayer Quantum Hall Systems. *arXiv:1302.2673*, 2013.

[5] Maissam Barkeshli and Xiao-Gang Wen. Phase transitions in $\mathbb{Z}_N$ gauge theory and twisted $\mathbb{Z}_N$ topological phases. *Phys. Rev. B*, 86:085114, Aug 2012.

[6] Héctor Bombin. Topological Order with a Twist: Ising Anyons from an Abelian Model. *Phys. Rev. Lett.*, 105:030403, Jul 2010.

[7] Robin Ming Chen, Yujin Guo, Daniel Spirn, and Yisong Yang. Electrically and magnetically charged vortices in the chern–simons–higgs theory. *Proceedings of the Royal Society A: Mathematical, Physical and Engineering Science*, 465(2111):3489–3516, 2009.

[8] Michael Freedman, Chetan Nayak, and Kevin Walker. Towards universal topological quantum computation in the $\nu = \frac{5}{2}$ fractional quantum hall state. *Phys. Rev. B*, 73:245307, Jun 2006.

[9] Jürgen Fuchs, Ingo Runkel, and Christoph Schweigert. Boundaries, Defects and Frobenius Algebras. In Daniel Iagolnitzer, Vincent Rivasseau, and Jean Zinn-Justin, editors, *International Conference on Theoretical Physics*, pages 175–182. Birkhäuser Basel, 2004.

[10] Jürgen Fuchs and Christoph Schweigert. A note on permutation twist defects in topological bilayer phases. *arXiv/1310.1329*, 2013.

[11] Daniel Gottesman. *Stabilizer codes and quantum error correction.* PhD thesis, California Institute of Technology, 2008.

[12] Alexei Kitaev. Fault tolerant quantum computation by anyons. *Annals of Physics*, 303:2–30, 2003.

[13] Alexei Kitaev. Anyons in an exactly solved model and beyond. *Annals of Physics*, 321(1):2–111, Jan 2006.

[14] Brennen G. K. Zoller P. Micheli, A. A toolbox for lattice-spin models with polar molecules. 2(341):1745–2473.

[15] Chetan Nayak, Steven H. Simon, Ady Stern, Michael Freedman, and Sankar Das Sarma. Non-Abelian anyons and topological quantum computation. *Rev. Mod. Phys.*, 80:1083–1159, Sep 2008.

[16] M.A. Nielsen and I.L. Chuang. *Quantum Computation and Quantum Information.* Cambridge Series on Information and the Natural Sciences. Cambridge University Press, 2000.

[17] Olga Petrova, Paula Mellado, and Oleg Tchernyshyov. Unpaired Majorana modes in the gapped phase of Kitaev's honeycomb model. *Physical Review B*, 88(14):140405, 2013.

[18] N. Read and Dmitry Green. Paired states of fermions in two dimensions with breaking of parity and time-reversal symmetries and the fractional quantum hall effect. *Phys. Rev. B*, 61:10267–10297, Apr 2000.

[19] Carlos E. Soliverez. An effective Hamiltonian and time-independent perturbation theory. *Journal of Physics C: Solid State Physics*, 2(12):2161, 1969.

[20] Carlos E. Soliverez. General theory of effective Hamiltonians. *Phys. Rev. A*, 24:4–9, Jul 1981.

[21] Jeffrey C. Y. Teo, Abhishek Roy, and Xiao Chen. Braiding Statistics and Congruent Invariance of Twist Defects in Bosonic Bilayer Fractional Quantum Hall States, 2013.

[22] Xiao-Gang Wen. Quantum orders in an exact soluble model. *Phys. Rev. Lett.*, 90:016803, Jan 2003.

[23] Xiao-Gang Wen. Topological Order: From Long-Range Entangled Quantum Matter to a Unified Origin of Light and Electrons. *ISRN Condensed Matter Physics*, 2013, 2013.

[24] Xing-Can Yao, Tian-Xiong Wang, Hao-Ze Chen, Wei-Bo Gao, Austin G. Fowler, Robert Raussendorf, Zeng-Bing Chen, Nai-Le Liu, Chao-Yang Lu, You-Jin Deng, and et al. Experimental demonstration of topological error correction. *Nature*, 482(7386):489–494, Feb 2012.

[25] Yi-Zhuang You, Chao-Ming Jian, and Xiao-Gang Wen. Synthetic non-Abelian statistics by Abelian anyon condensation. *Phys. Rev. B*, 87:045106, Jan 2013.

[26] Yi-Zhuang You and Xiao-Gang Wen. Projective non-Abelian statistics of dislocation defects in a $\mathbb{Z}_N$ rotor model. *Phys. Rev. B*, 86:161107, Oct 2012.